MULTIVARIATE IDENTIFICATION AND STOCHASTIC CONTROL OF A PILOT PLANT PACKED-BED REACTOR

MULTIVARIATE IDENTIFICATION AND STOCHASTIC CONTROL OF A PILOT PLANT PACKED BED REACTOR

by

ALLAN L.K. WONG, B.A.Sc.

A Thesis

Submitted to the Faculty of Graduate Studies

in Partial Fulfillment of the Requirements

for the Degree

Master of Engineering

McMaster University

May, 1977.

Master of Engineering
(Chemical Engineering)

McMaster University,
Hamilton, Ontario.

TITLE: MULTIVARIATE IDENTIFICATION AND STOCHASTIC CONTROL OF A PILOT PLANT PACKED BED REACTOR.

AUTHOR: ALLAN L.K. WONG, B.A.Sc. (University of Ottawa).

SUPERVISOR: DR. J.F. MacGregor.

NUMBER OF PAGES: xv, 176.

ABSTRACT

The modelling and control of a pilot plant packed bed catalytic reactor is investigated. The reactions considered are those of the hydrogenolysis of n-Butane over a nickel on silica gel catalyst. These involve several independent species and are highly exothermic. A multivariate transfer function model for process and a time series model for the disturbances are constructed through an iterative procedure of process identification, parameter estimation and diagnostic checking. Using exit concentrations inferred from reactor bed temperatures and inlet flow measurements, a multivariate stochastic controller, designed to minimize a quadratic function of the production rates of various intermediate products subject to constraints on the variances of the manipulated input flowrates is implemented on-line using a process minicomputer. The parameters of the inferential concentration equation are updated on-line using infrequent data from a process gas chromatograph. The performance of this feedback controller is found to be quite satisfactory.

ACKNOWLEDGEMENT

The author wishes to express his sincere gratitude to his research supervisor, Dr. J.F. MacGregor for his guidance and encouragement to make this thesis possible.

He is also indebted to the following persons during the course of the work:

Dr. A. Jutan for his help in the modelling of multivatiate processes;

J.P. Tremblay, Dr. J.D. Wright and especially to T. Harris for their assistance in minicomputer programming.

He also wishes to thank Mrs. Sheelagh Courtney for her patience and excellent work in typing this thesis; and to McMaster University for providing financial support.

TABLE OF CONTENTS

PAGE

LIST OF FIGURES

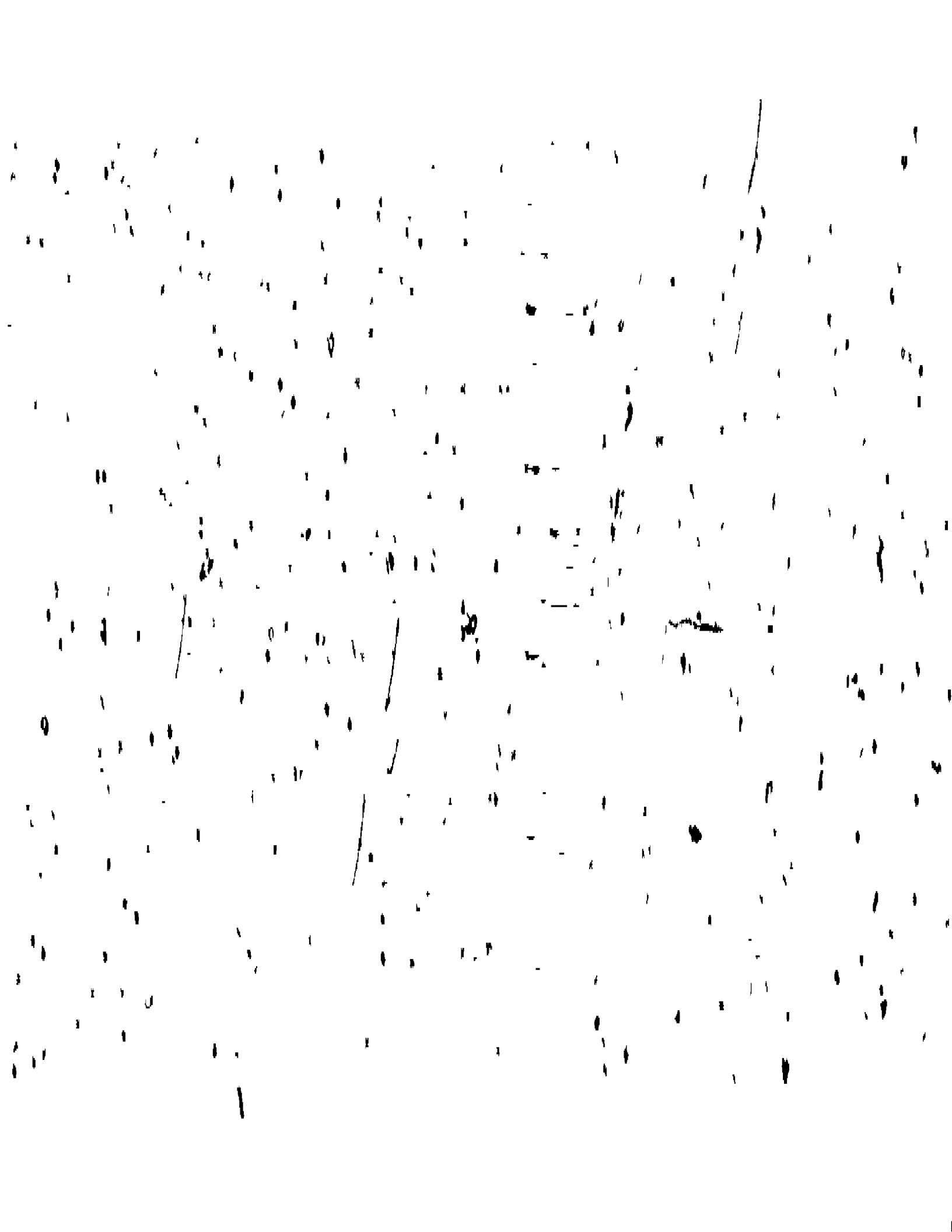

LIST OF TABLES

CHAPTER 1

INTRODUCTION AND REVIEW

Due to the recent breakthrough in minicomputer technology, extensive interest has been expressed on their application to chemical processes. The versatilities of digital minicomputers enables the interfacing of the computer with various process units and their real time on-line control. Although the applicability of various computer control schemes on chemical processes is still a point of debate, it is quite clear that the credibility of minicomputer application is continuously gaining support from industry and is no longer an academic exercise. The flexibility of the minicomputer makes the implementation of control theories more feasible.

Advanced control theories have been well developed for a long time. Previously, the problems related to their real time applications were three fold:

the lack of suitable computer systems,

large investment with doubtful economical returns, and

the lack of trained personnel.

The availability of minicomputers solves the first problem. The second obstacle hinges on the careful planning of the application. Large capital is indeed required initially, but in the long run, efficient

control of the process will increase product production rates, reduce the production cost and reduce problems caused by human errors. Modern sophisticated control schemes can also be applied and tested, thus ultimately improving the product quality. Besides, the increasingly modest computer hardware cost will offset part of the financial problem. The lack of trained people will still be a problem in the near future. However, as more industries adopt digital computer control systems, the necessity of the training of personnel will be extended to other academic and technical institutions.

The many advantages of minicomputer control applications have been pointed out by West [1976]. Various combinations of distributed control systems are rendered possible and operator/computer rapport is greatly improved. Data logging for process analysis and plant operation scheduling is becoming more efficient. Controls on process inputs-outputs, feedstock utilization and the reduction of utilities are the general objectives of most present computer applications. However, not many results are published in literature because of secrecy and company policies. As it is a relative new field, exciting new challenges in the future applications are abundant. The recent trend of industries moving to automation proves the computer control applications are beneficial and the usage of minicomputer systems will undoubtedly be expanded in the future.

1.1 Objectives of This Thesis

In this thesis, a pilot plant scale catalytic reactor is being studied. The work can be divided into two parts - process modelling and the direct digital control (DDC) of the process using modern stochastic control theory. The aim is to control the extents or production rates of the products about desired levels by adjusting the input reactant flowrates. A statistical approach is used for the development of a process model by fitting plant data empirically. This procedure includes the identification of the structure of the system, parameter estimation and diagnostic checking of the dynamic-stochastic model. From the resulting model, a multivariate optimal stochastic feedback controller is designed using dynamic programming and Kalman filtering theories for DDC purpose. Implementation of this controller on the reactor system will determine the effectiveness of this control procedure for such complex systems.

1.2 Modelling and Computer Control on Chemical Processes

The DDC computers have been widely adopted in many industries in the past decade, especially in the pulp and paper (Astrom et al [1975]), and steel making industries, where sophisticated control strategies have proven to be successful. Industrial applications on chemical processes are, however, limited to simple single loop control or occasionally cascade control on some linear, stable and well-known unit operations. Extensive control studies had been done by Fisher and Seborg [1976] on a double-effect evaporator. Marroquin et al [1973]

applied control on a batch reactor and a CSTR. Controls on an extractive distillation column had been carried out successfully by Jackson [1974], Hu and Ramirez [1972], just to name a few.

Reports on the computer control of complex chemical processes are extremely sparse. The problem may be accounted for by two reasons - the difficulties in understanding the process dynamics and the implementation of control theories on commercial plants. Lee and Weekman [1976] expressed an industrial viewpoint on the control of complex systems. Since many chemical processes have unknown dynamic characteristics, modelling is a major difficulty. Even with well understood kinetics, dynamic model development from basic physical equations is usually difficult because of large nonlinearities and the distributed parameter nature of the models. It has been shown that advanced control techniques such as multivariable control may improve process performances. (Fisher and Seborg [1976]). The additional performance gains from the advanced control techniques will be weighed against the extra work incurred in the controller designs and installation.

For complex packed bed reactors, various aspects of their transport and thermodynamics properties have been studied intensively. (Froment [1974], Sinai and Foss [1970], Ferguson and Finlayson [1970]). These studies all provided substantial insight necessary for the formulation of a mechanistic dynamic model. With the inclusion of axial and radial gradients, three dimensional partial differential equations (PDE) are involved. The PDE's can be converted into sets of ODE's and then linearized so that control theories and parameter estimation

can be applied. Finlayson [1972] applied the concept of orthogonal collocation for efficient solution of these complex dynamic equations. Vakil et al [1973] derived a control scheme for a fixed bed reactor using temperature data. Jutan [1976] obtained a dynamic model of an exothermic reactor suitable for on-line multivariable control applications. The reported application of control on these complex reactors is rare. Hong and MacGregor [1975] used a 'black box' transfer function-noise model approach to statistically identify a model and control a continuous stirred tank process. Wright and Bacon [1973] successfully identified such an empirical model for a dual input heat exchanger system. These results indicate that chemical processes can be modelled using different methods and various control strategies can then be designed accordingly.

1.3 Previous and Current Control Work on the Catalytic n-Butane Hydrogenolysis Reactor

The pilot plant tubular packed bed reactor was built by Tremblay [1977]. The flexibility and the complex nature of the system allow the testing of many advanced control schemes. Tremblay and Wright [1973] successfully used a single variable cascade control scheme for the control of butane conversion. Model reference adaptive control strategy was attempted by Tremblay [1977]. Jutan [1976] derived a dynamic-stochastic model from theoretical material and energy balances, and designed and implemented a multivariate stochastic controller. In this thesis, a similar multivariate stochastic control scheme will be developed using empirically identified multivariate

transfer function-noise models. Since this work and Jutan's are closely related, a discussion of his approach will be helpful in this study.

In Jutan's dynamic model building, the three dimensional PDE's representing the reactor dynamics were reduced to seven first order ODE's by using a quasi-steady state assumption on the concentration dynamics and approximating the partial derivatives using methods of orthogonal collocation. A seven dimensional discrete state space model resulted after linearization about operating profiles and discretization in time (Jutan et al [1976a]). The parameters of the state space model which described the axial temperature deviations were automatically determined for a given choice of three physical parameters - effective radial conductivity, effective radial diffusivity and the catalyst activity parameter (Jutan et al [1976b]). The axial temperatures at the collocation points were obtained by quadratic interpolation from nearby temperature measurements. A stochastic model for the disturbances was then incorporated into the dynamic state space model. An inferential relationship for the three theoretically independent exit concentrations in terms of temperature and inlet flow deviations was also derived and used in the controller objective function.

A multivariate feedback controller was designed from the resulting dynamic-stochastic model by dynamic programming, and was implemented under pilot plant operating conditions (Jutan et al [1976c]). Kalman filter theory was used to obtain the state estimates. Despite all the assumptions involved in the modelling, the controller performance was very satisfactory, and its performance when subjected to both the inherent stochastic disturbances in the system and to a deterministic load

change in wall temperature was considerably superior to a well-tuned single loop proportional-integral (PI) controller.

Jutan's result is one of the very few successful reports on the modelling and control of a complex packed bed reactor, proving that advanced control techniques are applicable to real world processes. However, the drawback of this work is the tremendous amount of time involved in the modelling part. The parameter estimation of the state space model was also time consuming. Lengthy and tedious mathematical operations have to be carried out in this procedure. Besides, in this case good models for the reaction kinetics of the hydrogenolysis of n-Butane had been established (Orlickas [1972]), Shaw [1974]), providing invaluable information in setting up the fundamental material and energy balances. In many cases, such information would be unavailable. All these factors make this approach difficult to apply industrially.

In view of these difficulties, an alternative approach which assumes the reactor as a 'black box' will be presented here. Dynamic and stochastic behaviours can be described by discrete transfer function-noise models which can be statistically identified from plant data. The procedure of this empirical model building has been systematically documented and will be discussed in Chapter 2. More important, it is applicable to any complex chemical reactor provided all the necessary plant data are measured. Although derivation of a multivariate stochastic controller directly from transfer function-type models is tedious, this model can be easily converted into a state space model form for which

straightforward design techniques exist. It is significant in this approach that all the independent controlled variables are measured or can be inferred from other measurable variables. Although the number of parameters involved will increase rapidly as the dimensionality of the inputs and outputs increase, this effect can be minimized by using the concept of principal component analysis on the output time series structure to reduce the dimensionality of the output. This will be outlined in Chapter 4. Many chemical processes seldom involve more than three inputs and three outputs. Thus, transfer function-noise models are often suitable for most regulatory control purposes.

In this work, a multivariate stochastic constrained feedback controller is derived from the transfer function-noise model. A similar controller design procedure to that used in Jutan's work is followed. Other projects currently being investigated on this reactor include self-tuning adaptive control, a dual cascade controller with decoupling effects and variations on model reference adaptive control.

1.4 Outline of the Following Chapters

Chapter 2 reviews the relevant material in the literature on the modelling techniques for multivariate processes. Section 2.1 gives a brief description of multivariate time series models and their various canonical forms. The three phases of formulation - identification, parameter estimation and diagnostic checking are presented in order. Section 2.2 deals with the formation of parsimonious multivariate transfer function-noise models. These multivariate forms are often

extensions from univariate models. Section 2.3 gives an example, illustrating the construction of multivariate models. An alternative representation of the dynamic-stochastic system in state space model form is shown in Section 2.4. Different methods for the conversion of transfer function models to this form are presented. The benefits of these two forms of model representation are also compared.

In Chapter 3, the configuration of the pilot plant reactor and the process digital minicomputer are reviewed. Section 3.1 presents the basic reaction kinetics of the catalytic hydrogenolysis of n-butane. A brief description of the equipment - tubular reactor, reactant flow network, circulating oil network and the process gas chromatograph-programmer is found in Section 3.2. Section 3.3 provides an overview of the real time process control Nova Computer system and its auxiliary facilities. A summary of the collection of basic software for the control of this particular reactor is also given. Section 3.4 indicates the necessary interfacing between the reactor system and the process computer.

Chapter 4 generally accounts for the actual modelling of the reactor system, the problems encountered and their solutions. Section 4.1 outlines the data acquisition scheme which is vital for the model building. Due to the configuration of the process gas chromatograph, exit concentrations are available only every six minutes which is far too long to base a practical control scheme on these measurements only. Section 4.2 will describe the development of an inferential scheme for

predicting the exit concentrations from the axial temperature measurement and the input flows present during the previous interval. Canonical variates are formed by the linear combinations of these measured predictor variables, and pseudo-concentrations in terms of extents are regenerated. The results from this canonical correlation analysis and the validity and advantages of the method are also discussed. Finally, a real time version of the recursive least squares fit is introduced to improve the parameter estimations in the prediction equation under drifting operation conditions. Section 4.3 is concerned with the building of a multivariate transfer function-noise model for the reactor system. Despite the success in model fitting, it was suspected that not all three output extents deviates needed to be controlled. In fact, in Section 4.4, a test for the reduction of the output dimension showed that only two independent outputs contain 'most of the activity' of the system. The formulation of this test is presented. With two independent outputs chosen, a two inputs-two outputs model is refitted and the final model is then transformed to the state space model form.

Chapter 5 outlines the optimal stochastic control theory from which the multivariate feedback controller is derived. Section 5.1 and 5.2 indicate the design procedure from transfer function and state space model forms. Kalman filter and controller design by dynamic programming are briefly discussed. A simulation study is carried out to confirm the performance of the various controllers. Section 5.3 describes the implementation of the multivariate controller and the results from this run are presented.

CHAPTER 2

MULTIVARIATE PROCESSES

2.1 Multivariate Time Series Analysis

2.1.1 General Formulation of Multivariate Time Series

A stochastic process is a statistical phenomenon in time governed by probabilistic laws. A time series is defined as a sequence of observations on a variable measured at different points in time. Thus, it is a realization of a stochastic process. In the case of more than one variable, a multivariate time series is represented by the vector $\underline{N}(t)$ which has elements $n_{i,t}$, where

$i = 1,2,\ldots,n$ $\quad$ n = number of variables

$t = 1,2,\ldots,\tau$ $\quad$ τ = total time intervals

In this thesis, only discrete time series models sampled at equispaced intervals of time are considered. A unified approach to modelling univariate time series has been presented by Box and Jenkins [1970]. Multivariate time series models of the forms considered in this thesis were first systematically presented by Quenouille [1957], and later by Wilson [1970], Alavi [1973] and many others. In general, a multivariate time series can be modelled as a weighted sum of past

values of a multivariate white noise sequence $\underline{a}_t$:

$$\underline{N}_t - \underline{\mu} = \underline{\psi}(B)\underline{a}_t \qquad (2.1)$$

where

$\underline{N}_t$ is the (nx1) vector of time series variates

$\underline{\mu}$ is the mean value of the series

$\underline{a}_t$ is a white noise sequence with mean $\underline{0}$ and covariance matrix $\underline{D}$

$$\underline{\psi}(B) = \underline{I} + \underline{\psi}_1 B + \underline{\psi}_2 B^2 + \ldots \qquad (2.1a)$$

is a matrix series in the operator B

B = backward shift operator, such that $B^k \underline{N}_t = \underline{N}_{t-k}$

It is assumed that from here on, all the series are mean corrected and equation (2.1) is rewritten as:

$$\underline{N}_t = \underline{\psi}(B)\underline{a}_t \qquad (2.2)$$

Equation (2.2) can be expressed in another form with $\underline{\pi}(B) = \underline{\psi}^{-1}(B)$, such that

$$\underline{\pi}(B)\underline{N}_t = \underline{a}_t \qquad (2.3)$$

Again, $\underline{\pi}(B)$ is a matrix series in the backward shift operator B. The uniqueness of Equation (2.2) and (2.3) hinges on the stationarity and invertibility conditions (Wilson [1970], Alavi [1973]). In brief, a process is stationary and invertible if $\underline{\psi}(B)$ and $\underline{\pi}(B)$ converge for all $|B| \leq 1$.

Defining the covariance matrix of the multivariate white noise sequence $\underline{a}_t$ as the expectation:

$$E(\underline{a}_t \underline{a}_s^T) = \underline{D}\, \delta_{ts} \qquad (2.4)$$

$$\delta_{ts} = \begin{cases} 0 & s \neq t \\ 1 & s = t \end{cases}$$

where

$\underline{D}$ is the dispersion matrix

$E(\ )$ is the expectation.

Superscript T is the transpose of the vector.

In other words, the white noise $\underline{a}_t$ are uncorrelated with $\underline{a}_s$ at different time periods. Correlation may exist among the components when t = s.

On many occasions, a time series is non-stationary, that is, the series has no fixed mean level. Data tends to drift away from the local mean level although local sequences of the series can be described by a stochastic model. Stationarity can be attained by means of differencing, which is represented by the inverted delta operator ∇, where $\nabla^d = (1-B)^d$. Generally, the value of d is rarely greater than 2.

In practice, a parsimonious model is required from modelling. It has the fewest number of parameters possible to best describe the series. It is the aim of achieving parsimony that different modelling techniques are developed.

Quenouille [1957] defined a discrete, stationary multivariate

time series model in the general form

$$\underline{\phi}(B)\ \underline{\nabla}^{d}\ \underline{N}_t = \underline{\theta}(B)\ \underline{a}_t \qquad (2.5)$$

where

$\underline{\phi}(B)$ and $\underline{\theta}(B)$ are finite matrix series in the operator B, such that

$$\underline{\phi}(B) = \underline{I} + \underline{\phi}_1 B + \underline{\phi}_2 B^2 + \ldots + \underline{\phi}_p B^p \qquad (2.5a)$$

$$\underline{\theta}(B) = \underline{I} + \underline{\theta}_1 B + \underline{\theta}_2 B^2 + \ldots + \underline{\theta}_q B^q \qquad (2.5b)$$

p, q is the order of matrix $\underline{\phi}(B)$ and $\underline{\theta}(B)$ respectively,

∇^d is a diagonal matrix of differencing operators.

Matrices $\underline{\phi}(B)$ and $\underline{\theta}(B)$ are both full; and the orders p_{ij} and q_{ij} of individual elements are not necessarily the same. Equation (2.5) designates an Autoregressive-Integrated-Moving-Average (ARIMA) process of order (p, d, q). When the AR operator $\underline{\phi}(B) = \underline{I}$,

$$\underline{\nabla}^{d}\ \underline{N}_t = \underline{\theta}(B)\ \underline{a}_b \qquad (2.6)$$

which is a moving average (MA) model of order q. Whereas when the MA operator $\underline{\theta}(B) = \underline{I}$,

$$\underline{\phi}(B)\ \underline{\nabla}^{d}\ \underline{N}_t = a(t) \qquad (2.7)$$

it is an autoregressive (AR) model of order p.

The general model Equation (2.5) although may be able to describe the process, the rapidly increasing number of parameters as the

number of series increases makes it impractical for efficient identification and estimation. More important, there are too many degrees of freedom in the full parameter matrices, $\underline{\phi}(B)$ and $\underline{\theta}(B)$. It is difficult to obtain unique identification since it can easily be shown that there are an infinite number of solutions to the full matrix model which will yield the same residual covariance structure (Rao and Kashyap [1976]). Thus, it is necessary to choose alternative canonical forms which will yield unique solutions corresponding to a given covariance structure.

Wilson [1970] suggested a canonical form having a diagonal $\underline{\phi}(B)$ matrix with order $p = \max(p_i)$, and with full $\underline{\theta}(B)$ and $\underline{\Sigma}$ matrices. No theoretical explanation is attempted for this particular selection. Rather, it is primarily for the ease with which one can identify the process structure from data. The diagonal $\underline{\phi}(B)$ matrix regenerates an intermediate multivariate series $\underline{b}_t$ from $\underline{N}_t$, facilitating series identification. However, by choosing full $\underline{\theta}(B)$ matrix operator, estimation is more difficult since MA parameters enter nonlinearly while the AR parameters enter linearly. Yet, subsequent tests indicate this model form provides adequate and satisfactory representation of many stochastic processes. This model formulation procedure will be presented in greater detail in the following sections.

Many other possible canonical model structures exit and each has its advantages and disadvantages (Rao and Kashyap [1976]). Alavi [1973] suggested an intermediate model form in which neither

$\underline{\phi}(B)$ nor $\underline{\psi}(B)$ is constrained to be full or diagonal. Both $\phi_{ij}(B)$ and $\theta_{ij}(B)$ are allowed to have different orders and the order of the model depends on the maximum values of p_{ij} and q_{ij}.

Other suggestions (Akaike [1974], Parzen [1974]) restrict the model to be pure autoregressive because of the ease in estimating their parameters, even though more parameters than necessary may be involved. The required order of the autoregressive model is found by successfully fitting higher order AR models and using some form of decision or hypothesis test to indicate whether more terms are necessary.

In viewing all the possible routes for modelling, the model suggested by Wilson is adopted for the most part of this thesis. The other forms are by no means inferior; rather it is an arbitrary choice from many equally adequate selections. Although Wilson's model may not give a perfect parsimonious representation, it is the author's feeling that with this structure, the readers with some knowledge in univariate time series will find the model development easy to follow. Other modelling techniques will, however, be supplemented whenever additional information is deemed necessary. More details on the properties of various time series representation can be formed in the literature mentioned above.

2.1.2 Identification, Estimation and Diagnostic Checking

Model building consists of three stages - identification, estimation and diagnostic checking. Identification of a process is the proper choice of a preliminary model with initial parameters and order

estimates. By estimation, the model is fitted statistically and the best parameter estimates are obtained. The final diagnostic checking involves testing for any inadequacies in the model. The model form will be adjusted and the procedure repeated until the diagnostic checks indicate no model inadequacies. These three stages are summarized below.

(a) Identification

In identification, the concepts of covariance, autocorrelation, cross-correlation and partial correlation functions are most commonly used. The formulations of these functions have been well defined (Box and Jenkins [1970], Quenouille [1957], Alavi [1973]) and thus will not be discussed here. A brief description of the behaviour of the auto- and partial correlation functions of the three classes of time series models - AR, MA and ARMA are summarized in Table 2.1

TABLE 2.1: AUTO- AND PARTIAL CORRELATION FUNCTIONS OF AR, MA AND ARMA PROCESSES

	Autocorrelation Functions ρ_k	Partial Correlation Functions, ϕ_{kk}
Autoregressive Process, AR $\underline{\phi}(B)\ \underline{N}_t = \underline{a}_t$	Tails off exponentially or as damped sine wave	Cuts off at lag p
Moving Average Process, MA. $\underline{N}_t = \underline{\theta}(B)\ \underline{a}_t$	Cuts off at lag q	Tails off exponentially or as damped sine wave
Autoregressive-Moving Average Process, ARMA	Tails off exponentially or damped sine wave after first (q-p) lags	Tails off exponentially or damped sine wave after first (p-q) lags

Following Wilson [1970], a univariate linear discrete model is first identified separately for each series such that

$$n_{i,t} = a_{i,t} - \sum_{k=1}^{q_i} \theta_{i,k}\, a_{i,t-k} + \sum_{k=1}^{p_i} \phi_{i,k}\, n_{i,t-k} \qquad (2.8)$$

The discrete parameters p_i, q_i of $\phi_{i,k}$ and $\theta_{i,k}$ are fitted and checked. The p_i and $\phi_{i,k}$ AR parameters are taken as good initial estimates for the corresponding elements in the multivariate model. The $n_{i,t}$ series are then checked for cross-correlations. If these $n_{i,t}$ are not cross-correlated, the multivariate model is simply the combination of all individual univariate models, i.e. $\underline{\phi}(B)$ and $\underline{\theta}(B)$ have diagonal elements only. For cross-correlated $n_{i,t}$, intermediate series $b_{i,t}$ are generated by filtering the original series through the $\underline{\phi}(B)$ operators.

$$b_{i,t} = n_{i,t} - \sum_{k=1}^{p_i} \phi_{i,k}\, n_{i,t-k} \qquad (2.9)$$

Sample cross-correlation functions between the $b_{i,t}$'s are then examined to find the lag k at which they appear to cut off. This lag k will be the order of the MA operator $\underline{\theta}(B)$ such that $q = \max(q_{ij})$, noting that q_{ij}'s are not necessarily the same.

(b) Estimation

When p and q are properly chosen, estimation can be carried out. The continuous parameters $\phi_{i,k}$ and $\theta_{ij,k}$ are estimated in this thesis by the maximum likelihood estimation procedure as outlined by Wilson [1970, 1973]. The algorithm which minimizes $\left| \sum_{t=1}^{\tau} \underline{a}_t\, \underline{a}_t^T \right|$ is based on iterating

between conditional estimation of residual dispersion matrix $\underline{D}$ and conditional estimation of parameter $\underline{\beta}$. Rapid convergence is often reached even with poor preliminary estimates. For any chosen value of the parameters, the residuals $a_{i,t}$ can be calculated recursively using

$$a_{i,t} = n_{i,t} - \sum_{k=1}^{p_i} \phi_{i,k}\, n_{i,t-k} + \sum_{j=1}^{n} \sum_{k=1}^{q_{ij}} \theta_{ij,k}\, a_{j,t-k} \qquad (2.10)$$

Initially, $\theta_{ij,k}$ values with $i \neq j$ can be set to zero. The $a_{i,t}$ before some time point t_1 are also set equal to zero in order to start the recursive calculation.

(c) Diagnostic Checking

The diagnostic checks are based on the fact that if the model is adequate the residual sequence $\underline{a}_t$ should appear to approximate a multivariate white noise sequence. This implies that each element of $\underline{a}_t$ should approximate a univariate white noise sequence and several tests can be performed to check this (Box and Jenkins [1970]). The sample autocorrelations of the residuals, $r_{a,ij}(k)$ can be calculated for each pair of series i,j and for lags k = 1,2,....,K; and compared with the two standard error limits $2/\sqrt{T'}$ where $T' = T - t_1 + 1$. If the model is correct, the $r_{a,ij}(k)$ would have an expected value zero and a standard error of approximately $1/\sqrt{T'}$. An approximate overall test can be obtained by comparing

$$\chi^2_{ij} = T' \sum_{k=1}^{K} \hat{r}^2_{a,ij}(k) \qquad (2.11)$$

with the critical value of a Chi-squared distribution with (K - p - q)

degrees of freedom. These two tests form the basis for model checking. If several models show no inadequacy, a model discrimination can be performed by examining the determinant of the residual dispersion matrix $\hat{\underline{D}}$ which is the generalized variance of the residuals. In fact, decisions on model improvement should be based on $|\hat{\underline{D}}|$ since Chi-square statistics are sometimes insensitive and misleading for model selection (Alavi [1973]).

The algorithm of identification, estimation and diagnostic checking is summarized in Figure 2.1.

In many cases, a pure AR process is desirable for time series modelling. AR parameter estimates from the identification step are fairly accurate estimates. A criterion for identification of the proper order of the AR operator was developed by Akaike [1974] for univariate series, and can be extended to multivariate case (Parzen [1974]). This procedure involves fitting multivariate AR models of increasing order and testing for the significance of the information contained in the additional parameters. Alavi [1973] presents an algorithm for recursively computing these higher order AR parameter matrices and thereby obtaining pseudo partial correlation matrices as well.

FIGURE 2.1 : ALGORITHM FOR MULTIVARIATE TIME SERIES MODELLING

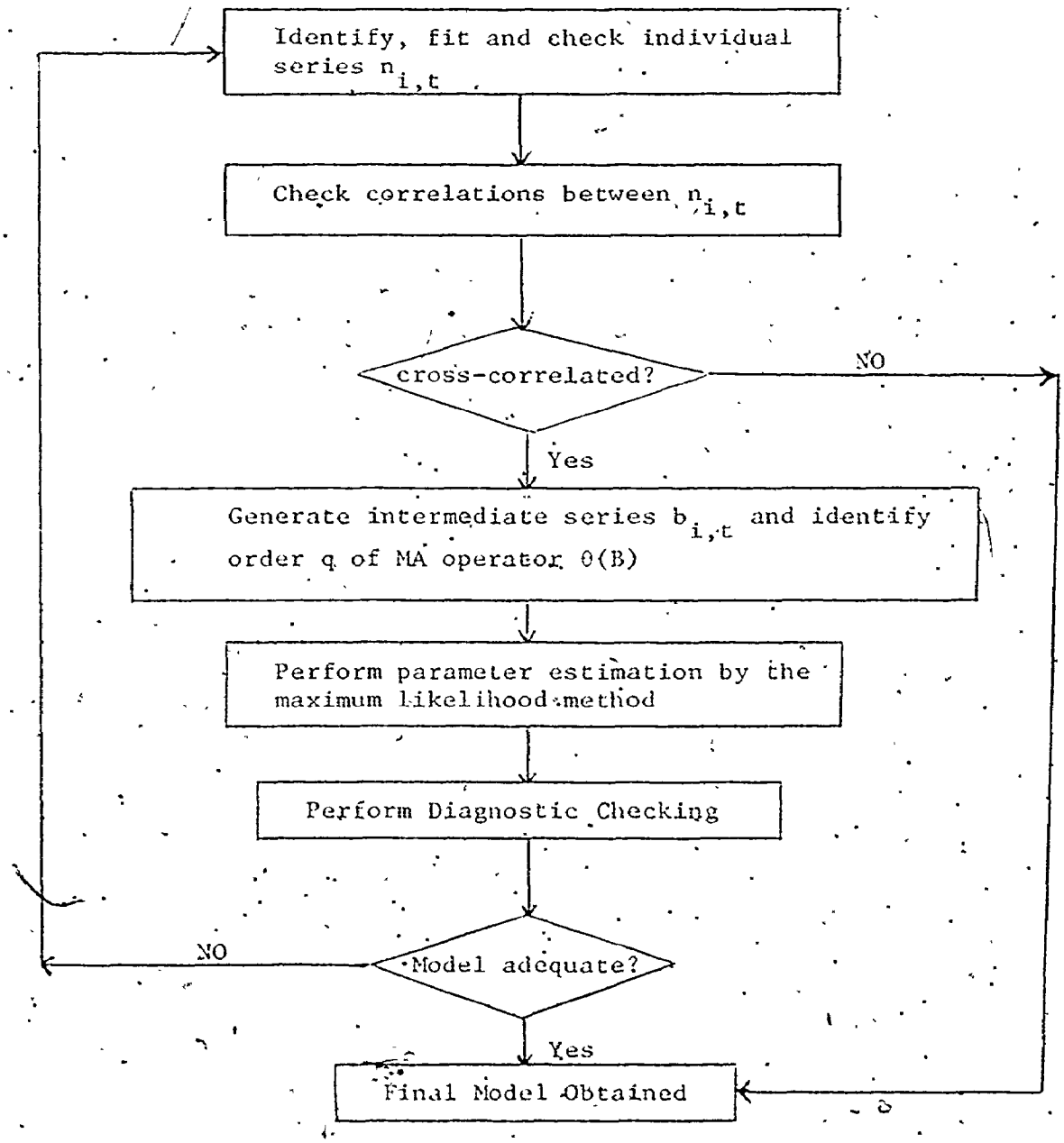

2.2 Multivariate Transfer Function - Noise Model

2.2.1 General Formulation of Transfer Function - Noise Model

In many chemical processes, the dynamic behaviour of the system can be represented by a transfer function which relates the inputs to the responses. Together with a noise term which describes all the uncontrollable disturbances in the system, Box and Jenkins [1970] defined a univariate transfer function-noise model for a discrete linear system:

$$y_t = \sum_{k=0}^{\infty} v_k u_{t-k} + N_t$$

$$\triangleq V(B) u_t + N_t \qquad (2.12)$$

with

$$V(B) = \frac{\omega(B)}{\delta(B)} B^b$$

$$= v_o + v_1 B + v_2 B^2 + \ldots \qquad (2.13)$$

where

$V(B)$ is the transfer function with impulse response weights $v_o, v_1, \ldots$

$\omega(B)$, $\delta(B)$ - polynomials of order r and s respectively

b is the dead time or delay

y_t - mean corrected stationary output series

u_t - mean corrected stationary input series

N_t - mean corrected stationary noise term

Similarly, a multivariate transfer function-noise model can be defined (Wilson [1970]) as:

$$\underline{Y}_t = \underline{V}(B)\,\underline{u}_t + \underline{N}_t \qquad (2.14)$$

where

$\underline{Y}_t$ is a (m x 1) vector of outputs

$\underline{u}_t$ is a (n x 1) vector of inputs

$\underline{V}(B)$ is a (m x n) transfer function matrix with the (i,j)-th element given by

$$V_{ij}(B) = \frac{\omega_{ij}(B)\,B^{b_{ij}}}{\delta_{ij}(B)} \qquad (2.15)$$

The multivariate disturbances $\underline{N}_t$ can be modelled by the ARIMA time series models discussed in the previous sections.

The discrete parameters b_{ij}, r_{ij}, s_{ij} of the transfer function and p_i, q_{ij}, d_{n_i} of the noise model, and the continuous parameters $\delta_{ij,k}$, $\omega_{ij,k}$, $\phi_{i,k}$, and $\theta_{ij,k}$ are to be identified from input and output data. The multivariate transfer function model is stable if and only if all the individual transfer functions are stable such that $\delta_{ij}(B)$ has no zero for $|B| \leq 1$. Similarly, the model is invertible if and only if m = n and the determinant of the multivariate transfer function $|\underline{V}(B)|$ has no zero for $|B| \leq 1$. Models can be unstable or non-invertible and in each case a controller is needed to stabilize the closed-loop system. Processes with non-invertible transfer functions are referred to as being non-minimum phase.

In practice, real world processes are very rarely noise-free and thus the inclusion of $\underline{N}_t$ is necessary. These stochastic disturbances will cause the responses to drift away from their operating mean level if left uncontrolled. It is assumed that $\underline{N}_t$ can be modelled independently of the transfer function of the system by the time series models of the last section. Thus, the model equation (2.14) consists of a transfer function model for the dynamic part and a time series model for the stochastic part of the system, as shown in Figure 2.2.

FIGURE 2.2: A SCHEMATIC DYNAMIC-STOCHASTIC PROCESS

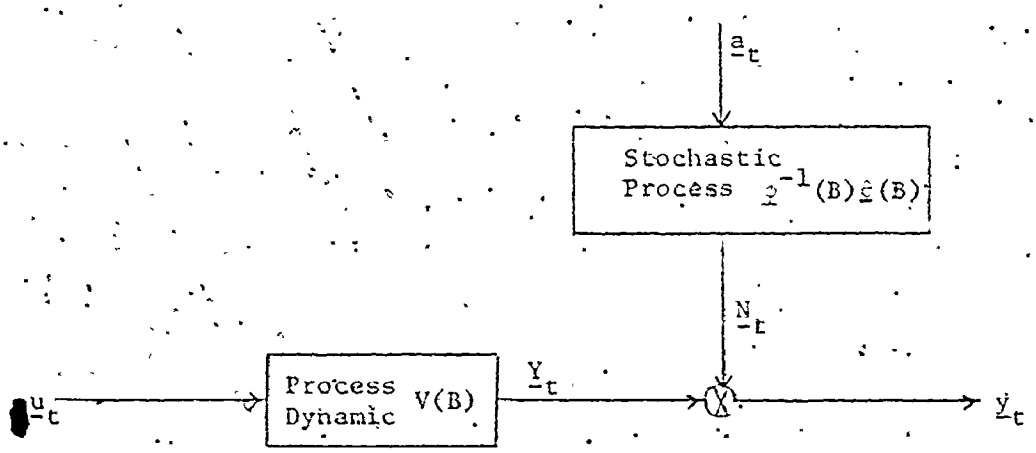

$\underline{Y}_t$ - deterministic output vector, (m x 1)

2.2.2 Identification, Estimation and Diagnostic Checking

(a) Identification of the Transfer Function:

The purpose of transfer function model identification is to determine the impulse response functions and the discrete parameters of the system. Postmultiplying Eq. (2.14) by $\underline{u}_{t-k}^{T}$, summing from $k = -\infty$ to ∞, and taking expectations with the condition that $\underline{N}_t$ and $\underline{u}_t$ are uncorrelated will give the general identification relationship

$$\underline{\Gamma}_{yu}(B) = \underline{V}(B)\ \underline{\Gamma}_{u}(B) \qquad (2.16)$$

where

$\underline{\Gamma}_{yu}(B)$ - cross-covariance matrix generating function between inputs and outputs, and is equal to $\sum_{k=-\infty}^{\infty} \underline{\Gamma}_{yu}(k)B^k$

$\underline{\Gamma}_{u}(B)$ - autocovariance matrix generating function of inputs, $= \sum_{k=-\infty}^{\infty} \underline{\Gamma}_{u}(k)B^k$

The procedure will start with the construction of univariate output and multivariate input systems. Three approaches to identify $\underline{V}(B)$ using Equation (2.16) are mentioned by Wilson [1970] - linear regression, prewhit-ening and spectral analysis. Only the prewhitening method will be presented here. The essence of this approach is to transform the input with known stochastic structure into a white noise sequence. A time series model is identified for the inputs such that

$$\underline{\tau}(B)\cdot\underline{u}_t = \underline{\alpha}_t \qquad (2.17)$$

where

$$\underline{\pi}(B) = \underline{\theta}^{-1}(B)\ \underline{\phi}(B)$$

Substituting Equation (2.17) into the transfer function model Equation (2.14) gives

$$\underline{y}_t = \underline{V}(B)\ \underline{\pi}^{-1}(B)\ \underline{\alpha}_t + \underline{N}_t$$

$$= \underline{U}(B)\ \underline{\alpha}_t + \underline{N}_t \qquad (2.18)$$

With the cross-covariance generating function $\underline{\Gamma}_{y\alpha}(B)$ and residual dispersion matrix $\underline{D}_\alpha$ formed

$$\underline{U}(B) = \underline{\Gamma}_{y\alpha}(B)\ \underline{D}_\alpha^{-1} \qquad (2.19)$$

Thus,

$$\underline{V}(B) = \underline{\Gamma}_{y\alpha}(B)\ \underline{D}_\alpha^{-1}\ \underline{\pi}(B) \qquad (2.20)$$

With the impulse response function $V_{ij,k}$ of each pair of input-output determined, the appropriate order of the $\omega_{ij}(B)$, $\delta_{ij}(B)$ operators and the delay order b_{ij} can be obtained. The $\underline{N}_t$ series can then be regenerated from Equation (2.14) and its stochastic structure identified separately by the methods of Section 2.1.2.

The advantages of transfer function model identification by prewhitening have been pointed out by Box and Jenkins [1970], and Wilson [1970]. The only significant disadvantage is the need of prior knowledge about the input structure. Since the input stochastic structure of many processes are quite simple and the identification is relatively easy, the prewhitening approach is recommended for

preliminary transfer function identification.

(b) Preliminary Estimation and Checking of the Transfer Function Model:

Rewriting the i-th row of Equation (2.14) with the discrete parameters properly identified,

$$y_{i,t} = \sum_{j=1}^{n} \frac{\omega_{ij}(B)}{\delta_{ij}(B)} u_{j,t-b_{ij}} + N_{i,t} \quad i = 1, \ldots, m \qquad (2.21)$$

and representing each $N_{i,t}$ by a univariate time series model

$$\phi_i(B) \nabla^d N_{i,t} = \theta_i(B) e_{i,t} \qquad (2.21a)$$

Equation (2.21) represents a multivariate input, univariate output model. The error terms $e_{i,t}$ for each output i is regenerated from Equation (2.21) and (2.21a) for any choice of the parameters. The non-linear least square estimation algorithm will be used, which minimizes $\sum_{t=1}^{\tau} e_t^2$. This algorithm resembles the univariate case except there are more than one input.

Two earlier assumptions form the basis of the model diagnostic checks:

(1) The input white noise $a_{j,t}$ and the output residuals $e_{i,t}$ ($i = 1, 2, \ldots, m$; $j = 1, 2, \ldots, n$) should not be cross-correlated.

(2) The residual sequences $e_{i,t}$ should be approximately a white noise sequence, which implies that they should not be autocorrelated.

The sample cross-correlations $r_{e\alpha,ij}(k)$ and sample autocorrelations $r_{e,ii}(k)$ can be tested by comparing them with their approximate 95% probability limits $\pm 2/\sqrt{T}$ and by computing the statistics

$$\chi^2_{e\alpha,ij} = T \sum_{k=1}^{K} r^2_{e\alpha,ij}(k) \qquad (2.22)$$

and

$$\chi^2_{e,ii} = T \sum_{k=1}^{K} r^2_{e,ii}(k) \qquad (2.23)$$

which should be distributed as Chi-square distributions with $(K - s_{ij} - r_{ij} - 1)$ and $(K - p_i - q_i)$ degrees of freedom, respectively if the model is adequate.

Proper model modification, if necessary, can be achieved by examining the resulting $r_{e\alpha,ij}(k)$ and $r_{e,ii}(k)$. If the transfer function is inadequate, there will be both significant cross-correlations and autocorrelations. When the transfer function model is correct but the noise model is inadequate, then significant autocorrelations should be observed. Model improvement can then be adjusted accordingly.

(c) Identification of the Multivariate Noise Model:

When the models Equation (2.21) have been correctly fitted and checked, the multivariate noise model can then be constructed. Cross-correlations between output disturbances series are first tested. Sample cross-correlations $r_{e,ij}(k)$ between the univariate residual series $e_{i,t}$'s are compared with their standard error $1/\sqrt{T}$. If $r_{e,ij}(k)$ are not greater than expected, the disturbances may be pure output series

measurement error and the multivariate model will be a combination of all multi-inputs, univariate output models. However, in many cases, if there are unmeasured and uncontrollable disturbances affecting all output series simultaneously, output noise series will then have significant cross-correlations and the $\underline{\theta}(B)$ operators of the stochastic model have to be re-estimated. Following the procedure outlined in Section 2.1.2, the $\underline{\phi}(B)$ operators are chosen to be diagonal with $\phi_{i,k}$ parameters from the univariate output model (2.21). The intermediate series $\underline{b}_t$ are again regenerated as before. For estimation, the identified diagonal $\theta_{i,k}$ parameters are retained and the $\theta_{ij,k}$ $(i \neq j)$ parameters are initially set to zero. The multivariate noise model can then be obtained through estimation and the diagnostic checking.

(d) Estimation and Diagnostic Checking of the Multivariate Dynamic-Stochastic Model:

The multivariate transfer function and multivariate noise models are combined for the final model fitting. All the parameters are re-estimated along with the new $\theta_{ij,k}$ parameters, although they are not expected to change significantly. The transfer function model should remain approximately the same since it is not adjusted. Multivariate residuals $\underline{a}_t$ are regenerated and are passed for parameter estimation by non-linear least squares fit. Wilson's algorithm [1970] in Section 2.1.2 can again be used to obtain the maximum likelihood estimates of the parameters by minimizing $\left| \sum_{t=1}^{T} \underline{a}_t \underline{a}_t^T \right|$, i.e. to minimize the

FIGURE 2.3: MULTIVARIATE TRANSFER FUNCTION - NOISE MODEL BUILDING

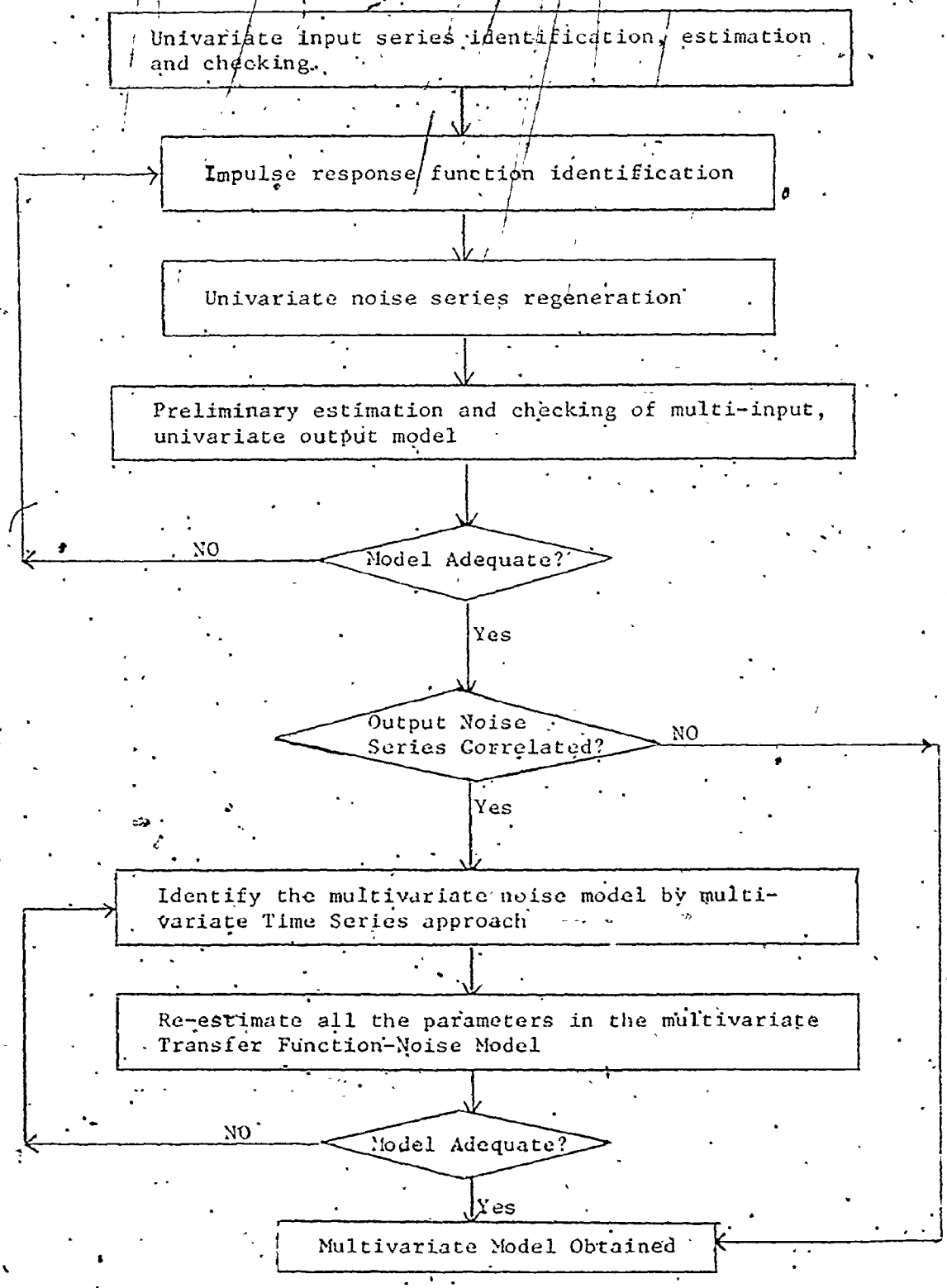

determinant of the variance-covariance matrix of the computed $\underline{a}_t$ vector. A computer program written for estimation and later modified by Jutan [1976] was used to carry out the estimation. The same tests as in (b) are used for model adequacy checking.

It should be noted that the above procedure is only a general guide for multivariate dynamic-stochastic model building and one need not follow the step by step construction strictly. Rather, good judgement is essential and some of the intermediate steps can be skipped without jeopardizing the model building. The procedure should be followed discreetly, depending on the particular process being studied. An algorithm of the whole procedure is illustrated in Figure 2.3.

2.3 Example

An example employing the model building technique described in the two previous sections is presented here. A two-input, two-output model was simulated with known random variable series, input series, and stochastic-dynamic structure. The time model has the following form:

$$\begin{bmatrix} y_{1,t} \\ y_{2,t} \end{bmatrix} = \begin{bmatrix} \left(\frac{10 - B}{1 - 0.5\,B}\right) B^2 & 2B \\ \left(\frac{3 + B}{1 - 0.8\,B}\right) B & \left(\frac{2}{1 - 0.3\,B}\right) B \end{bmatrix} \begin{bmatrix} u_{1,t} \\ u_{2,t} \end{bmatrix} + \begin{bmatrix} N_{1,t} \\ N_{2,t} \end{bmatrix} \quad (2.24)$$

$$\begin{bmatrix} 1 - 0.3\,B & 0 \\ 0 & 1 - 0.8\,B \end{bmatrix} \begin{bmatrix} N_{1,t} \\ N_{2,t} \end{bmatrix} = \begin{bmatrix} 1 + 0.2\,B & 0.5\,B \\ 0 & 1 \end{bmatrix} \begin{bmatrix} a_{1,t} \\ a_{2,t} \end{bmatrix} \quad (2.25)$$

With residual dispersion matrix

$$\underline{D} = E\,(\underline{a}_t \underline{a}_t^T) = \begin{bmatrix} 6 & 3 \\ 3 & 4.5 \end{bmatrix}$$

With only the input and output series, the procedure of identification, estimation and diagnostic checking were performed. Detailed step by step model construction is given in Appendix 1. The final fitted model based on these simulated input-output data is shown below, with parameter values corrected to 2 decimal places.

$$\begin{bmatrix} y_{1,t} \\ y_{2,t} \end{bmatrix} = \begin{bmatrix} \left(\frac{10 - 0.97\,B}{1 - 0.50\,B}\right) B & 2.02\,B \\ \left(\frac{3.03 + 1.03\,B}{1 - 0.80\,B}\right) B & \left(\frac{2.0}{1. - 0.31\,B}\right) B \end{bmatrix} \begin{bmatrix} u_{1,t} \\ u_{2,t} \end{bmatrix} + \begin{bmatrix} N_{1,t} \\ N_{2,t} \end{bmatrix} \tag{2.26}$$

$$\begin{bmatrix} 1 - 0.44\,B & 0 \\ 0 & 1 - 0.85\,B \end{bmatrix} \begin{bmatrix} N_{1,t} \\ N_{2,t} \end{bmatrix} = \begin{bmatrix} 1 & 0.54\,B \\ 0 & 1. - 0.10\,B \end{bmatrix} \begin{bmatrix} a_{1,t} \\ a_{2,t} \end{bmatrix} \tag{2.27}$$

$$\underline{D} = \begin{bmatrix} 6.05 & 2.52 \\ 2.52 & 3.93 \end{bmatrix}$$

A comparison of the true and fitted models shows excellent agreement. It should be emphasized that the author had no prior knowledge of the model structure before building the above model. Some comments can be drawn from this example.

The fitted transfer function agrees very well with the true form, probably because the signal to noise ratio is fairly large in this study. In fact, the ratio of the standard deviation of the output signal to its corresponding noise series is about 15 and 3 respectively. Experience has shown that most model building difficulties are due to the stochastic part of the model. Since the representation of the stochastic behaviour of the model is not unique, various model forms can describe the noise series adequately.

The designed input series u_t were uncorrelated white noise sequences, as confirmed by the identification. This simplified input series makes the model building procedure a little easier. In practice, whenever possible, the input series are designed to be uncorrelated. Its advantages are pointed out by Box and Jenkins [1970]. Thus, the choice of uncorrelated random variables as input in this example is reasonable. Although the model is relatively simple, this test does demonstrate that these model building techniques are capable of leading to the identification of a reasonable process dynamic-stochastic model from input-output data only.

2.4 Alternative Representation in State Space Model Form

2.4.1 General Formulation

State-space model development was made popular by Kalman [1963] who expressed the dynamic of the system by a set of linear first order ordinary differential equations

$$\dot{\underline{x}}(\tau) = \underline{A}\,\underline{x}(\tau) + \underline{B}\,\underline{u}(\tau)$$

$$\underline{y}(\tau) = \underline{H}\,\underline{x}(\tau) \qquad (2.28)$$

where

$\underline{A}$, $\underline{B}$, $\underline{H}$ - parameter matrices; τ - continuous time

$\underline{x}$ - (λ x 1) vector of state variables

$\dot{\underline{x}}$ - time derivative of $\underline{x}$

$\underline{u}$ - (n x 1) vector of manipulated input variables

$\underline{y}$ - (m x 1) vector of measured output variables

Physical equations from theoretical mass and energy balances are generally used to describe the dynamic behaviour of the process. These equations can usually be reduced and transformed into sets of purely deterministic ODE's as in Equation (2.28). Mechanistic models are frequently expressed in continuous time and then discretized if necessary by integration over the sampling interval.

An extension to include the stochastic disturbances produces the stochastic discrete linear state-space model Equation (2.29) capable of representing the input-output characteristics of many industrial processes

$$\underline{x}(t+1) = \underline{A}\,\underline{x}(t) + \underline{G}\,\underline{u}(t) + \underline{\Gamma}\,\underline{a}(t)$$

$$\underline{y}(t) = \underline{H}\,\underline{x}(t) + \underline{a}(t) \qquad (2.29)$$

where

$\underline{\Gamma}$ is a parameter matrix

$\underline{a}(t)$ is a vector of white noise sequence.

The whole system is represented by ℓ first order difference equations in the state variable $\underline{x}(t)$. These state variables are abstract quantities which may have physical meanings about the system. Upon close examination, they are made up of two groups - those states $\underline{x}^{+}(t)$ that identify to the dynamic part, the so called 'controllable' and 'observable' states; and those representing the stochastic part, the 'observable' but 'uncontrollable' states $\underline{x}^{*}(t)$.

Another commonly used equivalent linear discrete state-space model form is:

$$\begin{aligned} \underline{x}(t+1) &= \underline{A}\,\underline{x}(t) + \underline{G}\,\underline{u}(t) + \underline{w}(t) \\ \underline{y}(t) &= \underline{H}\,\underline{x}(t) + \underline{v}(t) \end{aligned} \tag{2.30}$$

where

$\underline{w}(t)$ - (ℓ^{*} x 1) vector white noise sequence due to disturbances and modelling error

$\underline{v}(t)$ - (n' x 1) vector white noise sequence due to measurement error

$\underline{w}(t)$ and $\underline{v}(t)$ are assumed independent of each other, with variance-covariance:

$$\begin{aligned} E(\underline{w}_t\,\underline{w}_t^{T}) &= R_1 \\ E(\underline{v}_t\,\underline{v}_t^{T}) &= R_2 \\ E(\underline{w}_t\,\underline{v}_{t+j}^{T}) &= \underline{0} \quad \text{for all } j \end{aligned} \tag{2.31}$$

This form is widely adopted in literature of filtering theory, yet, it is not uniquely identifiable from input-output data alone (MacGregor [1973]). The conversion between Equation (2.29) and (2.30) can be carried out easily.

2.4.2 Transformation from Transfer Function Form to State Variable Form

The transformation to discrete state model from transfer function form is obtained by the realization of the rational transfer function matrix into a minimal dimensional system of difference equations (Equation (2.29)). This minimal realization is known to be controllable and observable (Sinha and Rozsa [1974]) and many methods are available for the transformation. Sinha [1975] classified these methods into 3 main groups:

(a) Methods starting with non-minimal realization forms which are then reduced to get a realization that is both controllable and observable (Ho and Kalman, [1965]).

(b) Methods starting with the Markov parameters of system and then obtaining a suitable transformation of the resulting Hankel matrix (Sinha and Rozsa [1974]).

(c) Methods basing on system formulation introduced by Rosenbrock [1970].

A comparison of these three groups indicates that an algorithm proposed by Rozsa and Sinha [1974] requires less computation . A brief description of their algorithm will be presented here.

Consider a strictly proper (m x n) rational transfer function matrix $\underline{V}(s)$ in which m and n are the number of outputs and inputs respectively. The minimal realization procedure is to obtain the matrices, $\underline{A}$, $\underline{B}$ and $\underline{H}$ for a minimum number of states ℓ such that

$$\underline{V}(s) = \underline{H}\ (s\ \underline{I} - \underline{A})^{-1}\ \underline{B} \tag{2.32}$$

The transfer function matrix $\underline{V}(s)$ can be expressed as

$$\underline{V}(s) = \underline{J}_o\ s^{-1} + \underline{J}_1\ s^{-2} + \underline{J}_2\ s^{-3} + \ldots \tag{2.33}$$

where

$$\underline{J}_i = \underline{H}\ \underline{A}^i\ \underline{B} \qquad i = 0,\ 1,\ 2,\ \ldots.$$

The Hankel matrix $\underline{S}_{ij}$ is defined as

$$\underline{S}_{ij} = \begin{bmatrix} J_o & J_1 & \cdots & J_{j-1} \\ J_1 & J_2 & \cdots & J_j \\ \vdots & & & \\ J_{i-1} & J_i & \cdots & J_{i+j-2} \end{bmatrix} \tag{2.34}$$

$$= \begin{bmatrix} H \\ H\,A \\ H\,A^2 \\ \vdots \\ H\,A^{i-1} \end{bmatrix} \begin{bmatrix} B & A\,B & A^2B & \cdots & A^{j-1}B \end{bmatrix} = \underline{V}_i \underline{U}_j$$

$\underline{U}_j$ and $\underline{V}_i$ are the controllability and observability matrices, respectively. The Hankel matrix $\underline{S}_{ij}$ can be transformed into the Hermite normal form by outer product so that $\underline{A}$, $\underline{B}$ and $\underline{H}$ are directly obtainable. Due to the structure of $\underline{U}_j$, the matrix $\underline{B}$ is given by

$$\underline{B} = [\underline{e}_1, \underline{e}_2, \ldots, \underline{e}_n] \tag{2.35}$$

where $\underline{e}$ is a unit vector of dimension ℓ.

The $\underline{H}$ matrix is made up of the first m rows of the ℓ columns of the Hankel matrix $\underline{S}_{ij}$. The columns of matrix $\underline{A}$ are given by the $k + n$ columns of the matrix $\underline{U}_j$, with $k = 1, 2, \ldots, \ell$.

Thus, the basis of this method is to convert the Hankel matrix into its Hermite Normal form from which matrices $\underline{A}$, $\underline{B}$ and $\underline{H}$ can be read off directly. The transformation can be performed systematically in ℓ steps, with ℓ being the rank of the Hankel matrix. Hicklin et al [1976] have written a standard Fortran program for the minimal realization of a linear, time-invariant multivariable system from a strictly proper rational transfer function matrix.

It is noted that most of the formulations are designed for continuous time systems. However, since the transfer function here is discrete, the corresponding discrete state-space model parameters can be evaluated in the same manner.

2.4.3 Representation in State Model Form

The transfer function in Equation (2.14) can be transformed into discrete state-space form (2.29) by the concept of minimal realization of a transfer function matrix. Rewriting the transfer function-noise model (2.14):

$$\underline{y}(t) = \underline{V}(B)\,\underline{u}(t) + \underline{N}(t) \qquad (2.14)$$

which is made up of the stochastic model

$$\underline{N}(t) = \underline{\psi}(B)\,\underline{a}(t) \qquad (2.2)$$

and the deterministic model with output $\underline{Y}(t)$

$$\underline{Y}(t) = \underline{V}(B)\,\underline{u}(t) \qquad (2.36)$$

Equation (2.2) and (2.36) are analogous to a system with two transfer functions $\underline{V}(B)$ and $\underline{\psi}(B)$ with the corresponding inputs $\underline{u}(t)$ and $\underline{a}(t)$. Both $\underline{V}(B)$ and $\underline{\psi}(B)$ can be converted into the state model form. Assuming the dynamic transfer function $\underline{V}(B)$ and the stochastic transfer function $\underline{\psi}(B)$ are both proper or strictly proper rational matrices, that is, if we let $s = B^{-1}$, the degree of the polynomial in terms of s at the denominator of the transfer function is greater than or equal to that in the numerator. The linear system is stable when the transfer function matrix is either proper or strictly proper rational, whereas an irrational matrix implies non-stationarity and cannot be realized.

From minimal realization, V(B) can be expressed as

$$\underline{x}^{+}(t+1) = \underline{A}^{+}\,\underline{x}^{+}(t) + \underline{G}^{+}\,\underline{u}(t)$$
$$\underline{Y}(t) = \underline{H}^{+}\,\underline{x}^{+}(t) \qquad (2.37)$$

But the actual observed output is $\underline{y}(t)$ such that

$$\underline{y}(t) = \underline{Y}(t) + \underline{N}(t) \qquad (2.38)$$

Expressing $\underline{N}(B)$ into state model form,

$$\underline{x}^{*}(t+1) = \underline{A}^{*}\,\underline{x}^{*}(t) + \underline{B}^{*}\,\underline{a}(t)$$
$$\underline{N}(t) = \underline{H}^{*}\,\underline{x}^{*}(t) \qquad (2.39)$$

Incorporate $\underline{Y}(t)$ and $\underline{N}(t)$ in Equation (2.37) and (2.39) into Equation (2.38):

$$\begin{bmatrix} \underline{x}^{+}(t+1) \\ \hline \underline{x}^{*}(t+1) \end{bmatrix} = \left[\begin{array}{c|c} \underline{A}^{+} & 0 \\ \hline 0 & \underline{A}^{*} \end{array}\right] \begin{bmatrix} \underline{x}^{+}(t) \\ \hline \underline{x}^{*}(t) \end{bmatrix} + \begin{bmatrix} \underline{G}^{+} \\ \hline 0 \end{bmatrix} \underline{u}(t) + \begin{bmatrix} 0 \\ \hline \underline{B}^{*} \end{bmatrix} \underline{a}(t) \qquad (2.40)$$

and

$$\underline{y}(t) = \left[\begin{array}{c|c} \underline{H}^{+} & \underline{H}^{*} \end{array}\right] \begin{bmatrix} \underline{x}^{+}(t) \\ \hline \underline{x}^{*}(t) \end{bmatrix}$$

Equation (2.40) is a general complete representation of the multivariate transfer function-noise model in discrete state variable form.

2.4.4 Advantages and Disadvantages

The state space model has the advantage of unifying the representational form for linear dynamic-stochastic processes. For different linear systems, the state form is standard and only the parameter matrices have to be changed. The model unity is a great advantage in subsequent control and filtering calculations. Due to the first order difference equation form and its stagewise characteristic, the concept of dynamic programming can be introduced for optimal stochastic controller and filter designs. These equations are easily solved iteratively on digital computers. The state model is particularly suitable to the optimal stochastic control development on multi-input-output- systems where the derivation of control scheme from the transfer function-noise model is quite tedious.

On the other hand, the state representation does not usually provide the insight and understanding of the process and noise that is provided by transfer function ARIMA model. Identification of state space model is difficult and the estimation of parameters requires extensive knowledge about the process dynamics. It is much easier to identify the model structure from input-output data in the transfer-function ARIMA model form.

Traditional state modelling concerns mainly the dynamic part of the system . The stochastic representation of the disturbances is added as a hindsight to compensate for observed drifting. The combined model is required to describe the process.

The modelling choice between state model and transfer function-noise form is a matter of convenience since they can equally well represent the linear dynamic-stochastic systems. In this thesis, a compromised modelling approach is proposed. Both model forms are used to complement each other's deficiencies. In short, a multivariate transfer function-noise model is developed with plant empirical input-output data. This will provide a good understanding of the dynamic-stochastic behaviour of the process. This model is then transformed into the state variable form as in Equation (2.40). An optimal stochastic controller is then derived using filtering theories and dynamic programming. The detail modelling and control design procedure will be presented in Chapters 4 and 5.

CHAPTER 3

PROCESS REACTOR AND COMPUTER SYSTEM

An overall review of the pilot plant catalytic packed bed n-butane hydrogenolysis reactor system is presented here for completeness. Detailed information of instrumentation, equipment dimensions and construction, and calibrations are given by Tremblay [1977] who built and interfaced this reactor system. Figure 3.1 shows the configuration.

FIGURE 3.1: OVERALL CONFIGURATION OF REACTOR SYSTEM AND COMPUTER

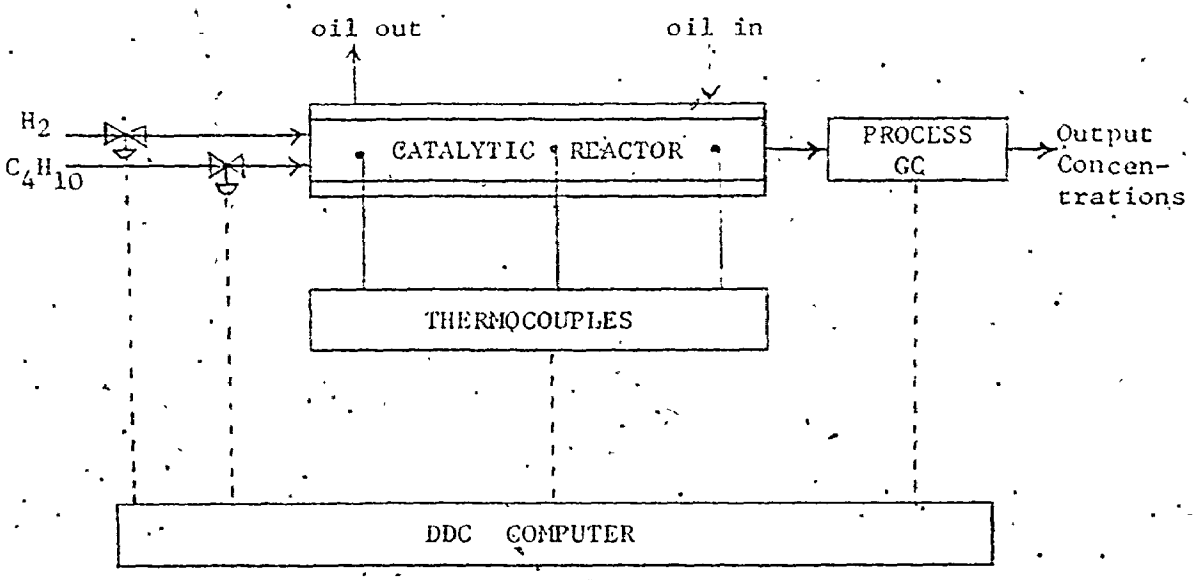

Very briefly, the following sections deal with the reactor kinetics, the reactor and its flow networks, the DDC computer and the interfacing between computer and process.

3.1 Reaction System Kinetics

The reaction being investigated is the catalytic hydrogenolysis of n-butane with excess hydrogen over a nickel-silica gel catalyst. The components in the exit product stream consist of methane, ethane, propane, unreacted butane and hydrogen. The reactions occur at high temperature environment and are highly exothermic.

The selection of this particular reaction scheme is due to the following reasons. Firstly, the chemical reaction kinetics are complex and also highly exothermic, exhibiting characteristics similar to many industrial catalytic packed bed reactions. The prime concern is to model and control a complex process resembling those industrial processes. Thus, various modelling techniques and the applicability of most modern control theories can be tested. Secondly, the kinetics of n-butane hydrogenolysis had been extensively studied (Orlikas [1970], Shaw [1974]). The understanding of the reactions provides great help during reactor modelling, though this is not strictly compulsory in this work. Also the analysis of product stream using gas chromatography techniques is relatively simple and well documented. All these factors favour the selection of this scheme for control studies.

An overall reaction mechanism for the hydrogenolysis of n-butane is shown in Figure 3.2.

The corresponding hydrogenolysis reactions can be represented by six equations of which only three are independent.

FIGURE 3.2: OVERALL REACTIONS SCHEME

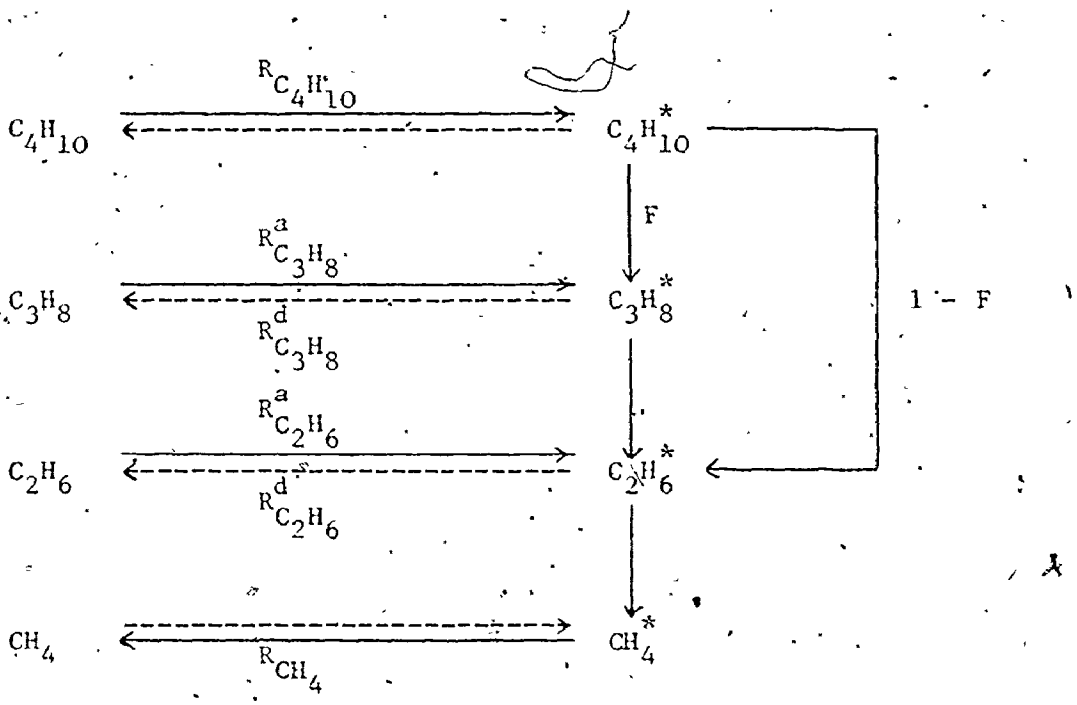

where

R – rate of production

R^d – rate of desorption

R^a – rate of adsorption

F – fraction of $C_4H_{10}^*$ that cracks to $C_3H_8^*$

$\longrightarrow$ – reaction path

$\dashrightarrow$ – assumed 0

$$
\begin{aligned}
C_4H_{10} + H_2 &\longrightarrow C_3H_8 + CH_4 \\
C_4H_{10} + H_2 &\longrightarrow 2\,C_2H_6 \\
C_3H_8 + H_2 &\longrightarrow C_2H_6 + CH_4 \\
C_2H_6 + H_2 &\longrightarrow 2\,CH_4 \\
C_4H_{10} + 3\,H_2 &\longrightarrow 4\,CH_4 \\
C_3H_8 + 2\,H_2 &\longrightarrow 3\,CH_4
\end{aligned}
\qquad (3.1)
$$

The reaction scheme in Figure 3.2 is based on two assumptions:

(1) Butane and Propane are absorbed on the catalyst surface before the reactions take place.

(2) The reaction products may react further or be desorbed.

An additional assumption suggests the conversion of butane and propane directly to methane does not occur because of the low probability of breaking two or three carbon bonds simultaneously. In this case, the last two reactions in Set (3.1) will not occur.

The overall rate balance of the six reactions is

$$R_{H_2} = 3\,R_{C_4H_{10}} - 2\,R_{C_3H_8} - R_{C_2H_6} \qquad (3.2)$$

3.2 Reactor Flow System and Networks

3.2.1 Reactor, Process Gases and Coolant Network

The reactor system was built by Tremblay [1970]. The process system consists of three main components: the packed bed tubular reactor, reactant flow system and the coolant network. For completeness, each of them will be discussed briefly in turn.

(1) Pilot Plant Tubular Packed Bed Reactor:

A detailed layout of the reactor is shown in Figure 3.3. It consists of two concentric sections of stainless steel pipe with diameters 1.5 and 2 in. respectively; and the inner tube is 28 cm. long. Nine chromel-alumel thermocouples are located along the reactor axis and three at the radial positions. The exact distribution of these thermocouples is shown in Table 3.1 a-b. The inner reactor tubes can be removed from the system through a gland at the top end. At either end are two plugs of steel rod and disks. The upper porous disk allows the distribution of reactant gases while the lower disk serves as a support for the catalyst. The bottom end is filled with inert silica gel to avoid direct contact of catalyst with the support disk, thus eliminating end effects. Coolant oil enters from the bottom and flows counter-currently in the annulus. The catalyst used is nickel on refrigeration grade silica gel, which is of approximately spherical shape. The preparation of this catalyst is outlined by Tremblay [1977].

FIGURE 3.3: SCHEMATIC LAYOUT OF THE TUBULAR PACKED BED REACTOR

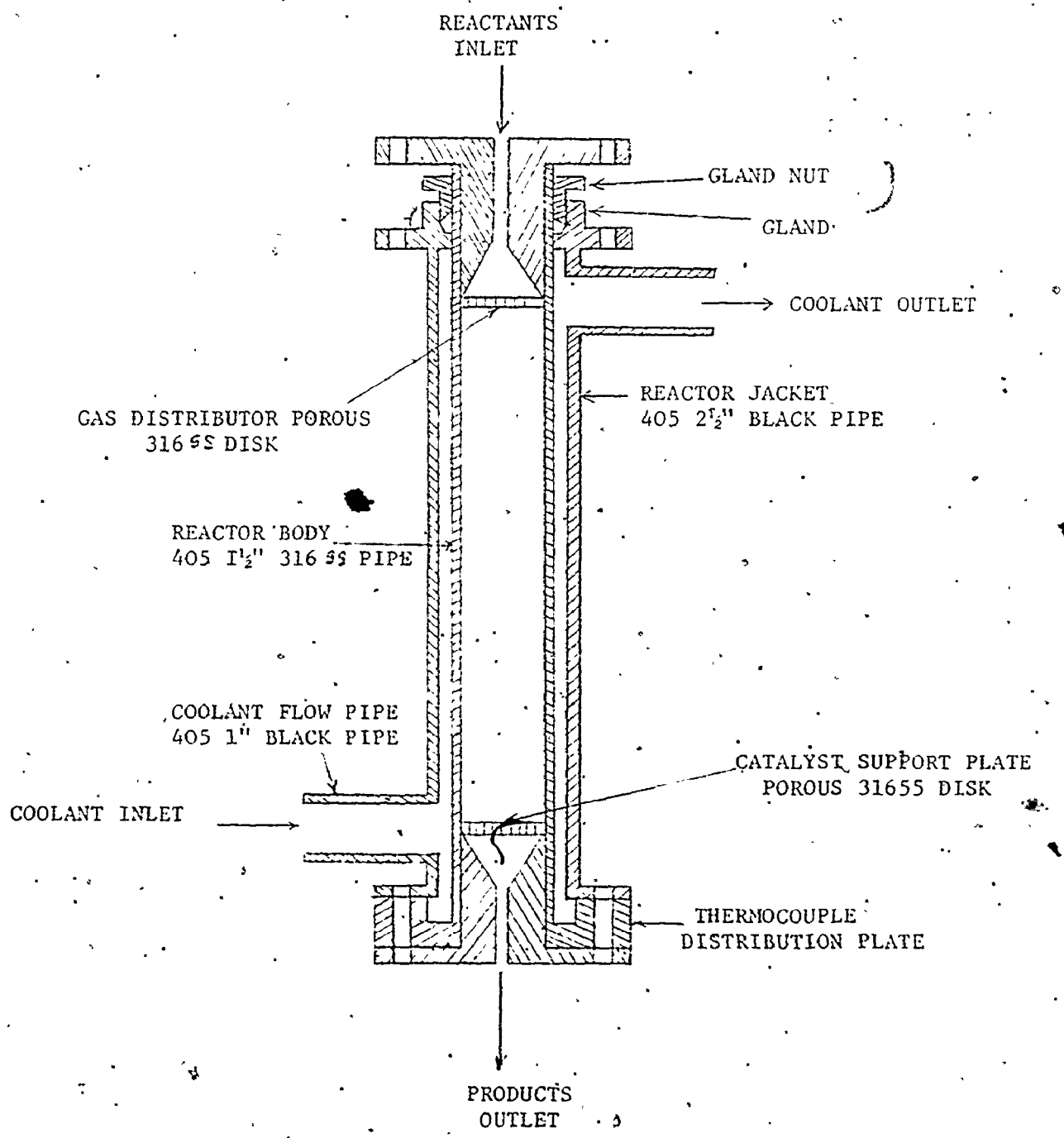

(2) Reactant Flow Network:

Figure 3.4 shows the schematic flow diagram of the reactant network. Four flow paths can be basically identified - the main path to the reactor, two paths for flow calibrations and the last for flushing the reactor with hydrogen. The input flowrates were determined from the pressure drops across a calibrated flowmeter, measured by a differential pressure transmitter. The maximum flowrates of n-butane and hydrogen can reach 30 and 160 cm^3/sec respectively at STP.

The gases are first mixed, flow through a back pressure regulator and the stream can then be directed into 3 sections of the system:

(a) during calibration, it is directed to the flowmeter calibration station;

(b) prior to plant startup, it is bypassed and vented;

(c) during operation, it is conveyed to the reactor.

During operation, the feed stream is preheated by an electrical heater before entering the reactor. The downstream pressure of the reactor is maintained by another back pressure regulator so that part of the exit product could be 'pushed' to the gas chromatograph.

The main gas supplies are pure hydrogen and n-butane. Hydrogen is needed for the reactor, calibrated mixture preparation station and the catalyst condition unit; and also acts as a carrier gas for the

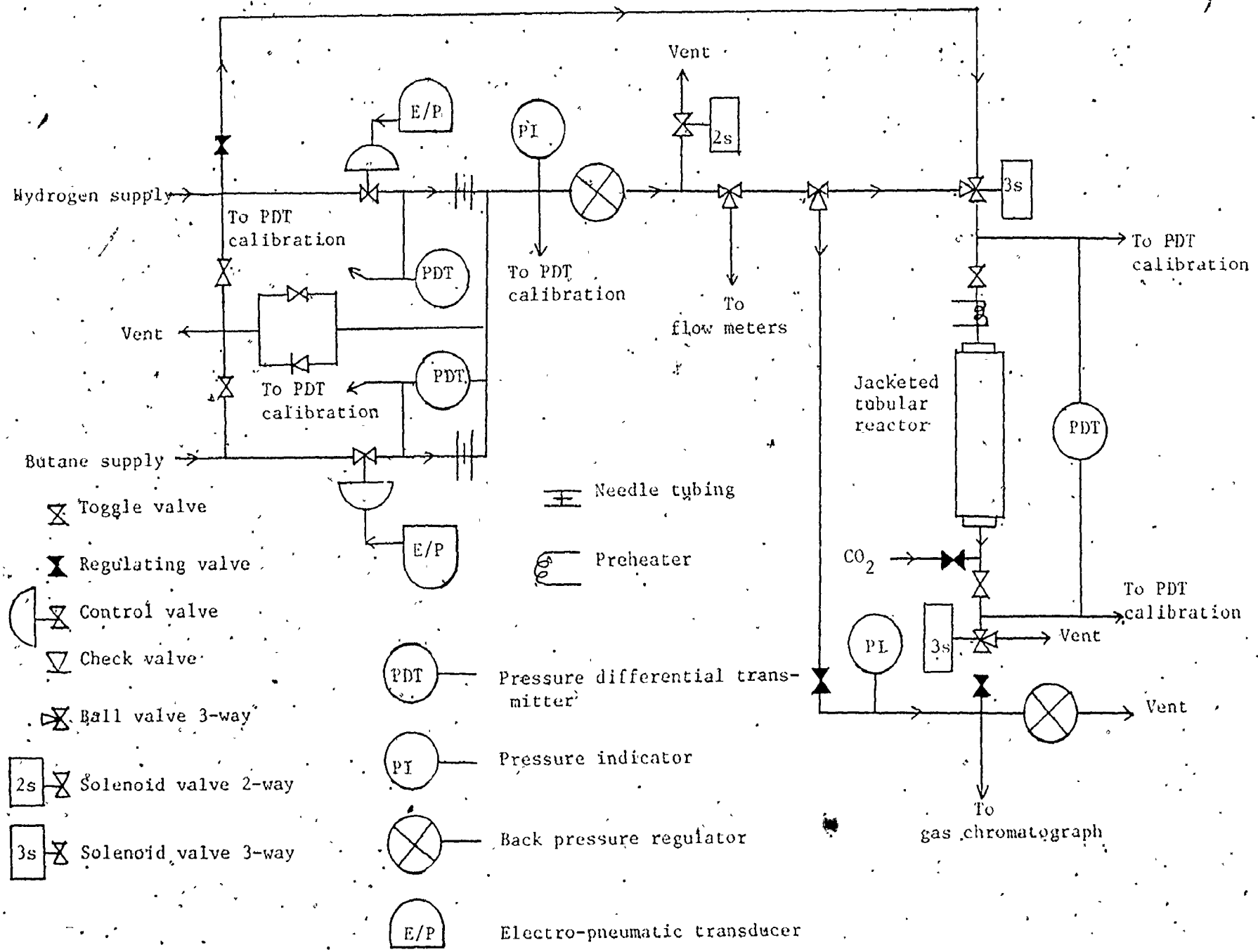

FIGURE 3.4: REACTANTS FLOW NETWORK

process gas chromatograph. n-Butane is required in the reactor and the calibrated mixture preparation station which in addition needs methane, propane and ethane gas. Carbon dioxide is necessary for the preparation of catalyst and its storage. An air supply is required for the heat exchanger of the coolant oil system, the gas chromatograph, the E/P transducers to actuate control valves and also the catalyst condition unit.

(3) Coolant Network:

The circulating coolant oil serves to maintain contstant reactor wall temperature and also initiate the reaction at start-up. A schematic flow diagram of the coolant system is in Figure 3.5. The coolant flow is continuously circulated at a constant rate by a centrifugal pump equipped with high temperature gland and gasket materials. The oil flows through the shell side of a single pass heat exchanger and is cooled by 25 psig. compressed air at the tube side. After passing through a flexible pipe which reduces thermal stress, it enters the jacket of the reactor. The exit coolant is heated by six electrical resistance heaters which have an overall capacity of about 6 kilowatts using low voltage, high current AC source.

The head tank has a capacity of about three imperial gallons. It serves as an expansion chamber for the oil during reactor startup, and also keeps the coolant system topped with oil. To ensure that the tank remains cool during high temperature reaction, a water cooler is installed. Five thermocouples are located at different positions in the coolant network and are indicated in Table 3.2. Detailed procedure

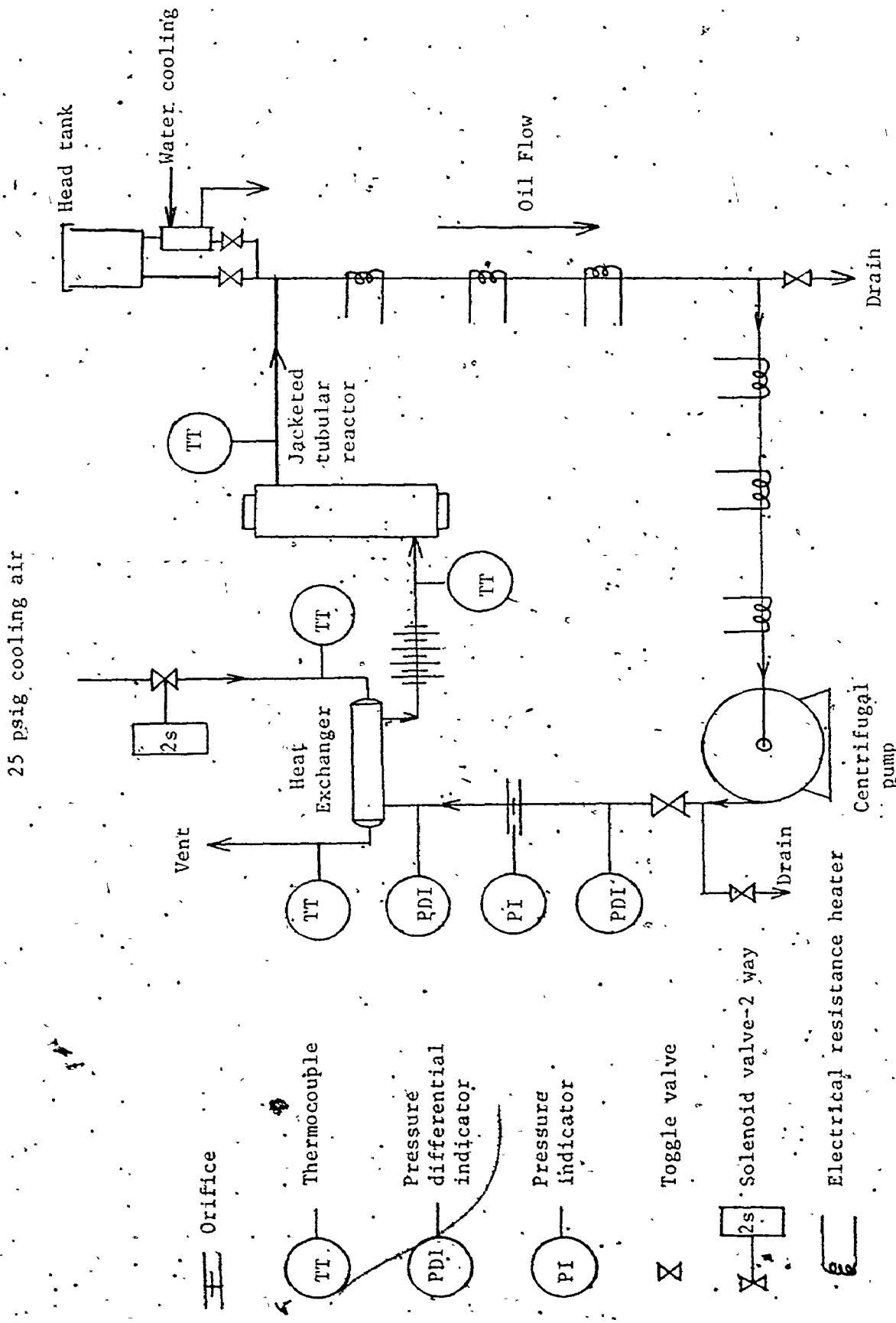

FIGURE 3.5: CIRCULATING COOLANT FLOW NETWORK

in the reactor startup, normal operations and shutdown sequence are given by Tremblay [1977].

TABLE 3.1a: LOCATIONS OF AXIAL THERMOCOUPLES ALONG REACTOR

Temperature Number	Thermocouple Temperature	Location, In. from Bottom Support	Normalized Axial Position from Support
T_9	T10	0.50	0.046
T_8	T6	1.75	0.159
T_7	T15	3.00	0.273
T_6	T18	4.25	0.386
T_5	T12	5.50	0.500
T_4	T9	6.75	0.614
T_3	T7	8.00	0.727
T_2	T13	9.25	0.841
T_1	T16	10.50	0.955

TABLE 3.1b: LOCATIONS OF RADIAL THERMOCOUPLES IN REACTOR

Thermocouple Temperature	Location, In. from Bottom Support	Normalized Position on Radial Direction
T8	5.50	0.60
T14	8.00	0.60
T17	1.75	0.60

TABLE 3.2: LOCATIONS OF THERMOCOUPLES ALONG COOLANT SYSTEM

Thermocouple Temperature	Locations
T1	Oil inlet of heat exchanger
T2	Air inlet of heat exchanger
T3	Air outlet of heat exchanger
T4	Oil inlet of reactor
T21	Oil outlet of reactor

3.2.2 Gas Chromatograph and Programmer

Frequently, gas chromatography is used to analyze the composition and distributions of the product stream. The gas chromatograph system employed here is the Beckman Instruments Inc. model 6700 Process Chromatograph equipped with thermal conductivity detector (Operation Manual [1973]). It consists of an analyzer and a programmer which can be interfaced to a computer. The programmer provides a control signal to operate the analyzer where products analysis is taking place.

Two different streams from the reactor system are usually fed to the chromatograph: a hydrocarbon gaseous mixture of known composition used for calibration and the effluent stream from the reactor exit. The analytical strategy was devised by Tremblay [1977]. Basically, hydrogen gas is adopted as the carrier gas. The relative mole fractions of hydrocarbons from a calibrated mixture and the carbon to hydrogen ratio in the feed stream enable the determination of product composition . This strategy is valid provided that a feed flow change does not occur within 3 seconds before sample injection.

A scheme for the analysis of methane, ethane, propane and butane is shown in Figure 3.6. A dual column, ten port valve and detector are in the analyzer. The sample (about 0.8 cm^3) is injected into column 1. The analysis cycle starts one second after the injection and valve A is energized. All the lighter components, methane and ethane enter column 2 after 39 seconds. Valve B is then energized, trapping methane and ethane inside column 2. Propane and

butane can then flow to the detector for analysis. At 199 seconds after the analysis cycle starts, valve B is de-energized, allowing methane and ethane to be analyzed. The whole cycle takes 360 seconds. Valve A will then be de-energized, picking up a new sample and a new cycle restarts. Table 3.3a and 3.3b indicate the time for the opening of valves and components analysis in the analyzer.

TABLE 3.3a: VALVE TIME (SECONDS)

Mode / Valve	Energized	De-energized
A	2	85
B	40	200

0 Second - Time for Injection

TABLE 3.3b: COMPONENT ANALYSIS TIME

Mode / Component	On	Off
Propane	45	80
Butane	108	199
Methane	217	280
Ethane	296	345

0 Second - Analysis Cycle Starts

FIGURE 3.6: ANALYZING SCHEME FOR PRODUCT STREAM

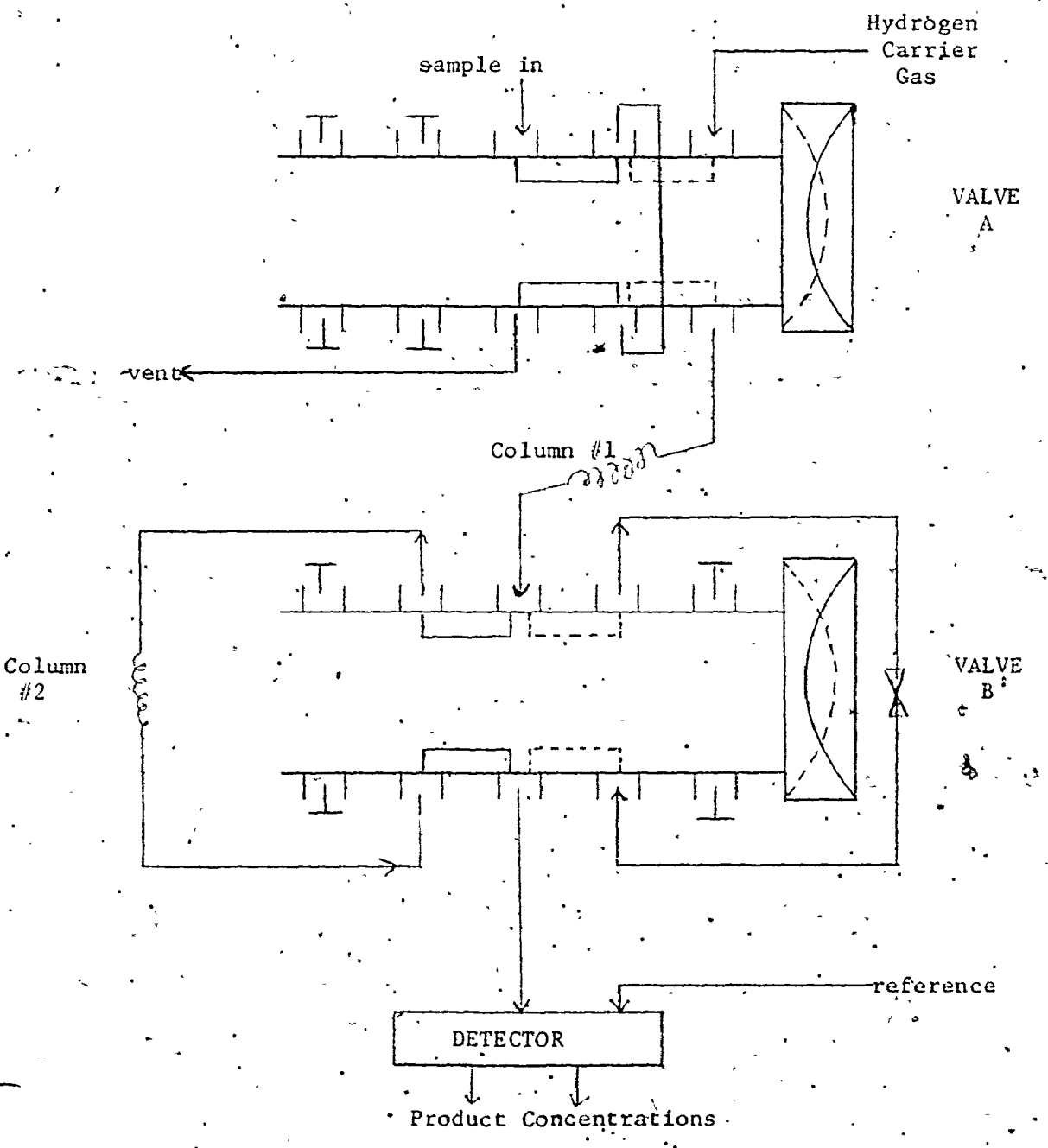

3.3 Mini-Computer System and Programming

3.3.1 Configuration of Process Control Computer

A layout of the computer facilities in the Chemical Engineering Process Control Laboratory of McMaster University at the time of this study is given in Figure 3.7. A dual process computer system consisting of a Nova 1200 and a Nova 2/10 computer is supported by Data General Corporation's Real Time Disk Operating System (RDOS). They share a 256 K fixed head disk without the interprocessor bus (IPB). Each computer consists of 32 K words of 16 bits central processor memory, real time clock and powerfail monitor. Peripheral devices attached to the system include two teletypes, a high speed paper tape reader and paper tape punch, and a lineprinter. More recently, two new fixed head disks (shown by dotted lines) were added and connected to the Nova 2/10 computer, increasing the flexibility and bulk storage capacity of the system tremendously.

The Nova 2/10 is configured for control applications while the Nova 1200 is mainly for program development and debugging. Interfacing devices to the Nova 2/10 include 16 channels of analog input multiplexed into a single 10 bit ADC, 16 contact sense inputs, 16 relay outputs and 6 channels of analog output from a 10 bit DAC. Both assembler language and real time Fortran IV program are used for control studies. A user-process communication executive program package has been developed for on-line control and data acquisition.

FIGURE 3.7: CONFIGURATION OF COMPUTER SYSTEM AT McMASTER UNIVERSITY

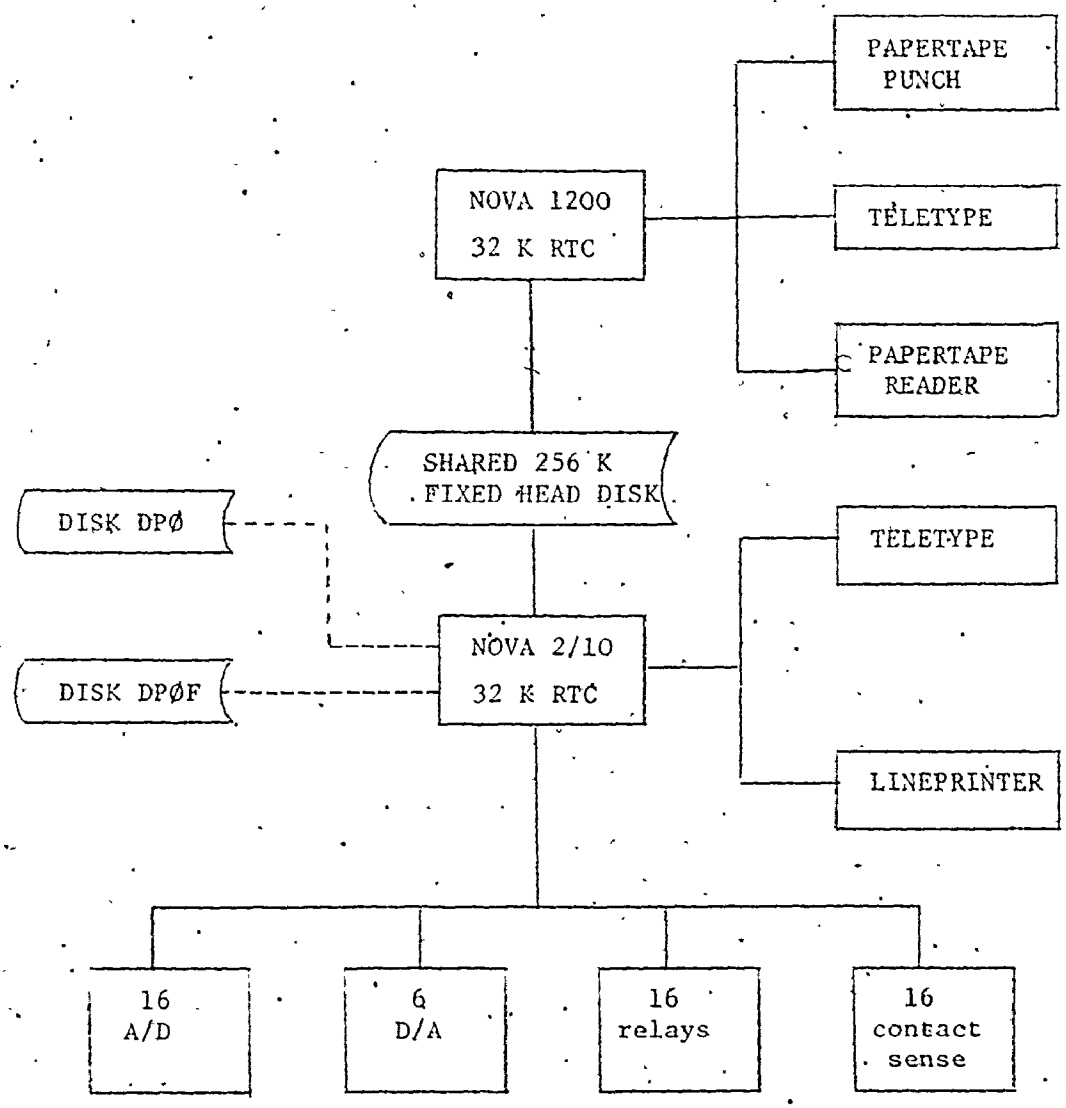

3.3.2 Real Time Programming

The details and structure of assembler and Fortran IV computer languages and the RDOS are given in the respective operating manuals [1975]. In control studies, on-line communication such as data logging and control outputs are an integral part of efficient monitoring of process operations. Tremblay [1975] developed an interactive on-line executive package for this purpose. This generalized operating system executive, known by its acronym "GOSEX", is based on the RDOS and is not application dependent. This package is capable of supporting high level language, displaying and changing parameters on-line, providing facilities for data plotting, profiling and storage; and the initiation and stoppage of user programs. Up to 30 output peripheral devices can be attached to the package. A general configuration is given by Tremblay [1975]. These include 2 teletypes, 2 lineprinters, 2 high speed paper tape punch, 8 magnetic tape transports, 8 cassette tape transports and 8 parallel disk channels. Proper linkage between the GOSEX package and user routines is maintained by an interfacing program.

3.3.3 Basic Reactor Software

The basic monitoring softwares for the reactor system are developed by Tremblay [1977]. A brief summary of these programs are shown in Table 3.4.

TABLE 3.4: BASIC SOFTWARES FOR REACTOR

PROGRAM	PURPOSES
PTAPE	GOSEX parameter tape
RTAPE	Reactor parameter tape
SYMBL	GOSEX symbols definitions
SYMBL1	Reactor symbols definitions
VISOR	Reactor supervising program
CSCON	Contact sense program
FLAG	Alarm flags for Fortran program
SETUP	Reactor initial conditions setup
QENCH	Quick cooling of reactor
PANIC	Emergency shutdown of system

Programs PTAPE and RTAPE are used to configure the executive programs to user's purposes. Only those parameters that relate to the peripherals may be changed, according to user's requirement. SYMBL and SYMBL1 define all the symbols that can be displayed on-line during operation. VISOR is the reactor supervising program which records the reactor temperatures, input flowrates and maintains the setpoint of the input flow controllers. CSCON supervises the contact sense and records the composition of exit stream from the gas chromatograph. Mole fractions of various species and the butane conversion will be calculated. Reactor axial temperatures and flow conditions at the time of sample injection are also stored. When Real Time Fortran IV programs are included, designed alarm messages can be transmitted through program FLAG. The SETUP program is responsible for the setting of reactor wall temperature at the startup procedure. It sets up conditions for program VISOR. When the reactor temperature is increasing rapidly and is unable to be controlled, e.g. reactor runaway, quick cooling can be achieved by initiating program QENCH. Under certain abnormal or emergency situations, program PANIC is used to shut down the reactor by cutting off the reactant flows and rapid cooling of circulating oil. To restart reactor monitoring, SETUP is initiated.

Usually, all these programs are not to be changed for this pilot plant tubular reactor, except in PTAPE where users can declare the number of peripherals required for their purposes. These programs form the backbone of the software on reactor control studies.

Additional programs for data acquisition, control action, etc. are incorporated with this basic software.

3.4 Process Reactor - Computer Interfacing

Proper interfacing is required to establish the linkage between process equipment and the computer. Process variables measured by transducers are transmitted to the process computer. These variables are the 19 thermocouple temperatures, two input flowrates and the product stream compositions. The temperatures and flowrates are recorded by computer programs while the concentrations are analyzed by a programmable gas chromatograph. The thermocouple signals are multiplexed into two identical thermocouple transmitters. A total of 22 inputs can be multiplexed into the two computer ADC's and unused thermocouples are to measure room temperature . A twelve point rotary relay selects the pair of thermocouples to be switched into the inputs of the thermocouple transmitters, limiting the multiplexer time cycle to twelve seconds.

Two differential pressure transmitters are used to determine the flowrates of hydrogen and n-butane; while a third one measures the pressure drop across the reactor. These transmitters consist of transducers and independent power supply.

It is necessary to manipulate the flowrates of inputs and cooling air during operation. Also, rapid venting of reactants and flushing the reactor with hydrogen are required at different stages of operation. Compressed air is supplied to the heat exchanger at the

coolant network by actuating a two-way solenoid valve in order to maintain constant oil temperature. The reactant flows are manipulated by applying a pneumatic signal to the diaphram of the control valves. These signals are generated by voltage to pressure (E/P) transducers. Rapid venting and hydrogen flushing are achieved by the actuating of a two-way solenoid valve and two three-way solenoid valves respectively.

Two modes of operation are possible for the reactor. An automatic mode where the process is monitored automatically by the computer during normal operations. During start-up, shutdown or abnormal conditions, a manual mode which over-rides the computer commands is needed. Under automatic positions, DAC signals from the computer are directed to an E/P transducer which actuates the control valve. To actuate the solenoid valve, a computer relay activates the transistor supplying the power. At manual position, DC manually operated voltage source supplies the necessary voltage to the E/P transducer. Manual actuation of the solenoid valves are required in this case.

Complete designs on switching networks of the control valves, solenoid valves and multiplexing are given by Tremblay [1977].

CHAPTER 4

DATA ACQUISITION AND MODEL BUILDING

4.1 Closed-Loop System

4.1.1 Closed-Loop Identification and Estimation

Ideally, a dynamic-stochastic model can be constructed with open-loop input-out data, following the procedure described in Sections 2.1 and 2.2. However, very few industrial processes, particularly those on which control is necessary, can be operated for any length of time in an open-loop mode because of product specifications or safety considerations. Their stability must be maintained either manually by an operator or by some simple feedforward-feedback control. The pilot plant butane hydrogenolysis reactor being investigated here is highly unstable if left uncontrolled, due to extreme nonlinearities and noisy disturbances. Therefore, a univariate feedback control scheme was implemented during data collection. The addition of this control presents a problem for the dynamic-stochastic model building.

Consider a univariate system under feedback control in Figure 4.1:

FIGURE 4.1: UNIVARIATE CLOSED-LOOP SYSTEM

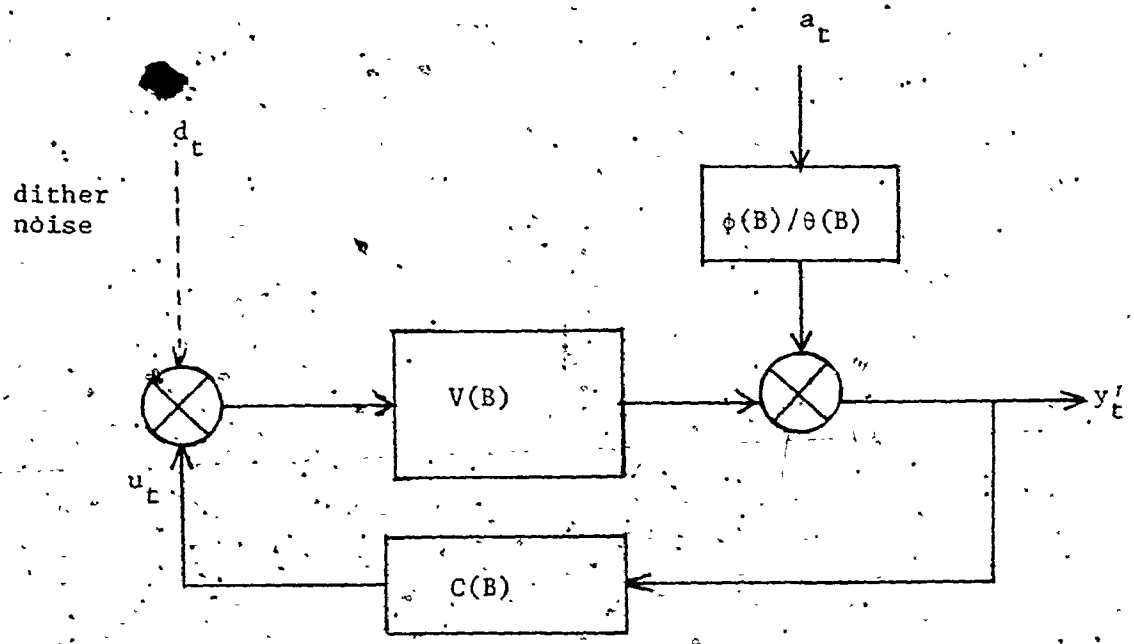

FIGURE 4.2: DATA ACQUISITION SCHEME

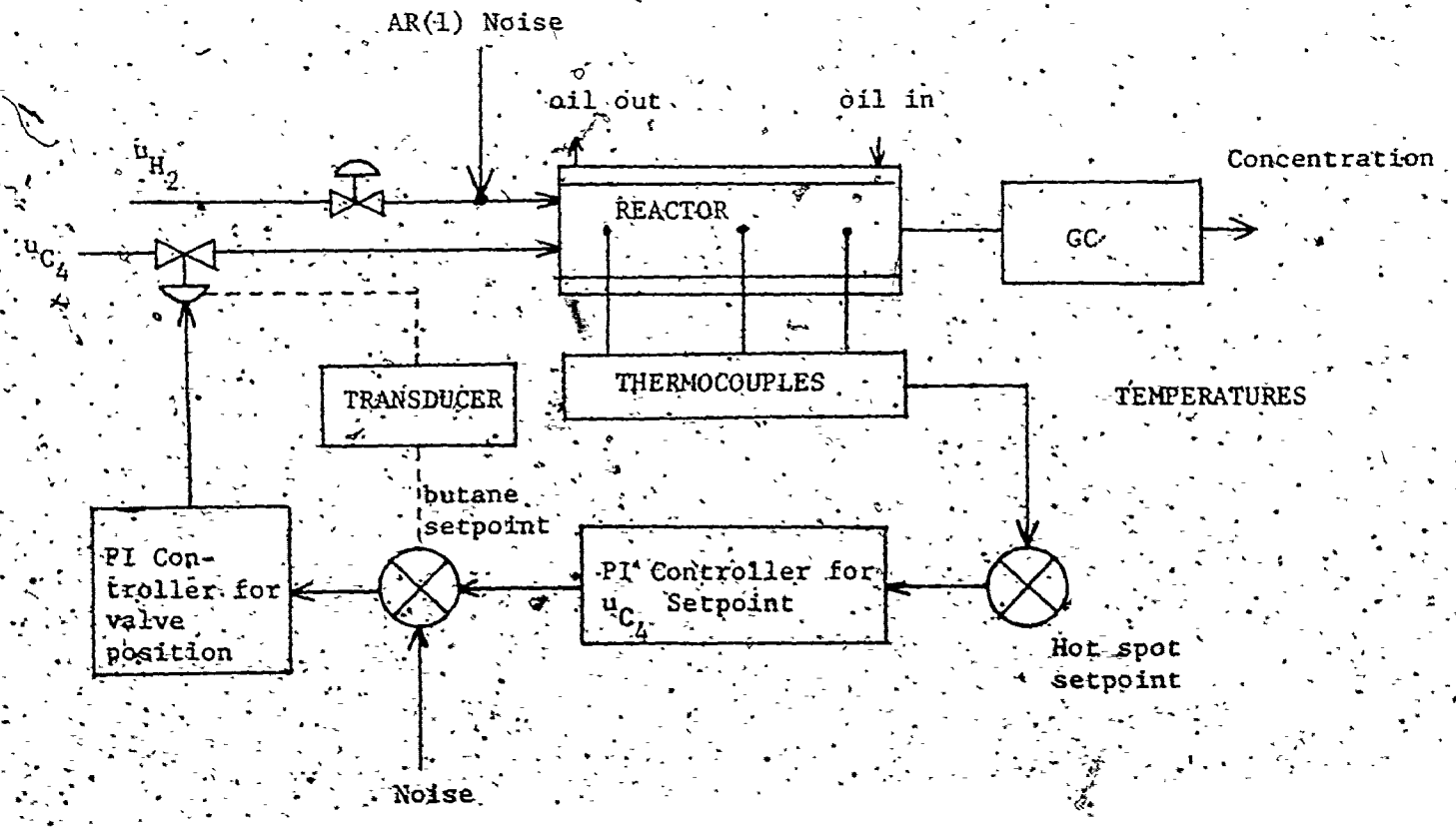

Recall the assumptions that u_t and N_t are uncorrelated for an open loop system. Therefore, the impulse response function can be determined by the sample cross-correlation functions between input and output. However, under closed-loop conditions, u_t and N_t are correlated; and the cross-correlation of y_t and u_t only gives the inverse of the controller coefficient (Box and MacGregor [1974]). No information about the transfer function is provided.

The closed-loop identification problem has been investigated extensively by Ljung et al [1974, 1975] and Box and MacGregor [1974]. They suggested the addition of a programmed 'dither' noise d_t with known structure to the input series, as shown by the dotted line in Figure 4.1. This 'dither' noise d_t is uncorrelated with the input and N_t. With the 'dither' noise-output and 'dither' noise-input sample cross-correlation generating functions determined ($r_{dy}(B)$ and $r_{du}(B)$), the impulse response function can be calculated by either long division $\frac{r_{dy}(B)}{r_{du}(B)}$ or equating the coefficients of the powers of B. This identification procedure is feasible no matter whether the controller C(B) structure is known or not. On occasions, one would have plant data without the knowledge of whether it is collected under closed-loop or open-loop. In this case, a significant cross-correlation between y_t and u_t at lag zero would indicate the presence of feedback control. Under open loop, since most systems do not have instantaneous transfer from input to output, v_o is practically zero.

In some systems, models can be derived successfully from closed-loop data without the addition of 'dither' noise if there is sufficient noise in the feedback loop. Box and MacGregor [1976] showed that parameter estimation can still be attained. Yet, with the inclusion of d_t to the input during data acquisition, parameter estimation efficiency is greatly improved. Sometimes, however, only the functions of the parameters that appear in the optimal control equation are required. In this case, no transfer function is involved and closed-loop data are adequate to provide efficient parameter function estimation without the 'dither' noise.

With the transfer function properly identified, parameter estimation and diagnostic checks can be carried out by methods mentioned earlier, as if they are in open loop situations.

4.1.2 Data Acquisition Scheme

Plant input-output data are required for dynamic-stochastic model building. A data acquisition scheme was devised and a schematic layout is shown in Figure 4.2.

The axial temperature profiles and the effluent product stream are the two groups of outputs. The characteristics of the input streams, coolant condition and the extent of reactions are reflected by the temperature profile and particularly the hot spot temperature. Also, temperature data is readily available at least every 12 seconds. During data acquisition, the reactor was kept under control by controlling the hot spot temperature. The target hot spot

setpoint was set to be about 25-30°C above the circulating oil temperature. The experimental hot spot was compared and the output error was passed to a univariate proportional-integral (PI) feedback controller which adjusted the setpoint of the butane flow. A second PI feedback controller was used to manipulate the butane flow stem valve position. This scheme resembles that of a cascade control system, where the first PI controller acts as a supervisory component. The purpose of this cascade setup is to avoid sudden drastic changes in the butane flow. The supervisory controller will smooth the adjustment of the butane valve.

Traditionally, hydrogen had been used as the manipulated variable. However, tests had shown that in this reactor, use of the hydrogen flow is unsatisfactory if the hot spot setpoint is more than 30°C above the oil temperature. Large excursions of hydrogen flow were experienced to keep the reactor about the desired operating level. With butane flow as the manipulated variable, a temperature difference of 50°C can be tolerated without the reactor running away. Besides, butane is the limiting reactant and this is, therefore, to be expected.

To facilitate closed-loop identification, a programmed white noise was added to the feedback loop manipulating the butane stream. A 30-second sampling interval was arbitrarily chosen. For the first 200 data, the hydrogen flow was maintained at its setpoint, with no noise added. This implied a univariate closed-loop system

and identification can be made easier. After the necessary data had been collected, another noise sequence following an AR(1) process was added to the hydrogen stream. The structure of these two noise series were formulated in Appendix 2.1. The purpose of the AR(1) disturbances was to excite the hydrogen flow such that more flow pattern variations were available to improve parameter estimation. The variances and intensity of these perturbations could be adjusted on-line. It is important that the minimum hydrogen to butane flow ratio was at least 3:1, otherwise the catalyst would be deactivated instantaneously due to carbon depositions from excess butane. On the other hand, the butane and hydrogen flows should not hit the upper and lower flow restrictions which maintain the critical ratio frequently. The closed-loop identification would not be feasible under this situation.

The effluent stream was analyzed by the process gas chromatograph and the compositions were available about every 6 minutes. Input flows were manipulated and recorded every 30 seconds. Profile temperatures were measured every 12 seconds. In order to smooth out the variations of the manipulated input flows and the controlled temperatures (Smith [1972]),filtered temperatures were calculated by Equation (4.1) every 30 seconds.

$$T(t) = \alpha_f T(t-1) + (1-\alpha_f) T_r(t) \qquad (4.1)$$

where

T is the filtered temperature

T_r is the measured raw temperature

α_f is the filtering constant.

These filtered temperatures were recorded in 30 second intervals and were used for modelling later. The experimental input flows and output products data are shown in Figures 4.3 to 4.7. Instead of mole fractions, the extents of various components were adopted as the responses. The extent is defined as the amount of species reacted or generated in gm mole/second. Because the production rate is a prime concern in plant operation, the extent of a reaction would provide necessary information for this purpose. Concentration in mole fraction is independent of the amount of product stream. By a suitable choice of total input flow, the extents would reflect the production of the required components.

The operating conditions for data acquisition and the formulation of the extents are given in Appendix 2.2 and 2.3. About seven hours of data were collected; and three hours of flowrates are shown in Figure 4.3 to 4.4. As discussed in Chapter 3, since there are only three independent components in the process reactions, the extents of propane, butane and hydrogen were chosen as the outputs. Henceforth, the extents will be used, instead of mole fractions.

4.2 Development of a Prediction Equation for Exit Products

4.2.1 The Problem

The exit concentrations of various components are intended to be used for controlling the reactor system. However, due to the restrictions on the process analyzer, concentration analysis results are only available about every 6 minutes. This large sampling interval

is impractical to be used for the control of this highly exothermic, potentially unstable reactor. Some means have to be devised to overcome this problem.

In earlier work by Jutan [1976], he developed a mechanistic model which simulated the dynamic behaviour of the reactor about a steady state situation. Although in reality unsteady state is always the case, a quasi-steady state condition can be assumed. For most catalyst gaseous reactors, the response of concentrations upon changes in reactor conditions is almost instantaneous, while the response rate of the temperature wave is at least 1000 times slower. This implies that upon perturbation, the reactor concentration will quickly attain a quasi-steady state. As the slower temperature dynamic response then moves to its new steady state level, the concentration will follow it.

Jutan derived a theoretical predictive relationship of the three independent exit concentrations in terms of the reactor axial temperature profile and inlet flow deviations during the past sampling interval.

$$\underline{C}(t) = \underline{R}^* \underline{T}(t) + \underline{S}^* \underline{u}(t-1) \qquad (4.2)$$

where

$\underline{R}^*$, $\underline{S}^*$ – parameter matrices, (3x7) and (3x2) respectively.

$\underline{C}$ – exit concentration deviations, (3x1)

$\underline{T}$ – axial temperature deviations, (7x1)

Since both $\underline{T}(t)$ and $\underline{u}(t-1)$ are available every 30 seconds, pseudo-concentration data can be regenerated from the above relationship. The assumption of quasi-steady state enables us to express concentrations as an algebraic function of the inputs and the axial temperatures.

In Jutan's analysis, the parameter matrices $\underline{R}^*$ and $\underline{S}^*$ came directly out of the theoretical model once it was fitted with plant concentration, temperature and flow data. However, it was shown that the temperatures are highly correlated among themselves (Tremblay [1977]), and therefore not all the temperature data is needed to provide good predictions. A more parsimonious form can be employed. Here, the concept of canonical variables and correlations is introduced to formulate a prediction equation similar to Equation (4.2) in the following parts. It involves a statistical study of various combinations of variables and linear canonical transformations are then carried out. Another approach was proposed by Tremblay [1977], where a reduced subset of three temperature variables were chosen on physical and engineering judgement. These three variables were the hot spot temperature, its normalized axial position and the area under the temperature profile. The concentrations were then fitted using these three pseudo temperature variables plus the two output flow deviations.

$$\underline{C}(t) = \underline{P}\,\underline{F}(t) + \underline{Q}\,\underline{u}(t-1) \qquad (4.3)$$

where

$\underline{P}$, $\underline{Q}$ - parameter matrices, (3x3) and (3x2) respectively

$\underline{F}$ - vector of temperature functions (3x1).

A comparison of these two approaches will be given in Section 4.3.2.

4.2.2 Prediction Equation Formulation and Concentrations (Extents) Regeneration

The idea of canonical correlation analysis is to determine a new coordinate system for two sets of variables such that the correlations between them is maximized. The linear combination of variables in each set that have the maximum correlation will define the first new coordinate. A second linear combination in each set, which are uncorrelated with the first linear combination, and which have maximum correlation are then defined. The procedure is repeated until the new system is completely specified.

A description of this canonical correlation procedure is given by Anderson [1958]. Briefly, two sets of variables are first defined. In this case,

$$\underline{M}_1^T = [C_1, C_2, C_3]$$

and (4.4)

$$\underline{M}_2^T = [T_1, T_2, \ldots\ldots T_9 \mid u_{1,t-1}, u_{2,t-1}]$$

where the $\underline{u}$ data are those that existed during the last sampling period. Let

$$\underline{M} = \begin{bmatrix} \underline{M}_1 \\ \hline \underline{M}_2 \end{bmatrix} \qquad (4.5)$$

and let the covariance matrix of $\underline{M}$ be denoted by

$$\Sigma = \left[\begin{array}{c|c} \Sigma_{11} & \Sigma_{12} \\ \hline \Sigma_{21} & \Sigma_{22} \end{array}\right] \tag{4.6}$$

where

$$\begin{aligned} \Sigma_{11} &= E(\underline{M}_1 \underline{M}_1^T), \quad (3\text{x}3) \\ \Sigma_{12} &= E(\underline{M}_1 \underline{M}_2^T), \quad (3\text{x}11) \\ \Sigma_{21} &= E(\underline{M}_2 \underline{M}_1^T), \quad (11\text{x}3) \\ \Sigma_{22} &= E(\underline{M}_2 \underline{M}_2^T), \quad (11\text{x}11) \end{aligned} \tag{4.7}$$

It can be shown that the 3 linear combinations of the predictor variables in $\underline{M}_2$ that are most highly correlated with the three concentration variables in $\underline{M}_1$ are given by the eigenvectors $\underline{\gamma}$ corresponding to the 3 largest eigenvalues in the following equation:

$$[\Sigma_{21} \Sigma_{11}^{-1} \Sigma_{12} - \lambda^2 \Sigma_{22}] \underline{\gamma} = \underline{0} \tag{4.8}$$

where

λ^2 is the eigenvalue

$\underline{\gamma}$ is the corresponding eigenvector

Equation (4.12) is analogous to the real symmetric generalized matrix eigen-problem of the form

$$\underline{A}_e \gamma = \lambda \underline{B}_e \gamma \tag{4.9}$$

Theoretically, three eigenvectors $\underline{Y}_i$ corresponding to the eigenvalues λ^2 will be determined since Σ_{11} is of rank 3. These eigenvectors are the three different linear combinations of T_1, T_2, ..., T_9, u_1, u_2 which are most highly correlated with the linear combinations of concentrations. The square root of individual eigenvalue i.e., λ_1^2, λ_2^2 and λ_3^2, is equal to the magnitude of correlations between the new canonical variates. With these eigenvectors defined, new canonical variates are then defined as

$$Z_i = \underline{Y}_i^T \underline{M}_2 \quad , \quad i = 1, 2, 3 \tag{4.10}$$

The new canonical variates Z_i's are orthogonal to each other, i.e. no correlation among themselves. Statistically, the Z_i's are the optimal choice of the sets of temperatures and flowrates to predict the concentrations. Assuming a linear model, the prediction equation will be

$$\underline{C}(t) = \underline{\beta}\ \underline{Z}(t) \tag{4.11}$$

where $\underline{\beta}$ is the prediction parameter matrix (3x3). By a linear least squares fit, $\underline{\beta}$ can be determined.

An alternative canonical system is also suggested here. Assuming the the two input flows are known to be important, only the temperature data is transformed into canonical variates, i.e.

$$\underline{M}_2^* = [T_1, \ldots, T_9]^T \tag{4.12}$$

The same formulation as above is repeated; and the new pseudo-concentration prediction equation is:

$$\underline{C}(t) = \underline{\beta}_1^* \underline{Z}^*(t) + \underline{\beta}_2^* \underline{u}(t-1) \qquad (4.13)$$

Parameter matrices $\underline{\beta}_1^*$ (3x3) and $\underline{\beta}_2^*$ (3x2) are fitted as before by least squares.

4.2.3 Results from the Canonical Correlation Analysis

The seven-hours exit concentration data from the gas chromatograph and their corresponding temperatures and input flows are used to set up the prediction equation. Since the input flow variables are collected at room temperature and pressure (assume STP conditions), they have to be corrected to the reactor operating conditions. Also, they are converted into their mean deviates which are being used for model construction. A total of 62 concentration data sets are avilable.

Table 4.1a and 4.1b show the results of the eigenvalue-eigenvector analysis and the corresponding least square fit for the three independent variables (Equation 4.11). The last row of these parameters in Table 4.1b corresponds to the canonical variate Z_3 with the smallest eigenvalue and the first row corresponds to Z_1 with the largest λ_1^2.

Parameters $\underline{\beta}_1$, $\underline{\beta}_2$ and $\underline{\beta}_3$ are corresponding to the responses C_1, C_2 and C_3 respectively. In equation form,

$$\begin{bmatrix} C_1 \\ C_2 \\ C_3 \end{bmatrix} = \begin{bmatrix} .2307E-04 & .1016E-05 & .4795E-06 \\ .2914E-04 & -.4077E-05 & .2572E-07 \\ .4087E-04 & -.1466E-04 & .1227E-05 \end{bmatrix} \begin{bmatrix} Z_1 \\ Z_2 \\ Z_3 \end{bmatrix} \qquad (4.14)$$

where C_i - mean corrected extents $\quad i = \begin{cases} 1, \text{ propane} \\ 2, \text{ butane} \\ 3, \text{ hydrogen} \end{cases}$

Tables 4.2a and 4.2b give the same information with the five independent variables in the form of Equation (4.13). Fifteen parameters are involved in this case. In equation form,

$$\begin{bmatrix} C_1 \\ C_2 \\ C_3 \end{bmatrix} = \begin{bmatrix} .2307E\text{-}04 & .1016E\text{-}05 & .4821E\text{-}06 & -.2571E\text{-}08 & -.1586E\text{-}08 \\ .2914E\text{-}04 & -.4077E\text{-}05 & .2712E\text{-}07 & -.1598E\text{-}08 & -.2144E\text{-}09 \\ .4087E\text{-}04 & -.1466E\text{-}04 & .1227E\text{-}05 & -.2004E\text{-}10 & .2468E\text{-}08 \end{bmatrix} \begin{bmatrix} z_1^* \\ z_2^* \\ z_3^* \\ u_1 \\ u_2 \end{bmatrix}$$

where

u_1 = mean corrected butane flowrate

u_2 = mean corrected hydrogen flowrate

(4.15)

TABLE 4.1a: EIGENVALUES AND EIGENVECTORS OF THE GENERALIZED SYMMETRIC MATRIX EQUATION (4.8) - LINEAR COMBINATIONS OF NINE TEMPERATURES AND TWO FLOWRATES

EIGENVALUES			u_1 butane flowrate u_2 hydrogen flowrate
λ_1^2	λ_2^2	λ_3^2	
0.8908	0.5402	0.0767	
CORRESPONDING EIGENVECTOR, γ			PREDICTOR VARIABLES
γ_1	γ_2	γ_3	
-0.0881	0.2129	-0.1620	$T_{1,t}$
0.1688	-0.2225	-0.0703	$T_{2,t}$
-0.0489	0.1160	0.0492	$T_{3,t}$
0.1590	-0.1725	-0.1028	$T_{4,t}$
0.0775	-0.0476	0.8894	$T_{5,t}$
-0.0281	0.1087	0.0482	$T_{6,t}$
-0.0038	-0.0161	-0.5722	$T_{7,t}$
0.1121	-0.3118	-0.1172	$T_{8,t}$
-0.0693	0.1694	0.0698	$T_{9,t}$
0.2815	0.0101	-0.1046	$u_{1,t-1}$
-0.0160	-0.1358	0.1334	$u_{2,t-1}$

TABLE 4.1b: PARAMETER ESTIMATIONS FROM LS FIT OF $\underline{C}_i = \underline{Z}^T \cdot \underline{\beta}_i$

(WITH CONFIDENCE INTERVALS)

Propane, C_1	Butane, C_1	Hydrogen, C_3	Canonical Variates
$\underline{\beta}_1$	$\underline{\beta}_2$	$\underline{\beta}_3$	
.2307E-04 (± .02E-04)	.2914E-04 (± .03E-04)	.4087E-04 (± .05E-04)	Z_1
.1016E-05 (± .21E-05)	-.4077E-05 (± .28E-05)	-.1466E-04 (± .05E-04)	Z_2
.4795E-06 (± .22E-05)	.2572E-07 (± .27E-05)	.1227E-05 (± .52E-05)	Z_3

TABLE 4.2a: EIGENVALUES AND EIGENVECTORS - LINEAR COMBINATIONS OF NINE TEMPERATURES

EIGENVALUES			
λ_1^2	λ_2^2	λ_3^2	
0.4730	0.3396	0.0533	
CORRESPONDING EIGENVECTOR			PREDICTOR VARIABLES
$\underline{Y}_1$	$\underline{Y}_2$	$\underline{Y}_3$	
-0.1546	-0.1542	-0.1143	$T_1(t)$
0.2004	-0.2000	0.1055	$T_2(t)$
-0.1127	0.0144	0.0167	$T_3(t)$
0.1494	0.1901	-0.1694	$T_4(t)$
-0.0708	0.4024	0.7776	$T_5(t)$
-0.1050	0.1927	-0.0739	$T_6(t)$
0.1110	-0.0647	-0.5555	$T_7(t)$
0.2794	-0.1436	-0.0077	$T_8(t)$
-0.1085	-0.2707	0.2636	$T_9(t)$

TABLE 4.2b: PARAMETER ESTIMATES FROM LS FIT FOR 5 VARIABLES

Propane, C_1	Butane, C_2	Hydrogen, C_3	Variates
$\underline{\beta}_1$	$\underline{\beta}_2$	$\underline{\beta}_3$	
.2307E-04	.2914E-04	.4087E-04	z_1^*
.1016E-05	-.4077E-05	-.1466E-04	z_2^*
.4821E-06	.2712E-07	.1227E-05	z_3^*
-.2571E-08	-.1598E-08	-.2004E-10	u_1
-.1586E-08	-.2144E-09	.2468E-08	u_2

The residual variances from the linear least squares fit of these two approaches are given in Table 4.3.

TABLE 4.3: RESIDUAL VARIANCES COMPARISON

Measured Output	Residual Variances x 10^{10}	
	Three Canonical Variates	Three Variates Plus Two Flows
C_1	0.724	0.750
C_2	1.243	1.286
C_3	4.266	4.416

A comparison of these two approaches indicates that they have essentially identical residual variances. There is, therefore, no preference for either approach on the basis of LS. The first approach is however chosen since less parameters are involved. Thus, the prediction equation is represented by Equation (4.11).

An analysis of the result shows that those parameters (last row in Table 4.1b) corresponding to the smallest eigenvalue λ_3^2 are small and have wide confidence intervals. This implies that Z_3 is relatively insignificant and the other two canonical variates Z_1, Z_2 are able to represent most information about the set of variables. Nevertheless, Z_3 is included in the prediction equation for a complete description of the system.

With the prediction equation properly set up, pseudo-extent deviates are generated from the 30 seconds interval data on temperatures and flowrates. The fact that they are not independent would not affect the identification procedure. Each response is fitted separately similar to a single response system.

4.2.4 Comments on Canonical Correlations

The three canonical variates represent the optimal choice of independent variables for the prediction of concentrations. The canonical correlation procedure determines the three linear combinations of measured independent variables that are most highly

correlated with the linear combinations of the responses. Statistically, the canonical variates are orthogonal, i.e. they are independent variates. This orthogonal feature is particularly attractive in the subsequent least squares fitting because it gives rise to independent and accurate parameter estimates. Also, in the recursive least squares algorithm described in the next section it will result in faster convergence of the estimation.

It had been pointed out that, (Tremblay [1977]), although this concept is adequate as long as the reactor conditions at run time remain the same as when the data was collected, a shift of operating levels on parameters such as catalyst decay, setpoint change may jeopardize the adequacy of the fitting. Refitting under new conditions will then be required. Although this is correct to a certain extent, the prediction errors can be minimized by parameter updating in the prediction equation. These updated parameters are adjusted to improve the response predictions and they will also be capable of partially cancelling out any effects of changes in the canonical variates as well. Besides, an on-line updating scheme of the eigenvector elements can be derived easily. Whenever conditions shift , a number of temperature and flow data are collected and an on-line eigenvalue-eigenvector analysis is carried out. For this work, this on-line analysis is not being done because it is believed that the recursive least squares parameter updating can eliminate the errors incurred from shifting conditions.

On the other hand, the canonical analysis has proved to be superior to the approach used by Tremblay [1977] in which temperature variates were chosen somewhat arbitrarily - hot spot temperature, its position and the integral under the temperature curve plus the two flowrates - and fit them empirically. For a test, the same set of data used by Tremblay (61 data) was used to fit the prediction equation (4.11) using canonical variates. Comparing the residual variances of the predicted responses in Table 4.4.

TABLE 4.4: RESIDUAL SUM OF SQUARES COMPARISON

Response	Residuals Variances ($\times 10^{11}$)	
	Canonical Analysis	Arbitrary Fitting
C_1	0.946	1.79
C_2	5.42	8.92
C_3	19.2	38.90

A 50% improvement in terms of residual variances is achieved. The correlation matrix of the canonical variates is shown in Appendix 3.1 together with the correlation matrix from arbitrary fitting. By examining individual parameter confidence intervals (Appendix 3.1), the parameter estimates from canonical analysis are greatly improved, except for the least important linear combination. Although a direct comparison is impossible due to different number of

parameters involved, it is obvious that canonical correlation is a better method for the prediction equation construction, even though it uses fewer parameters.

Another advantage of canonical correlation is that their variates are normalized since the eigenvector elements are scaled such that $\gamma^T \Sigma_{22} \gamma = I$ (see Appendix 3.1). As shown in Table 4.1b, the parameters from the same response have equal confidence intervals. It is a direct result of this normalization.

A modified representation of the responses might be suggested for use in the subsequent model building and control. In view of the success of canonical correlation, probable dependencies among responses could be effectively eliminated if, rather than using the extents C_i's as the responses to be predicted and controlled, one were to use the canonical variates $w_i = \underline{\alpha}_i \underline{C}$ (analogous to the z_i) as the response variables since they are orthogonal. The dynamic-stochastic model could then be identified with these linear combinations against the measured input flows. This is particularly useful when a large number of outputs and inputs are involved. Since there are at most three output responses and two inputs in this work, for simplification, this approach is not adopted.

It is interesting to compare the characteristics of the data set collected in this work and that collected by Tremblay [1977] in his Ph.D. thesis. Both sets of data were collected under similar circumstances, except with different operating conditions. In his

study, it was under a more extreme condition with the hot spot temperature about 50°C above the coolant oil setpoint. The variance of the added 'dither' noise to the butane flow was unchanged while the variance of the AR(1) noise series to the hydrogen stream was increased periodically. Applying the canonical correlation on the data, the residual variances of the two data sets after LS fit are given in Table 4.5.

TABLE 4.5: COMPARISON OF RESIDUAL VARIANCES IN TWO DIFFERENT DATA SETS

RESPONSES	Residual Variances ($\times 10^{11}$)	
	This Work	Tremblay's Work
C_1	7.24	0.946
C_2	12.43	5.42
C_3	42.66	19.2

It is obvious that Tremblay's data results in smaller residual variances, especially for the response propane extents. It is expected since the butane conversion increases under a higher temperature profile, giving a more significant amount of propane and reducing the effects of the incurred errors. However, under such severe conditions, the butane flow hits the upper and lower flow limit frequently in order to control the hot spot temperature, exhibiting the characteristics of the so called 'bang-bang' control. The

closed-loop identification using this flow data would not be feasible and no transfer function model can be built, although the data set is still useful for the dynamic-stochastic model fitting and controller designs. Thus, there is a trade-off between these two data sets. In the view that transfer function-stochastic model building is an integral part of our object, the data collected in this work is used. Additional details can be obtained from Tremblay's data when it is necessary.

4.2.5 Parameter Updating by Recursive Least Squares

It is worthwhile to investigate the accuracy of the parameter matrix $\underline{\beta}$ in Equation (4.11) in subsequent control runs. These parameters are first fitted off-line, based on the data collected at the time of the experiment. It has been observed that the conditions of the reactor characteristics change with time, e.g. a new bed of catalyst may be used or the 'old' catalyst deactivates gradually. A different coolant temperature would then be needed to initiate the reaction. Also, there may be a setpoint change or load change at the time of on-line control. All these condition changes may throw the prediction equation off-balance when applied during on-line control. The prediction parameters may have changed in the new situation. Thus, an on-line re-estimation scheme is required to update the parameter matrix $\underline{\beta}$. It was decided that the eigenvectors forming the canonical variates need not be updated, although updating on-line is not impossible. Rather, only the regression parameters $\underline{\beta}$ in Equation (4.11)

were to be updated. The appropriate eigenvector space may change but most of the changes can probably be accounted for by adapting $\underline{B}$.

The essence of parameter updating is that whenever new concentration extents are available, they are compared with their predicted values from Equation (4.11). The prediction errors, ε which are the residuals will be used for updating. Several recursive identification methods have been compared (Soderstrom et al [1974]). A real time version of the recursive linear least squares (RLS) method is discussed here. Recall that the least squares estimates of parameter vector $\underline{\beta}$ in the equation $\underline{Y} = \underline{x}\,\underline{\beta} + \underline{\varepsilon}$ is given by,

$$\hat{\underline{\beta}} = (\underline{x}^T\underline{x})^{-1}\,\underline{x}^T\,\underline{Y} \qquad (4.16)$$

where

$\underline{x}$, $\underline{Y}$ - vectors of independent and dependent variables respectively.

If the data is becoming available in a sequential manner, it is advantageous to make this algorithm recursive. The recursive least squares parameter updating formulation is given as follows:

$$\hat{\underline{\beta}}(t+1) = \hat{\underline{\beta}}(t) + \underline{K}_w(t+1)\,\varepsilon(t+1) \qquad (4.17)$$

$$\underline{K}_w(t+1) = \frac{\underline{P}(t)\,\underline{z}(t+1)}{\lambda_f + \underline{z}(t+1)^T\,\underline{P}(t)\,\underline{z}(t+1)} \qquad (4.18)$$

$$\underline{P}(t+1) = \left[\underline{P}(t) - \frac{\underline{P}(t)\,\underline{z}(t+1)\,\underline{z}(t+1)^T\,\underline{P}(t)}{\lambda_f + \underline{z}(t+1)^T\,\underline{P}(t)\,\underline{z}(t+1)}\right] \Big/ \lambda_f \qquad (4.19)$$

$$\varepsilon(t+1) = y(t+1) - \underline{z}(t+1)^T \hat{\underline{\theta}}(t) \qquad (4.20)$$

where $\hat{\underline{\theta}}$ - parameter estimates vector (3 x 1)

$\underline{z}$ - independent variable vector (3 x 1)
equal to the (t+1)-th row of $\underline{x}$

$\underline{p}$ - a matrix proportional to the covariance matrix
of independent variables (3 x 3)

$\underline{K}_w$ - weighting factor vector, (3 x 1)

y - measured dependent variable

λ_f - forgetting factor

ε - prediction error, difference between measured
and predicted y

The above RLS method actually minimizes the exponentially discounted sum of squares function $\sum_{s=1}^{t} \lambda^{t-s} \varepsilon(s)^2$. The forgetting factor λ_f is chosen to be smaller than one if it is desired to adapt to changing conditions. In this way, old residuals will be discounted and have little influence on the estimates. If $\lambda_f < 1.0$, the weighting factor $\underline{K}_w$ does not tend to zero, which is a necessary condition if one wishes to track changing parameter values. For starting values, $\hat{\underline{\theta}}(0) = \underline{0}$ and $p(0) = \alpha \underline{I}$ could be assumed. α is assigned a large number, about 10 times the variances of the corresponding y. Convergence can be reached rapidly in this manner.

The appropriateness of the RLS method depends on the assumption that the prediction error ε is a white noise sequence. If this condition is not fulfilled, consistent estimates cannot be obtained. In this study, since the concentration data is available every six minutes, the parameters will be updated only every 12 sampling intervals and it is felt that little serial correlation will exist.

4.3 Modelling

4.3.1 Multivariate Transfer Function-Noise Model Formation

Table 4.6 gives the resulting impulse response functions v_j for the three transfer functions (Equation 4.2). They are plotted in Figure 4.9 to 4.11. Also, Figure 4.12 to 4.14 show the corresponding step response functions.

From Figure 4.9 to 4.11, a dead time delay of one period can be identified in each case. Apparently, the dynamics cannot be identified easily. It is because the thermal waves are slow to respond. Their impulse response functions stretch out to a large lag giving the illusion of no immediate dynamics. However, from the step

responses and based on the known kinetics and previous work, first order transfer function can be identified. The transfer function model form with first order dynamics is given by

$$y_t = \left(\frac{\omega_o - \omega_1 B}{1 - \delta_1 B}\right) u_{t-1} \qquad (4.21)$$

Equation (4.21) is referred as a (1, 1, 1) model, i.e. order r = 1, s = 1 and delay b = 1.

TABLE 4.6: IMPULSE RESPONSE FUNCTIONS v_j

Lag j	Impulse Response Function $v_j \times 10^6$		
	C_1 and $u_{C_4H_{10}}$	C_2 and $u_{C_4H_{10}}$	C_3 and $u_{C_4H_{10}}$
0	0.281	0.235	0.184
1	0.841	0.812	0.749
2	0.098	0.129	0.162
3	0.161	0.234	0.252
4	0.155	0.273	0.384
5	0.131	0.125	0.124
6	0.163	0.188	0.206
7	0.173	0.213	0.098

A problem arises in the identification of the dynamic responses against hydrogen flow. The hydrogen flow is left uncontrolled, i.e. under open-loop while the exit concentrations are under closed-loop.

Both open and closed-loop identification methods would not be applicable. However, it can reasonably be assumed that the hydrogen dynamics resembles that of butane. Previous work of open-loop univariate identification on hydrogen flow had indicated a similar v_j pattern. Although they were done under very different conditions, they do provide a preliminary model form for the hydrogen flow. For tentative identification purposes, the elements of the transfer function matrix are all chosen to have the same form as in Equation (4.21). In general,

$$Y_{i,t} = \left(\frac{\omega_o - \omega_1 B}{1 - \delta_1 B}\right) u_{j,t-b_{ij}} \qquad i = 1,2,3; \quad j = 1,2 \qquad (4.22)$$

145 data in which both hydrogen and butane flows were perturbed were available. With preliminary transfer function parameters, noise series were generated and identified. The results of noise identification of the original series and its first difference are given in Figure 4.15 to 4.20. Two stochastic forms are possible, multivariate AR(1) or integrated MA(1). In order to design a controller equipped with integral action, an unstationary noise series is needed. Thus, the IMA(1) model is chosen. Significant cross-correlations among the noise series are observed and are shown in Figure 4.21 to 4.23.

The multivariate transfer function-noise model is refitted by the multivariate estimation algorithm outlined in Section 2.2. Subsequent fittings indicated the δ parameters related to the hydrogen

input were extremely poorly estimated and did not significantly improve the fit and so were dropped. Due to the large number of parameters involved (24 parameters) and the memory capacity of the CDC 6400 computer system, only 145 data sets can be used for estimation. Thus, the fitting was carried out twice and the average values of the parameters were listed in the final model. The result of each fitting is given in Appendix 3.2 and the final model given below (with the approximate 95% confidence intervals of each parameter shown in brackets).

$$10^{+6} \times \begin{bmatrix} C_{1,t} \\ C_{2,t} \\ C_{3,t} \end{bmatrix} = \begin{bmatrix} \underset{(\pm.03)}{\left(\frac{5.97 - 4.28B}{1 - 0.866B}\right)B} & \begin{matrix}(\pm.22) & (\pm.37)\\ (-0.63 - 0.125B)B & \end{matrix} & \begin{matrix}(\pm.17) & (\pm.18)\end{matrix} \\ \begin{matrix}(\pm.37) & (\pm.51)\\ (-0.257 - 0.250B)B & \end{matrix} & \underset{(\pm.02)}{\left(\frac{7.25 - 4.92B}{1 - 0.884B}\right)B} & \begin{matrix}(\pm.28) & (\pm.30)\end{matrix} \\ \underset{(\pm.03)}{\left(\frac{9.62 - 5.73B}{1 - 0.890B}\right)B} & \begin{matrix}(\pm.65) & (\pm.85)\\ (0.900 - 0.484)B & \end{matrix} & \begin{matrix}(\pm.52) & (\pm.52)\end{matrix} \end{bmatrix} \begin{bmatrix} u_{C_4H_{10},t} \\ u_{H_2,t} \end{bmatrix} + N_t \tag{4.23}$$

$$(1-B)N_t = \begin{bmatrix} \underset{1 - 0.502B}{(\pm.28)} & \underset{0.021B}{(\pm.33)} & \underset{-0.085B}{(\pm.12)} \\ \underset{0.368B}{(\pm.44)} & \underset{1 - 0.543B}{(\pm.50)} & \underset{-0.226B}{(\pm.19)} \\ \underset{0.250B}{(\pm.80)} & \underset{0.281B}{(\pm.90)} & \underset{1 - 1.402B}{(\pm.34)} \end{bmatrix} a_t \tag{4.24}$$

Covariance matrix of residuals vector is

$$\underline{D} = \begin{bmatrix} 47.7 & 76.5 & 132.5 \\ 76.5 & 122.1 & 218.2 \\ 132.5 & 218.2 & 394.6 \end{bmatrix} \times 10^{-2}$$

A comparison between the average residual variances and the predicted response variances is given in Table 4.7.

TABLE 4.7: RESIDUAL VARIANCES AND PREDICTED RESPONSE VARIANCES

RESPONSES	RESIDUAL VARIANCES $\times 10^{12}$	PREDICTED RESPONSE VARIANCES $\times 10^{12}$
C_1	47.7	635
C_2	122.1	1094
C_3	394.6	2446

The autocorrelation and cross-correlation of the residuals are determined and examined. No substantial correlations are observed and these residuals are practically white noise sequences. A more detailed description of the model building is presented in Appendix 3.2.

4.3.2 Comments on the Fitted Model

The fitted transfer function, Equation (4.23), shows that the dynamics relating to butane flow are the dominant components of the process. Their transfer function gains are much larger than that with the hydrogen flow. This confirms the characteristics of the hydrogenolysis reactions whose reactivity is very sensitive to the amount of the key reactant butane. Since the hydrogen flow was in large excess (at least 5:1 in flow ratio) and the magnitude of the input perturbations in it were small relative to this gain, limited dynamic information was extracted from the collected data. Besides, no initial identification of this model form is available. The relatively insignificant hydrogen dynamic effect is illustrated by the small transfer function gains and the absence of δ parameters. Parameters with the butane flow are more accurate due to proper preliminary identification and larger input perturbations. Since the system dynamics are heavily dependent on these parameters, Equation (4.23) should be able to represent the deterministic part of the process reactor model.

It is observed that positive dynamic gains associate the outputs with the butane flow, while the hydrogen flow and the outputs are related with effective negative gains. This confirms the theoretical reaction behaviour in which the production and conversion of output products increases with the butane flow and decreases with hydrogen flow.

The noise model, Equation (4.24) indicates a full moving

average parameter matrix with most parameters having large confidence intervals. However, the model Equation (4.23) and (4.24) are formed by averaging parameter values of two fitted models which are fitted with two different sets of data (see Appendix 3.2 for these model forms). The added perturbations to both hydrogen and butane in the second set have larger variances. The noise parameters of the resulting fitted model, Equation A3.8b), have relatively smaller confidence intervals and thus are more reliable. This is because the dynamic effects are better estimated and therefore the noise is more apparent and is easier to be detected. Another indication of a better overall model form is given by the determinant of the residual covariance matrix $\underline{D}$. It has a $|\underline{D}| = 564.3$ as opposed to 618.5 resulting from the first 145 data. Equation (A3.8a) and (A3.8b) can be alternatively used as the final fitted model.

From Table 4.7 the variance values of the residuals are about 10-15% that of the corresponding predicted responses. Thus, the noise effects would not overshadow the effects of the dynamics in the data set.

In the fitted model, there are high correlations among the parameters that are related to the same input flow, and also in the noise model. These are probably due to the correlated regenerated pseudo-extents. The correlations cannot be avoided because of the nature of closed-loop conditions. All the output extents depend on the manipulated butane flow. Since the aim is to design a feedback

controller to maintain the output levels, the correlated outputs will not hinder the design of control scheme.

Due to the large number of parameters (24) involved and the limited number (145) of data used for fitting, the fitted model is less precise than it could be, though adequate. A larger number of data should provide more accurate parameter estimations. In order to investigate the possibility of reducing parameter numbers, the output structure must be reviewed. Under the conditions during data acquisition, the amount of ethane produced was practically zero (< 0.1%). It implies that a modification of the reaction kinetics is possible. It sheds some light about reducing the output dimensions without misinterpreting the dynamic-stochastic behaviour of the process. This possibility is considered in the following section.

4.4 Dimensionality Reduction of Multivariate System

4.4.1 General Formulation

The dimensionality reduction of non-dynamic multiresponse data has been studied by Box et. al [1973]. Arguing in a similar manner, Box and Tiao [1976] proposed the reduction of multivariate time series into vectors of canonical variates. Consider a general multivariate linear dynamic-stochastic system

$$\underline{y}_t = \underline{V}(B)\ \underline{u}_t + \underline{N}_t \qquad (4.25)$$

Although there are m outputs, there may be only m-p linear combinations of them which exhibit significant disturbances and that are in need of

control. The remaining linear combinations express the natural dependencies among themselves and are represented by random errors. Consider a multivariate first order autoregressive model.

$$\underline{N}_t = \underline{\phi}\, \underline{N}_{t-1} + \underline{a}_t \tag{4.26}$$

Define the autocovariances of lag k as

$$\underline{\Gamma}_k = E[\underline{N}_t\, \underline{N}_{t+k}^T]$$

$$\underline{\Gamma}_k^T = E[\underline{N}_t\, \underline{N}_{t-k}^T] \tag{4.27}$$

It follows from Equation (4.26)

$$\underline{\Gamma}_k^T = \underline{\phi}\, \underline{\Gamma}_{k-1}^T \tag{4.28}$$

or

$$\underline{\phi} = \underline{\Gamma}_1^T\, \underline{\Gamma}_o^{-1} \tag{4.29}$$

with k = 1 and $\underline{\Gamma}_o$ symmetric.

If k = 0,

$$\underline{\Gamma}_o = \underline{\phi}\, \underline{\Gamma}_1 + \underline{\Sigma} \tag{4.30}$$

where

$$\underline{\Gamma}_{-k}^T = \underline{\Gamma}_k$$

Substitute Equation (4.29) into (4.30)

$$\underline{\Gamma}_o = \underline{\Gamma}_1^T\, \underline{\Gamma}_o^{-1}\, \underline{\Gamma}_2 + \underline{\Sigma} \tag{4.31}$$

MacGregor [1972] showed that a canonical form of several linear combinations of $\underline{N}_t$ where $\dot{N}_{1t} = \underline{\ell}_1^T\, \underline{N}_t$, $\dot{N}_{2t} = \underline{\ell}_2^T\, \underline{N}_t$, etc. can

respresent 'most of the activity' of the process. This activity is measured by the idea of the 'most forecastable variation'. The first principal component

$$\dot{N}_{1t} = \underline{\ell}_1^T \underline{\dot{N}}_t = \underline{\ell}_1^T \underline{\Phi} \underline{\dot{N}}_{t-1} + \underline{\ell}_1^T \underline{a}_t$$

$$= \dot{N}_{1,t-1}(1) + a_{1t} \qquad (4.32)$$

is obtained by choosing $\underline{\ell}_1$ which maximizes the ratio of the variance of the forecast $\hat{\dot{N}}_{1t}(1)$ to the variance of the forecast error $\dot{a}_{1t}$.

$$\max_{\underline{\ell}_1} \frac{V[\hat{\dot{N}}_{1t}(1)]}{V[\dot{a}_{1t}]} = \frac{\underline{\ell}_1^T \underline{\Phi} \underline{\Gamma}_o \underline{\Phi}^T \underline{\ell}_1}{\underline{\ell}_1^T \underline{\Sigma} \underline{\ell}_1} \qquad (4.33)$$

Equation (4.33) is known as the Rayleigh Quotient (Noble [1969]) and the solution is solved by the generalized eigen-problem

$$[\underline{\Gamma}_1^T \underline{\Gamma}_o^{-1} \underline{\Gamma}_1 - \lambda_1^* \underline{\Sigma}]\underline{\ell}_1 = 0 \qquad (4.34)$$

λ_1^* is a non-zero eigenvalue corresponding to the eigenvector $\underline{\ell}_1$ which forms the linear combination $\underline{\ell}_1^T \underline{\dot{N}}_t$. Equivalently, the same solution can be obtained by maximizing the ratio

$$\max_{\underline{\ell}_1} \frac{V[\hat{\dot{N}}_{1t}(1)]}{V[\dot{N}_{1t}]} = \frac{\underline{\ell}_1^T \underline{\Gamma}_1^T \underline{\Gamma}_o^{-1} \underline{\Gamma}_1 \underline{\ell}_1}{\underline{\ell}_1^T \underline{\Gamma}_o \underline{\ell}_1} = \mu_1 \qquad (4.35)$$

with $0 < \mu_1 < 1$.

μ_1 is the largest root of the determinant equation

$$| \underline{\Gamma}_1^T \underline{\Gamma}_o^{-1} \underline{\Gamma}_1 - \mu \underline{\Gamma}_o | = 0 \qquad (4.36)$$

μ_1 is related to λ_1^* such that

$$\frac{\lambda_1^*}{\lambda_1^* + 1} = \mu_1 \qquad (4.37)$$

Since $\underline{\Gamma}_o$ and $\underline{\Gamma}_1^T \underline{\Gamma}_o^{-1} \underline{\Gamma}_1$ are positive definite, there are m positive roots $\mu_1, \mu_2, \ldots, \mu_m$ to Equation (4.36) with m corresponding vectors $\underline{\ell}_1^T, \underline{\ell}_2^T, \ldots, \underline{\ell}_m^T$. Let $\underline{\ell}_j^T$ form the rows of the m x m matrix $\underline{L}$ which is then normalized, $\underline{L}\ \underline{\Sigma}\ \underline{L}^T = \underline{I}$. By a non-singular transformation of Equation (4.26)

$$\dot{\underline{N}}_t = \underline{L}\ \underline{N}_t = (\underline{L} \pm \underline{L}^{-1})\ \underline{L}\ \underline{N}_{t-1} + \underline{L}\ \underline{a}_t$$

$$= \hat{\dot{\underline{N}}}_{t-1}(1) + \dot{\underline{a}}_t \qquad (4.38)$$

The canonical variates $\dot{N}_{1t}, \ldots, \dot{N}_{mt}$ are the most forecastable, next most forecastable etc.

A statistical test is designed (MacGregor [1972]) to determine the significance of the roots $\mu_1, \ldots \mu_m$. Assume (m-p) roots have values significantly larger than zero. It was shown that the remaining roots $\mu_{m-p+1}, \mu_{m-p+2}, \ldots, \mu_m$ should be asymptotically distributed as a Chi-square distribution with 2 p degrees of freedom.

$$-[(n-m)+\frac{1}{2}(2m+1)]\ln\Lambda = \chi^2_{2p} \tag{4.39}$$

with

$$\Lambda = \prod_{j=m-p+1}^{m} (1-\mu_j) \tag{4.40}$$

The above formulation is based on the assumption that $\underline{N}_t$ can be adequately represented by a multivariate AR(1) model. The procedure can be extended for a general AR(p) model. Since the AR(1) form can readily be applied to many multivariate processes, in the sense that only the multivariate series dimensions are of interest, the formulation based on an AR(1) model is adequate.

4.4.2 Application to the Reactor Extent Data

Applying the canonical reduction to the three output series $\underline{y}_t$ of 358 data each, the eigenvalues λ^* and μ obtained are listed in Table 4.8. The corresponding eigenvectors are given in Table 4.9. The Chi-square statistic test of assuming the smallest eigenvalue is not significant from zero is given by Table 4.10.

The three output canonical variates $\dot{C}_j$ are:

$$\begin{aligned}
\dot{C}_1 &= 1.498\ C_1 - 0.702\ C_2 + 0.038\ C_3 \\
\dot{C}_2 &= 5.212\ C_1 - 5.355\ C_2 + 0.875\ C_3 \\
\dot{C}_3 &= 7.79\ C_1 - 11.99\ C_2 + 4.157\ C_3
\end{aligned} \tag{4.41}$$

Obviously, all three eigenvalues are significantly different from zero. However, eigenvalue λ_3^* is much smaller than λ_1^* and λ_2^*. Although it is still significantly different from zero, only 6.9% of its

variation is forecastable (since $\mu_3 = .069$).

TABLE 4.8: EIGENVALUES FROM CANONICAL REDUCTION

i	Generalized Eigenvalues λ_i^*	$\mu_i = \frac{\lambda_i^*}{\lambda_{i+1}^*}$
1	1.829	0.6465
2	1.039	0.5096
3	0.0744	0.0692

TABLE 4.9: GENERALIZED EIGENVECTORS ASSOCIATED WITH THE EIGENVALUES

Eigenvectors ($\times 10^{+5}$)			Variables
$\underline{\ell}_1$	$\underline{\ell}_2$	$\underline{\ell}_3$	
1.498	5.212	7.79	C_1
-0.702	-5.355	-11.99	C_2
0.038	0.875	4.157	C_3

$\underline{\ell}_1$ corresponding to the largest eigenvalue x_1

TABLE 4.10: CHI-SQUARED TEST THAT λ_2^* AND λ_3^* ARE ZERO

r Roots that are Insignificant	$-[(n-m)-\frac{1}{2}(2m+1)]\ln \Lambda$	$\chi^2_{2r}(.05)$
r = 1	25.1	6.00
r = 2	274.5	9.49

Box et al [1973] show that small eigenvalues will result if there is a linear relationship among the responses. This led us to suspect that some such relationship existed among the extents of the form

$$C_3 = 7.79\ C_1 - 11.99\ C_2 + 4.16\ C_3 = 0$$

or approximating the relative ratio of the various extents,

$$2\ C_1 - 3\ C_2 + C_3 = 0$$

Upon analyzing the data of Tremblay taken at somewhat more extreme conditions (50°C temperature rise), the same linear relationship associated with the small eigenvalue appeared. Comparing this with the stochiometric equation (3.2) when the rate of generation of ethane is negligible

$$R_{H_2} = 3\ R_{C_4H_{10}} - 2\ R_{C_3H_8} \qquad (4.42)$$

Thus, this analysis has uncovered what in hindsight is a basic

redundancy among the responses at these conditions. Hence, rather than having three independent output extents, there are in reality only two independent ones which need to be controlled. Therefore, it was decided that a two-dimensional output would be adequate to describe the system. In this case, less parameters are involved (14 compared to 24), and thus more data can be used and model fitting would be more efficient. A little information about the dynamic behaviour might be lost from the reduction of output dimension. However, it is a worthwhile trade-off since 'most of the activity' of the dynamics can still be retained by an appropriate choice of outputs.

There are two choices of output combinations:

(a) The two linear combinations of the three extents corresponding to the large effects λ_1^* and λ_2^*.

(b) The extents of any two species among hydrogen, propane and butane.

The first choice (a) may carry more information about the three output structures but they are not as physically meaningful. The relationship between these linear combinations and the input flows are not clear, leading to difficulties in identification. Besides, controller design may cause complication in setting the output level to be controlled. Nevertheless, it does provide an alternative to fit a dynamic-stochastic model. Good model can be constructed by choosing the appropriate set of two outputs (b). It is believed that butane extents should be included due to the importance of

the butane component and its conversion rate.. The remaining component is either the hydrogen or propane extent . It is required to have a component that can best be predicted from Equation (4.11). This logical deduction leads to the choice of propane extent. To justify this selection, the ability of these three components to be predicted can be tested by taking the ratio of the standard deviations of the responses and their corresponding residuals when they are generated by Equation (4.11). The results are shown in Table 4.11.

TABLE 4.11: RATIO OF SIGNALS TO NOISE

Component	σ Response (signal)	σ Residual (noise)	Signal/Noise
C_1	.252E-04	.850E-05	2.96
C_2	.331E-04	1.11E-05	2.98
C_3	.495E-04	2.06E-05	2.40

The results indicate the extents of propane and butane provide a higher signal to noise ratio.

Refitting of Dynamic-Stochastic Model:

Using 300 data sets, the two inputs, two outputs dynamic-stochastic model is refitted with the same transfer function and noise

structures. Residuals auto- and cross-correlations are shown in Figure 4.24 to Figure 4.27.

$$10^6 \times \begin{bmatrix} C_{1,t} \\ C_{2,t} \end{bmatrix} = \begin{bmatrix} \underset{(\pm.026)}{\left(\frac{5.900 - 4.231\ B}{1 - 0.868\ B}\right)B} & (-0.614 - 0.121\ B)B \\ \underset{(\pm.023)}{\left(\frac{7.170 - 4.862\ B}{1 - 0.887\ B}\right)B} & (-0.183 - 0.237\ B)B \end{bmatrix} \begin{bmatrix} u_{1,t} \\ u_{2,t} \end{bmatrix} + N_t \qquad (4.43)$$

$$(1-B)\ N_t = \begin{bmatrix} 1 - 0.326\ B & -0.221\ B \\ 0.698\ B & 1 - 1.121\ B \end{bmatrix} a_t \qquad (4.44)$$

Covariance matrix of residuals

$$D = \begin{bmatrix} 48.55 & 76.44 \\ 76.44 & 124.55 \end{bmatrix}$$

Considerable improvements are generally obtained, especially for the noise model. The new model will be used for the controller design.

4.4.3 Transformation to State Model Form

Before taking the transformation of dynamic-stochastic model to the state model form, a slight modification on u_t is necessary. Because an integrated form of the noise model is involved, the optimal

controller will be in the form of $\nabla \underline{u}_t$ (i.e.; it will contain integral action). Therefore, anticipating this one can express the dynamic-stochastic model in terms of $\nabla \underline{u}_t$ by combining Equation (4.43) and (4.44) together to give

$$\underline{y}_t = (\underline{I} - \underline{I}\, B)^{-1}\, \underline{V}(B)\, \nabla \underline{u}_t + (\underline{I} - \underline{I}\, B)^{-1}\, \underline{\theta}(B)\, \underline{a}_t \qquad (4.45)$$

The corresponding augumented state-space model is in the form similar to Equation (2.40).

$$\begin{aligned} \underline{x}(t+1) &= \underline{A}\, \underline{x}(t) + \underline{G}\, \nabla\, \underline{u}(t) + \underline{\Gamma}\, \underline{a}(t+1) \\ \underline{y}(t) &= \underline{H}\, \underline{x}(t) \end{aligned} \qquad (4.46)$$

Applying the minimal realization transformation described in Section 2.4 to the model Equation (4.43) and (4.44), the augmented parameter matrices $\underline{A}$, $\underline{G}$, $\underline{\Gamma}$ and $\underline{H}$ are set up and are given in Appendix 3.3. The final state vector contains 9 states, in which 5 identify to the dynamic part and 4 correspond to the stochastic part.

FIGURE 4.3: n-BUTANE FLOWRATES

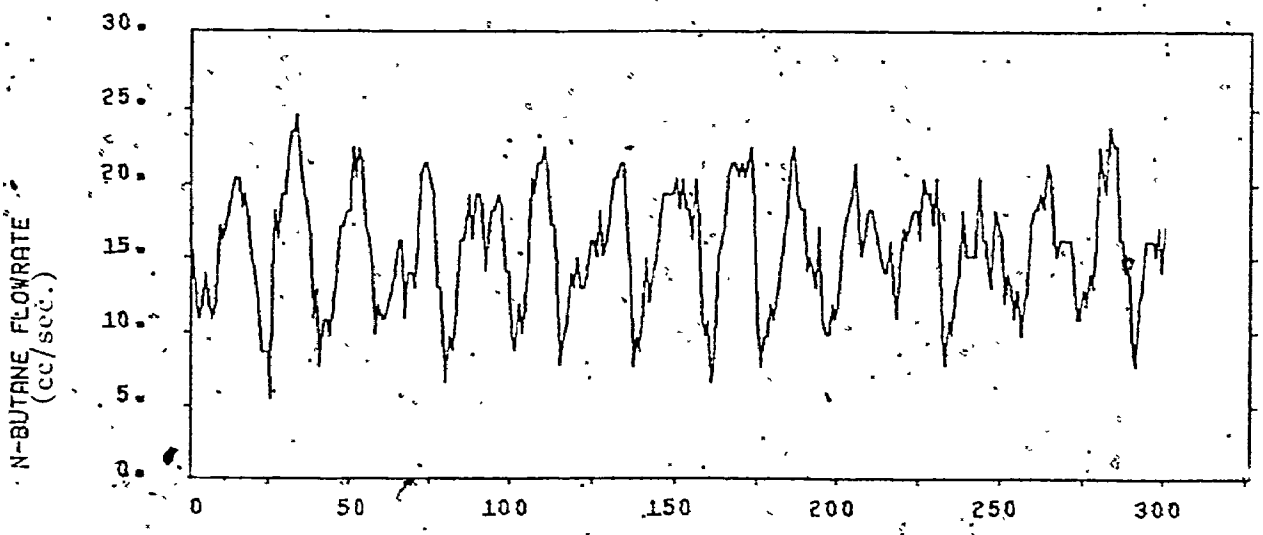

FIGURE 4.4: HYDROGEN FLOWRATES

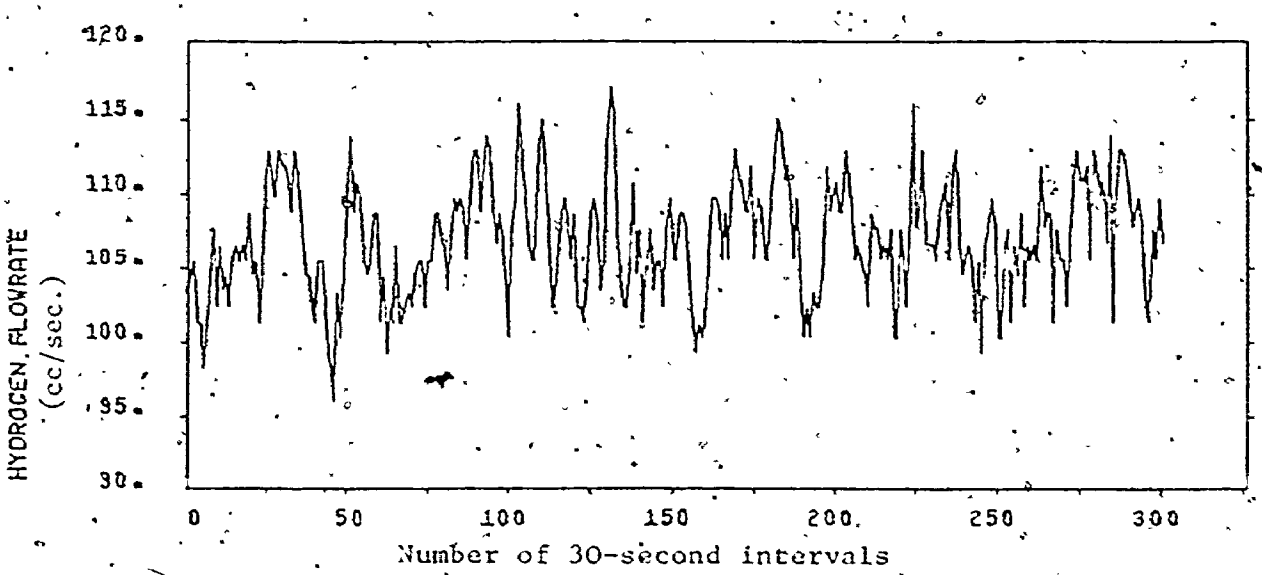

FIGURE 4.5a: MEASURED PROPANE EXTENTS

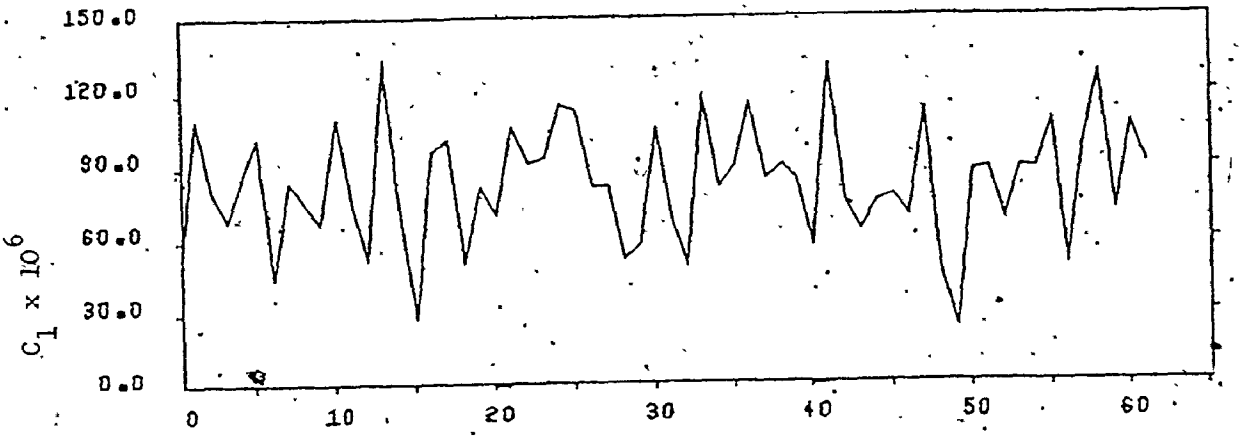

FIGURE 4.6a: MEASURED BUTANE EXTENTS

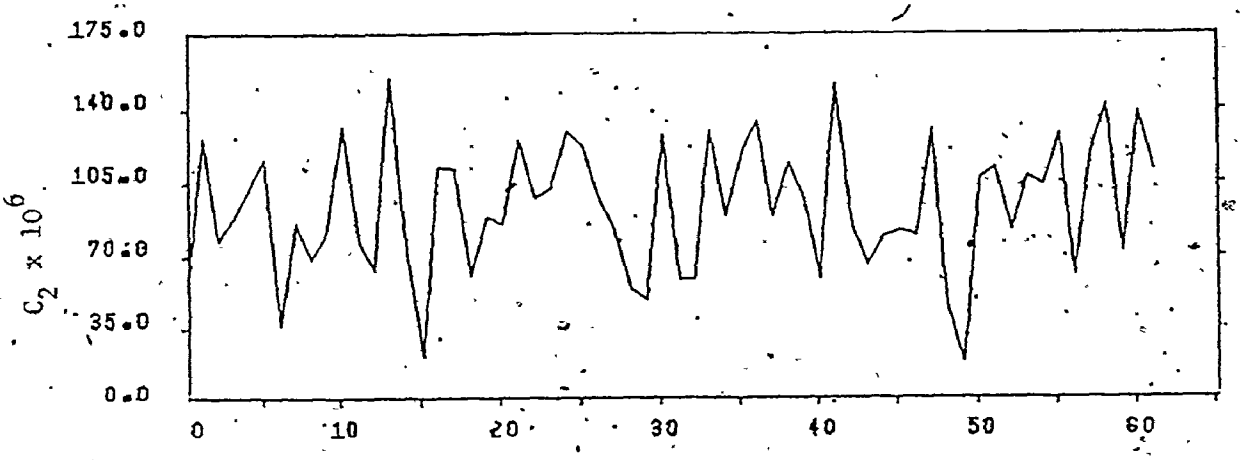

FIGURE 4.7a: MEASURED HYDROGEN EXTENTS

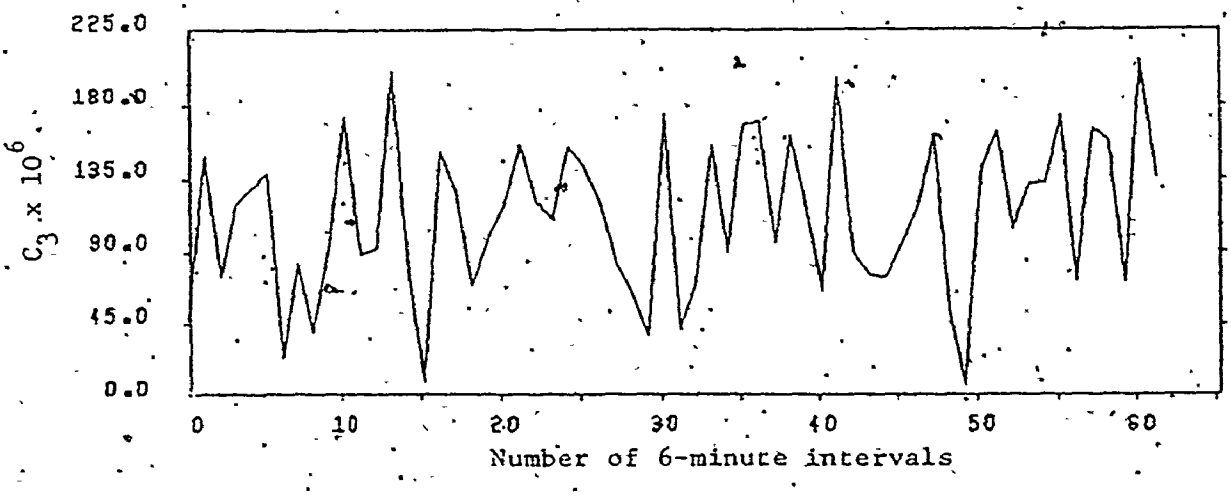

FIGURE 4.5b: REGENERATED PROPANE EXTENTS

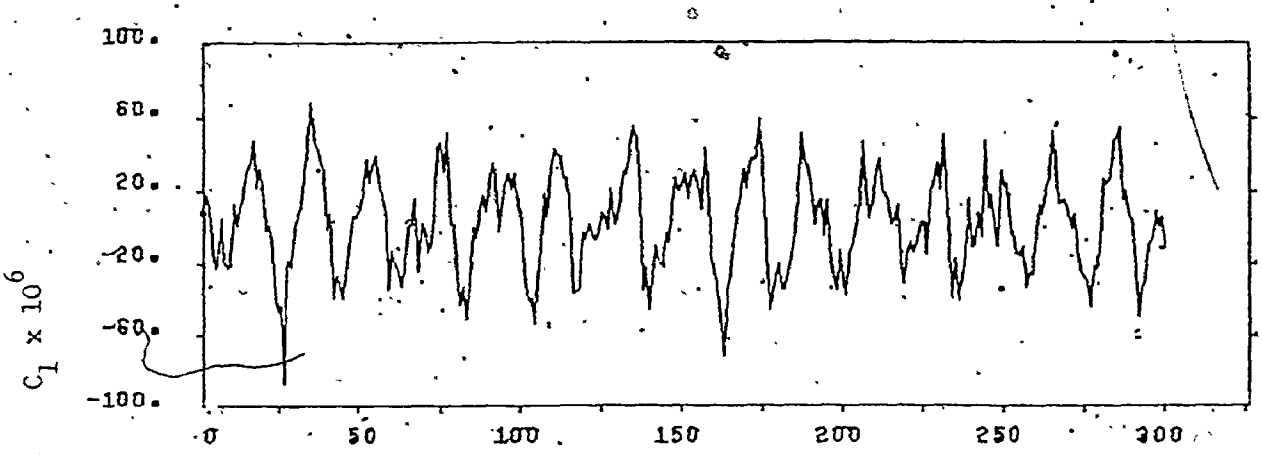

FIGURE 4.6b: REGENERATED BUTANE EXTENTS

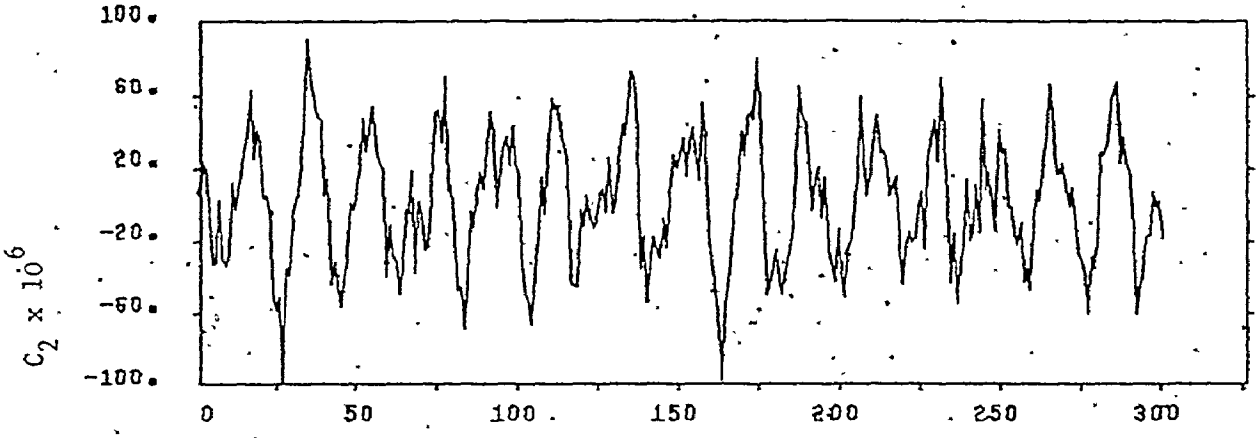

FIGURE 4.7b: REGENERATED HYDROGEN EXTENTS

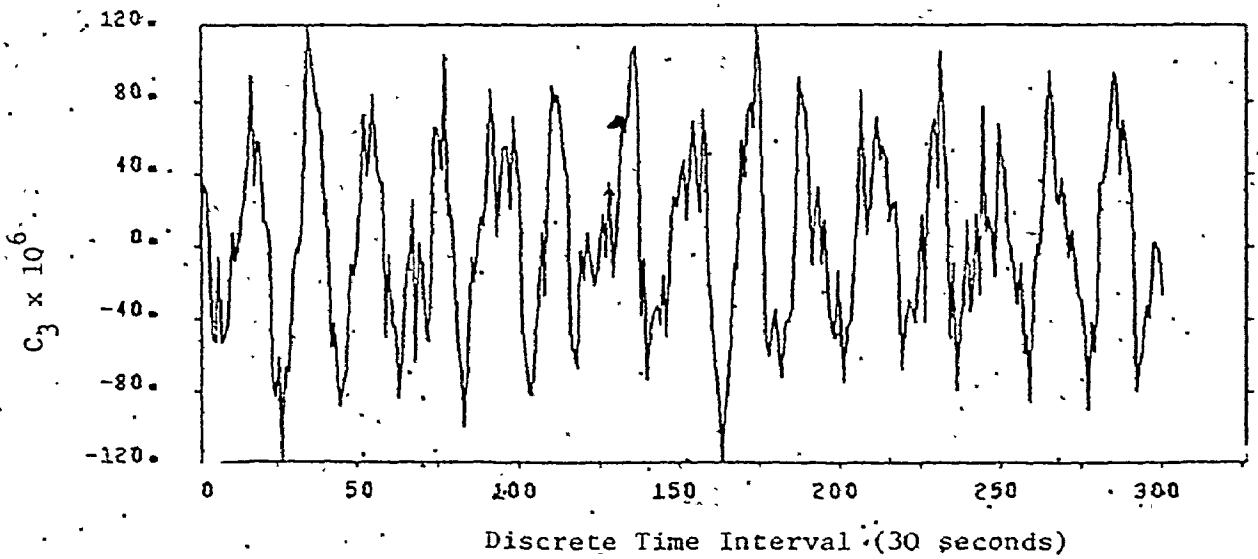

Impulse Response Function

FIGURE 4.9: $u_{1,t}$ and $C_{1,t}$

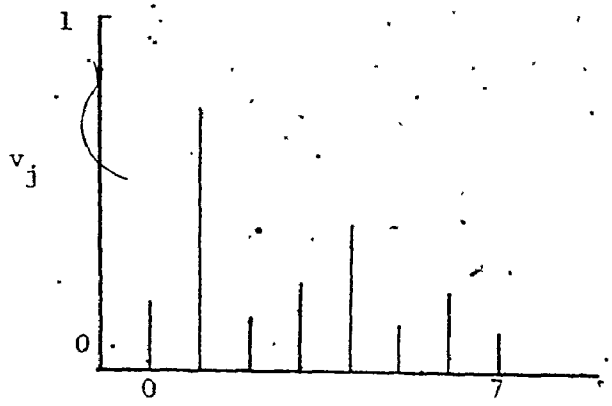

FIGURE 4.10: $u_{1;t}$ and $C_{2,t}$

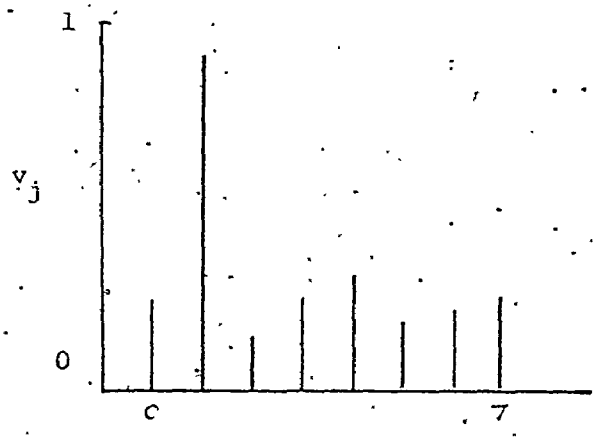

FIGURE 4.11: $u_{1,t}$ and $C_{3,t}$

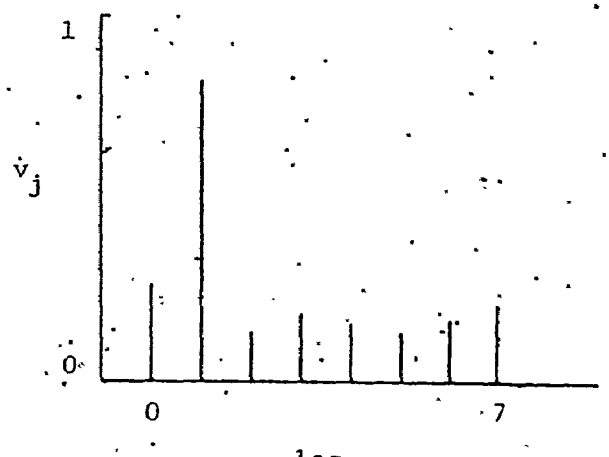

Step Response Function

FIGURE 4.12: $u_{1,t}$ and $C_{1,t}$

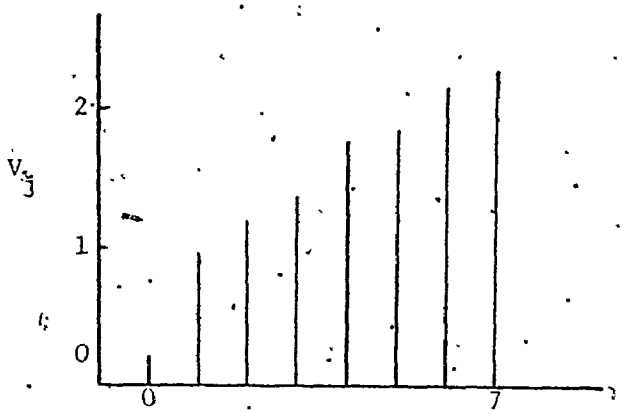

FIGURE 4.13: $u_{1,t}$ and $C_{2,t}$

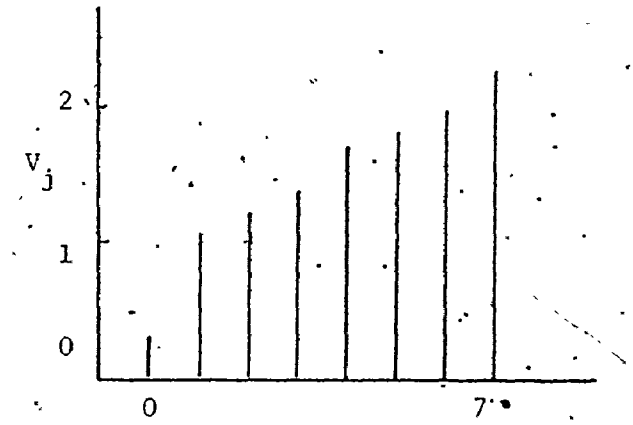

FIGURE 4.14: $u_{1,t}$ and $C_{3,t}$

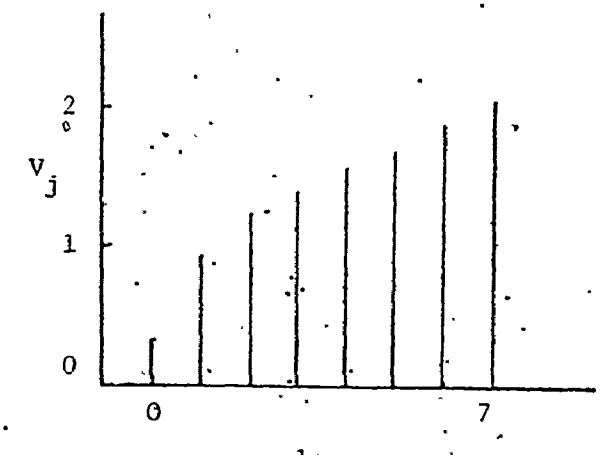

$$V_j = \sum_{j=1}^{k} v_j$$

Noise Series Identification (no differencing)

FIGURE 4.15: $n_{1,t}$

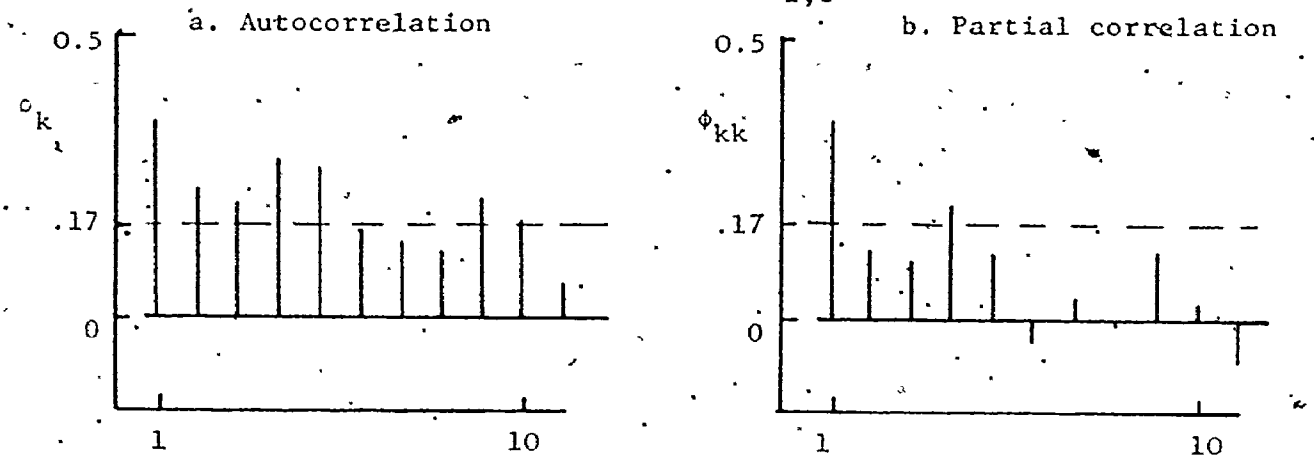

FIGURE 4.16: $n_{2,t}$

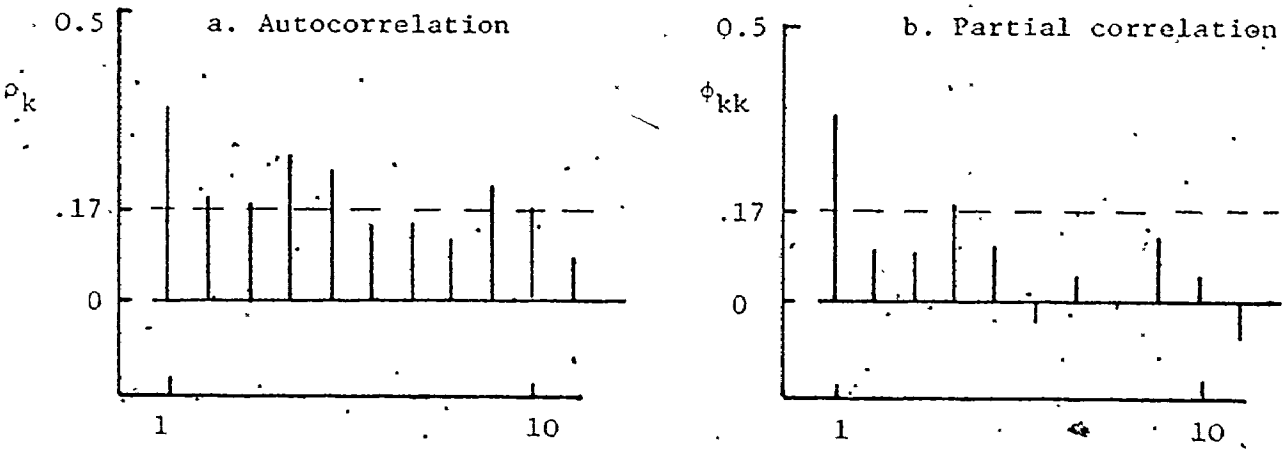

FIGURE 4.17: $n_{3,t}$

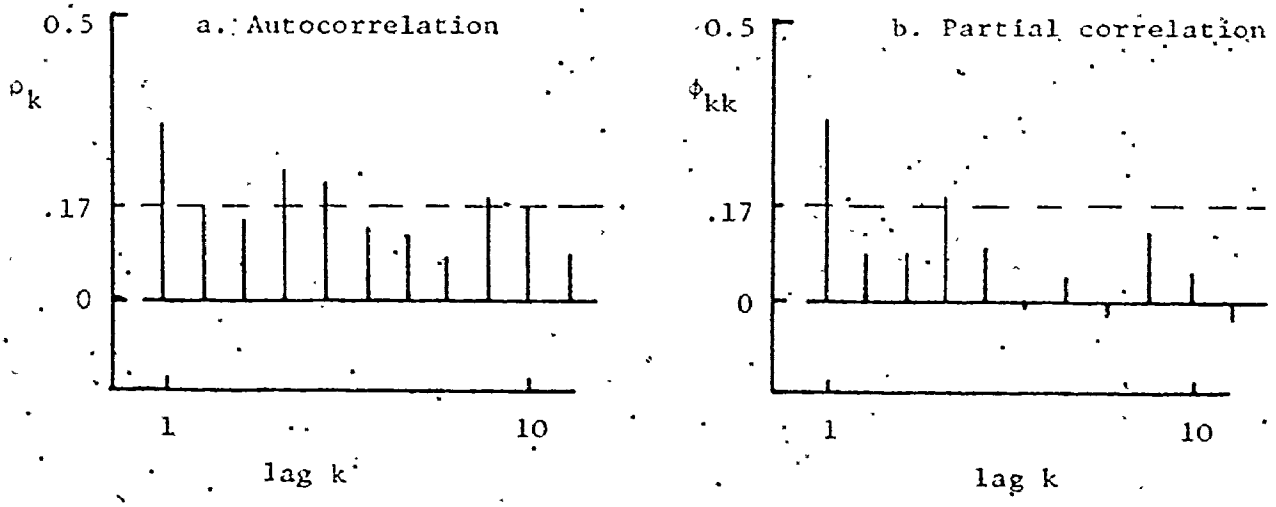

Noise Series Identification (1st difference)

FIGURE 4.18: $\nabla n_{1,t}$

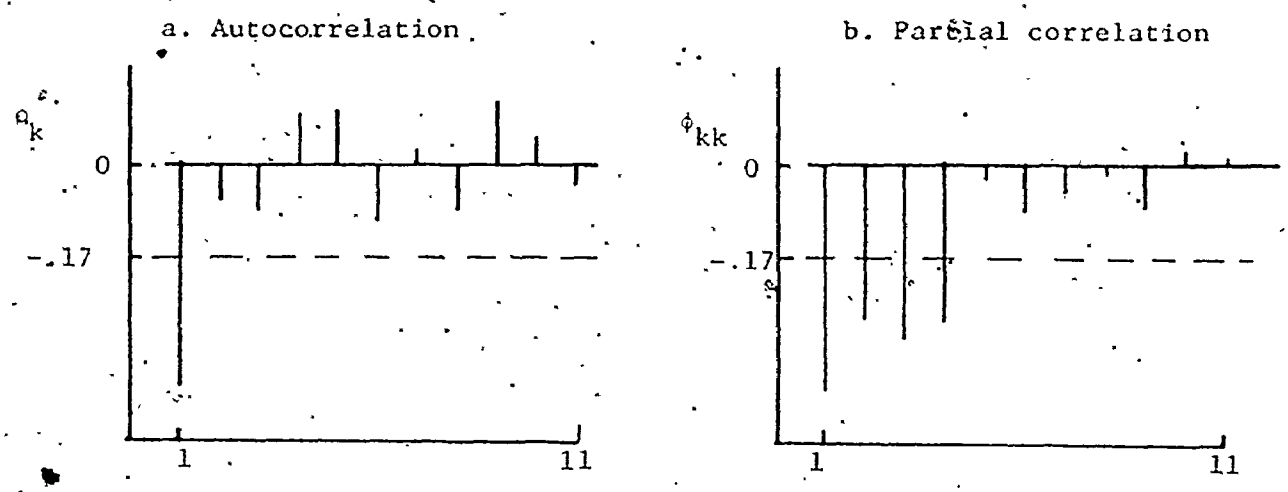

FIGURE 4.19: $\nabla n_{2,t}$

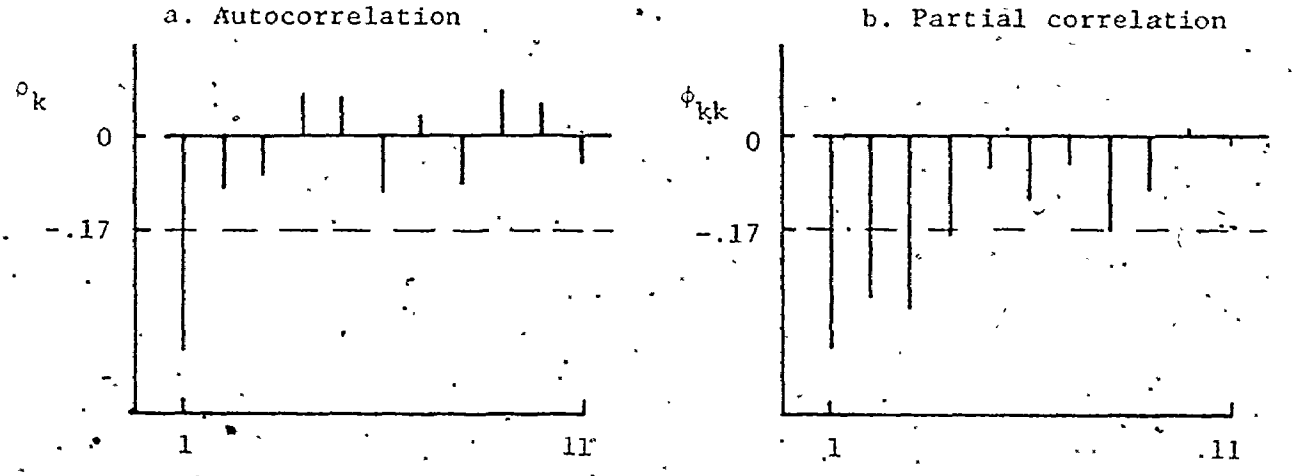

FIGURE 4.20: $\nabla n_{3,t}$

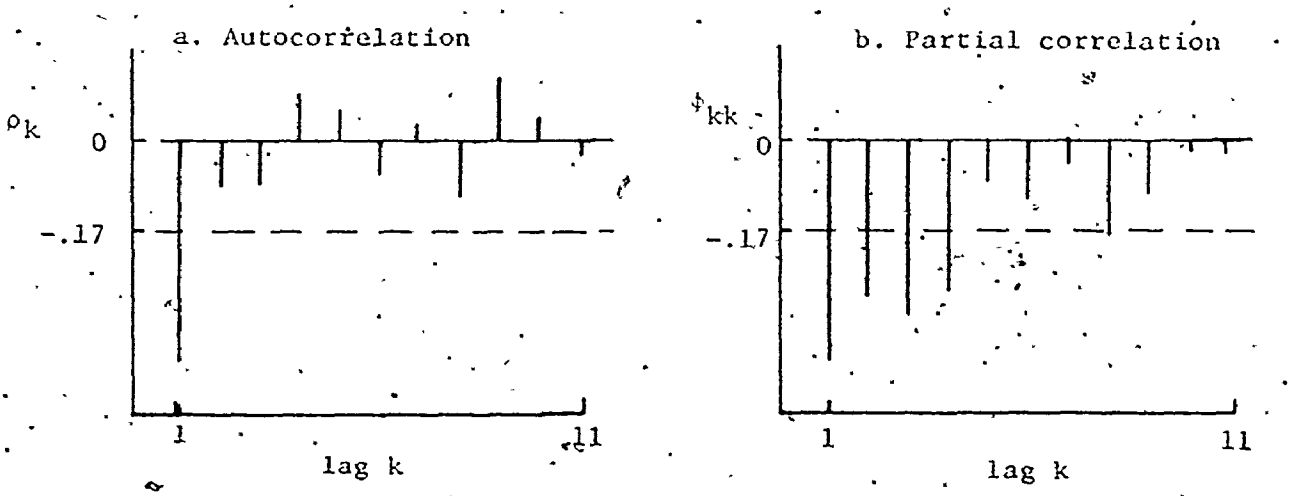

FIGURE 4.21: CROSS-CORRELATION BETWEEN $n_{1,t}$ and $n_{2,t}$

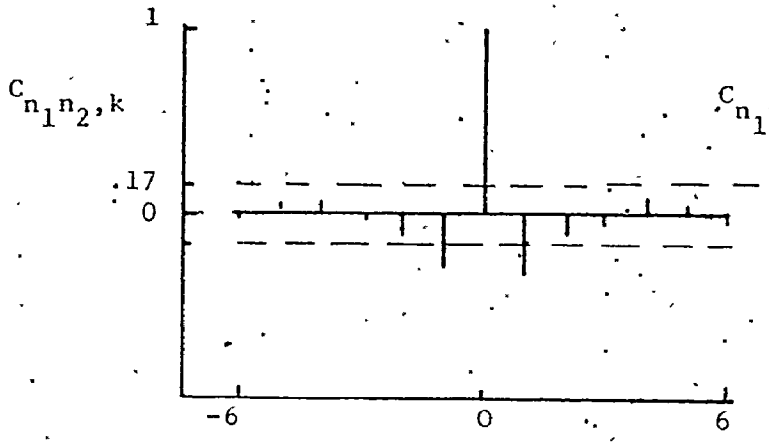

FIGURE 4.22: CROSS-CORRELATION BETWEEN $n_{1,t}$ and $n_{3,t}$

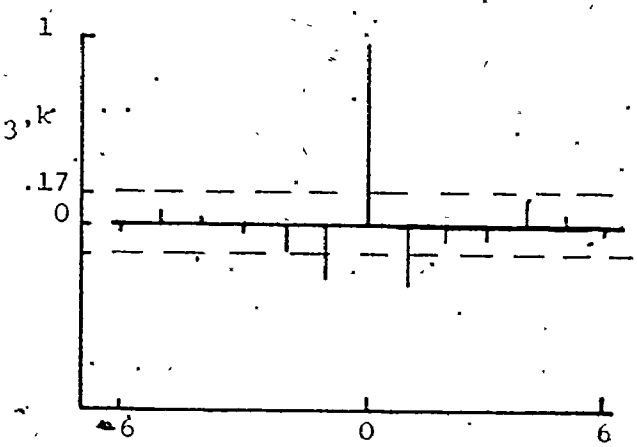

FIGURE 4.23: CROSS-CORRELATION BETWEEN $n_{2,t}$ and $n_{3,t}$

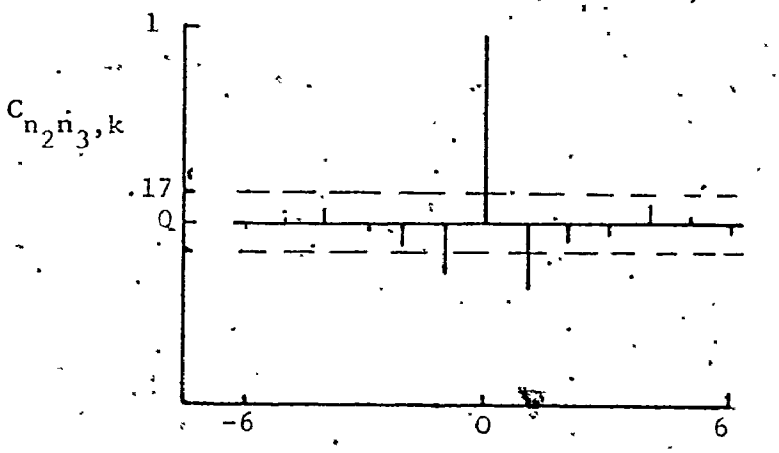

FIGURE 4.24: AUTOCORRELATION OF $a_{1,t}$

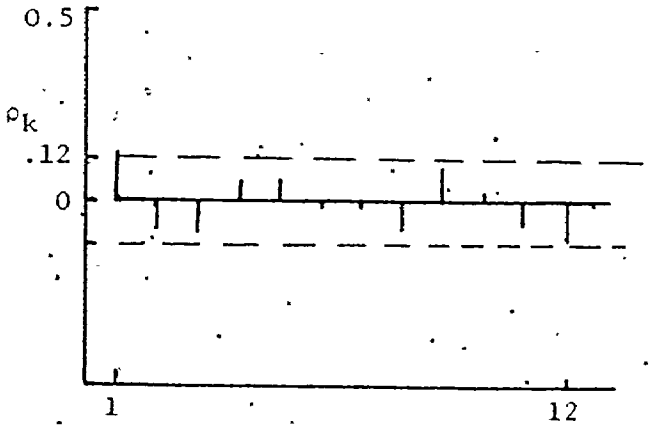

FIGURE 4.25: AUTOCORRELATION OF $a_{2,t}$

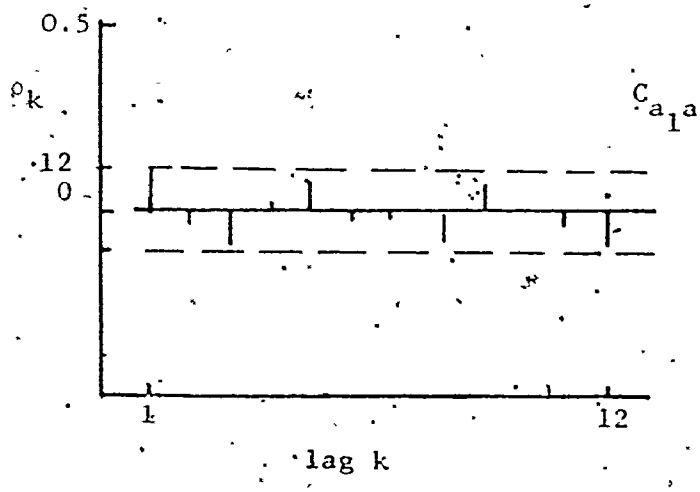

FIGURE 4.26: CROSS-CORRELATION BETWEEN $a_{1,t}$ and $a_{2,t}$

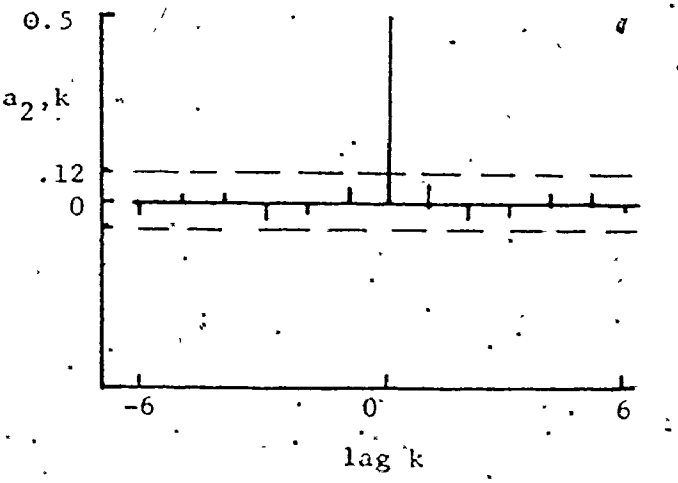

CHAPTER 5

OPTIMAL MULTIVARIATE STOCHASTIC CONTROL

5.1 Stochastic Control Theory Using Transfer Function Noise Models

Discrete stochastic feedback control on a univariate transfer function-noise model was developed by Box and Jenkins [1970] and Astrom [1970]. Extension to include multivariate dynamic-stochastic systems was outlined by Wilson [1970]. Basically, the object is to minimize the output deviations from target values by adjusting the manipulated inputs - a minimum variance criterion. An optimal controller is designed to satisfy this criterion. In practice, a quadratic objective function is normally used which includes possible restrictions on the variances of the inputs

$$\min_{\underline{u}(t)} E[\underline{y}^T(t)\ \underline{Q}_3\ \underline{y}(t) + \underline{u}^T(t)\ \underline{Q}_2\ \underline{u}(t)] \qquad (5.1)$$

where $\underline{Q}_3$, $\underline{Q}_2$ are positive semi-definite matrices.

The detailed formulation of the univariate optimal feedback controller is given by Box and Jenkins [1970]. In essence, the output noise represents the disturbances that drive the output off target if no control action is taken. This noise series is forecasted at a time t, for (b+1) steps ahead (b - dead time of process dynamics). The next input setting is then fixed so as to cancel out this forecasted noise value. Equivalently, the process output variance is minimized with

proper manipulation of input series. The formulation of a multivariate control scheme is quite complicated because of variations in the individual transfer functions of the matrix. Computation is lengthy and is not suitable for computer solution. A generalization of the development is presented by Wilson [1970]. A more commonly used approach is to derive the control scheme from an equivalent state space model.

5.2 Optimal Stochastic Control Using State Space Model

5.2.1 Feedback Control Design

(a) Optimal Controller Via Dynamic Programming:

The optimal stochastic feedback controller on linear discrete state variable models was first developed by Kalman [1960]. The design of optimal stochastic control schemes with the concept of dynamic programming and Kalman filter has been widely adopted (Noton [1965], Astrom [1970], Meditch [1969]).

For a general linear, discrete state space model in the form of Equation (2.29) or (2.30), one optimizes the quadratic performance criterion

$$\min_{\underline{u}(t) \quad t=1,\ldots,N} E[\underline{x}_N^T \underline{Q}_1 \underline{x}_N + \sum_{i=t}^{N-1} (\underline{x}_i^T \underline{Q}_1 \underline{x}_i + \underline{u}_i^T \underline{Q}_2 \underline{u}_i)] \qquad (5.2)$$

where $\underline{Q}_1$, $\underline{Q}_2$ are positive semi-definite matrices.

The dynamic programming solution of the optimal control problem is (Astrom [1970]):

$$\underline{u}(t) = -\underline{L}(t)\,\hat{\underline{x}}(t/\tau) \qquad (5.3)$$

where

$\underline{u}(t)$ is the optimal control setting to be applied at time t, $(n \times 1)$.

$\hat{\underline{x}}(t/\tau)$ is the conditional expectation of the state vector $E[\underline{x}(t)/\underline{y}(\tau)]$ where $\underline{y}(\tau)$ are the known output data available at time t, i.e. $\underline{y}(\tau) = (\underline{y}_\tau, \underline{y}_{\tau-1}, \ldots, \underline{y}_0)$.

$\underline{L}(t)$ is the control matrix given by

$$\underline{L}(t) = [\underline{Q}_2 + \underline{G}^T\underline{S}(t)\underline{G}]^{-1}\underline{G}^T\underline{S}(t)\underline{A} \qquad (5.4)$$

where

$$\underline{S}(t) = \underline{A}^T\underline{S}(t+1)\underline{A} + \underline{Q}_1 - \underline{A}^T\underline{S}(t+1)\underline{G}[\underline{Q}_2 + \underline{G}^T\underline{S}(t+1)\underline{G}]^{-1}\underline{G}^T\underline{S}(t+1)\underline{A} \qquad (5.5)$$

with initial condition $\underline{S}(N) = \underline{Q}_1$.

The convergence of the matrix $\underline{S}(t)$ to a fixed constant steady state value $\underline{S}_\infty$ will usually occur quite rapidly. $\underline{S}_\infty$ and the steady state control matrix $\underline{L}_\infty$ are obtained by iterating between Equation (5.4) and (5.5) until convergence. Thus,

$$\underline{L}_\infty = [\underline{Q}_2 + \underline{G}\,\underline{S}_\infty\,\underline{G}]^{-1}\,\underline{G}^T\,\underline{S}_\infty\,\underline{A} \qquad (5.6)$$

The matrix $\underline{Q}_1$ is formed by choosing

$$\underline{Q}_1 = \underline{H}^T\,\underline{C}^*\,\underline{H} \qquad (5.7)$$

$\underline{C}^*$ is a weighting matrix (often diagonal) which determines the relative weighting placed on the variances and covariances of the

output $\underline{y}(t)$. $\underline{Q}_2$ is a diagonal matrix which places constraints on the variances of various inputs $\underline{u}(t)$.

$$\underline{Q}_2 = \underline{I}\ \underline{\lambda} \tag{5.8}$$

where $\underline{\lambda}$ is a vector of constraints.

In practice, $\underline{Q}_2$ and $\underline{C}^*$ are both unknown. A trial and error iteration is applied until the variances of the inputs and outputs as predicted from the model are jointly acceptable.

(b) Kalman Filter:

For the general state variable model Equation (2.30) it is shown (Jazwinski [1970]) that the estimates of the state vector $\hat{\underline{x}}(t)$ and $\hat{\underline{x}}(t+1)$ given $\underline{y}(t)$ and $\underline{u}(t)$ information up to and including time t are expressed by

$$\hat{\underline{x}}(t/t) = \hat{\underline{x}}(t/t-1) + \underline{K}[\underline{y}(t) - \underline{H}\ \hat{\underline{x}}(t/t-1)] \tag{5.9}$$

$$\hat{\underline{x}}(t/t-1) = \underline{A}\ \hat{\underline{x}}(t-1/t-1) + \underline{G}\ \underline{u}(t-1) \tag{5.10}$$

with covariance matrices

$$\underline{P}(t/t) = \underline{P}(t/t-1) - \underline{K}\ \underline{H}\ \underline{P}(t/t-1). \tag{5.11}$$

$$\underline{P}(t/t-1) = \underline{A}\ \underline{P}(t-1/t-1)\underline{A}^T + \underline{R}_1 \tag{5.12}$$

The Kalman filter matrix $\underline{K}$ is defined as

$$\underline{K} = \underline{P}(t/t-1)\underline{H}^T[\underline{H}\ \underline{P}(t/t-1)\underline{H}^T + \underline{R}_2]^{-1} \tag{5.13}$$

In some cases, the time period between a change in the input and the effect on the output is less than one whole period of delay. A state model representation for a process with nonstationary noise and no appreciable transport delay (f=0), as the case here, is given by Equation (4.44):

$$\begin{aligned} \underline{x}(t+1) &= \underline{A}\,\underline{x}(t) + \underline{G}\,\nabla\,\underline{u}(t) + \underline{\Gamma}\,\underline{a}(t+1) \\ \underline{y}(t) &= \underline{H}\,\underline{x}(t) \end{aligned} \qquad (4.44)$$

In this case, the simultaneous state estimator $\hat{\underline{x}}(t/t)$ is required for the control equation (5.3). Substitute Equation (5.10) into (5.9), with $\nabla\,\underline{u}_t$ replacing $\underline{u}_t$

$$\hat{\underline{x}}(t/t) = \underline{A}\,\hat{\underline{x}}(t-1/t-1) + \underline{G}\,\nabla\,\underline{u}(t-1)$$

$$+ \underline{K}[\underline{y}(t) - \underline{H}\,\underline{A}\,\hat{\underline{x}}(t-1/t-1) - \underline{H}\,\underline{G}\,\nabla\,\underline{u}(t-1)]$$

or

$$\hat{\underline{x}}(t/t) = [\underline{A} - \underline{K}\,\underline{H}\,\underline{A}]\hat{\underline{x}}(t-1/t-1) + [\underline{G} - \underline{K}\,\underline{H}\,\underline{G}]\nabla\,\underline{u}(t-1)$$

$$+ \underline{K}\,\underline{y}(t) \qquad (5.14)$$

The matrices $\underline{R}_1$ and $\underline{R}_2$ for this case are defined as

$$\begin{aligned} \underline{R}_1 &= \underline{\Gamma}\,\underline{\Sigma}\,\underline{\Gamma}^T \\ \underline{R}_2 &= \underline{0} \end{aligned} \qquad (5.15)$$

The nonstationary nature of disturbances leads to adjustment on the change of the manipulated variable $\nabla \underline{u}(t)$ in Equation (5.3). Thus,

$$\nabla \underline{u}(t) = - \underline{L}_\infty \hat{\underline{x}}(t/t) \tag{5.16}$$

When there is a time lag of f sampling periods, the state estimator for Equation (4.46) is given by

$$\hat{\underline{x}}(t+1/t) = \underline{A}\, \hat{\underline{x}}(t/t-1) + \underline{G}\, \nabla \underline{u}(t-f) + \underline{\Gamma}[\underline{y}(t) - \underline{H}\, \hat{\underline{x}}(t/t-1)] \tag{5.17}$$

The f-step ahead forecast $\hat{\underline{x}}(t+f/t)$ will then displace $\hat{\underline{x}}(t/t)$ in Equation (5.16).

(c) Constraining of the Input Variances:

In order to obtain smoothed control action, drastic changes of the manipulated variable $\nabla \underline{u}(t)$ are avoided. In addition, sometimes the feedback control matrix $\underline{L}_\infty$ calls for large input variations which are physically impossible, e.g. a valve reading to be 110% opened to suit the required control action. MacGregor [1973] suggested a procedure for control scheme design with constraints placed on the inputs. In essence, for a control matrix $\underline{L}_\infty$, the variances of $\underline{u}(t)$ and variance-covariance matrix of $\underline{y}(t)$ are calculated and this is repeated until these variances are acceptable. Various constraint matrices $\underline{Q}_1$ and $\underline{Q}_2$ can be tried for the design of $\underline{L}_\infty$.

The formulation of the input and output variances of the control equation (5.16) is given by MacGregor [1973]:

$$\text{Var}[\underline{y}(t)] = E[\underline{y}(t)\ \underline{y}^T(t)] = \underline{H}\ \underline{V}_x\ \underline{H}^T + \underline{R}_2 \tag{5.18}$$

$$\text{Var}[\nabla\ \underline{u}(t)] = E[\nabla\ \underline{u}(t)\ \nabla\ \underline{u}^T(t)] = \underline{L}_\infty[\underline{V}_x - \underline{P}^\infty(t/t)]\underline{L}_\infty^T \tag{5.19}$$

where $\underline{V}_x$ is the variance matrix of the state vector $\underline{x}(t)$ and is given by

$$\underline{V}_x = E[\underline{x}(t+1)\underline{x}^T(t+1)]$$

$$= \underline{W}\ \underline{V}_x\ \underline{W}^T + \underline{W}\ \underline{P}^\infty(t/t)\underline{L}_\infty^T\ \underline{G}^T + \underline{G}\ \underline{L}_\infty\ \underline{P}^\infty(t/t)\underline{W}^T$$

$$+ \underline{G}\ \underline{L}_\infty\ \underline{P}^\infty(t/t)\ \underline{L}_\infty^T\ \underline{G}^T + \underline{R}_1 \tag{5.20}$$

where

$$\underline{W} = [\underline{A} - \underline{G}\ \underline{L}_\infty] \tag{5.21}$$

$\underline{P}^\infty(t/t)$ is the converged solution of Equation (5.9) and (5.11). MacGregor [1973] shows that with one period of delay in the process dynamics, the variances of inputs and outputs are

$$\text{Var}[\nabla\ \underline{u}(t)] = \underline{L}_\infty\ \underline{V}_{\hat{x}}\ \underline{L}_\infty^T \tag{5.22}$$

$$\text{Var}[\underline{y}(t)] = \underline{H}\ \underline{V}_{\hat{x}}\ \underline{H}^T + \underline{\Sigma} \tag{5.23}$$

where $\underline{V}_{\hat{x}}$ of the state vector $\underline{x}(t+1/t)$ is

$$\underline{V}_{\hat{x}} = \underline{W}\ \underline{V}_{\hat{x}}\ \underline{W}^T + \underline{\Gamma}\ \underline{\Sigma}\ \underline{\Gamma}^T \tag{5.24}$$

In either case, an iterative solution to a matrix equation (5.20) or (5.24) is required to obtain Var[$\nabla \underline{u}(t)$] and Var[$\underline{y}(t)$]. Computer programs written in Fortran IV had been developed for the design of $\underline{L}_\infty$, $\underline{K}$ and the examination of the input, output variance-covariance matrices.

Reduction of Var[$\nabla \underline{u}(t)$] by constraining is at the expense of increasing Var[$\underline{y}(t)$], and the minimum variance values cannot be maintained. However, output variance will usually increase very slightly while a large reduction of Var[$\nabla \underline{u}(t)$] is obtained. Thus, the success of the constraining strategy is judged on the basis of relative changes in the input and output variances. An overall algorithm for the optimal stochastic control scheme is presented in Figure 5.1.

5.2.2 Controller Design for Reactor

A multivariate optimal stochastic feedback controller is designed for the dynamic-stochastic model in state space form, Equation (4.44) in which the change of the butane and hydrogen flowrates deviates are the inputs, while propane and butane extents deviates are the outputs. With the Kalman filter matrix $\underline{K}$ determined, the simultaneous estimator $\hat{\underline{x}}(t/t)$ is set up as in Equation (5.12). The results of $\underline{K}$ and the sets of equations of the estimator $\hat{\underline{x}}(t/t)$ are listed in Appendix 4.

The control matrix $\underline{L}_\infty$ is designed with the weighting matrix $\underline{C}^*$ chosen to be the identity matrix $\underline{I}$, that is, minimizing the

FIGURE 5.1: ALGORITHM OF OPTIMAL STOCHASTIC CONTROL DESIGN

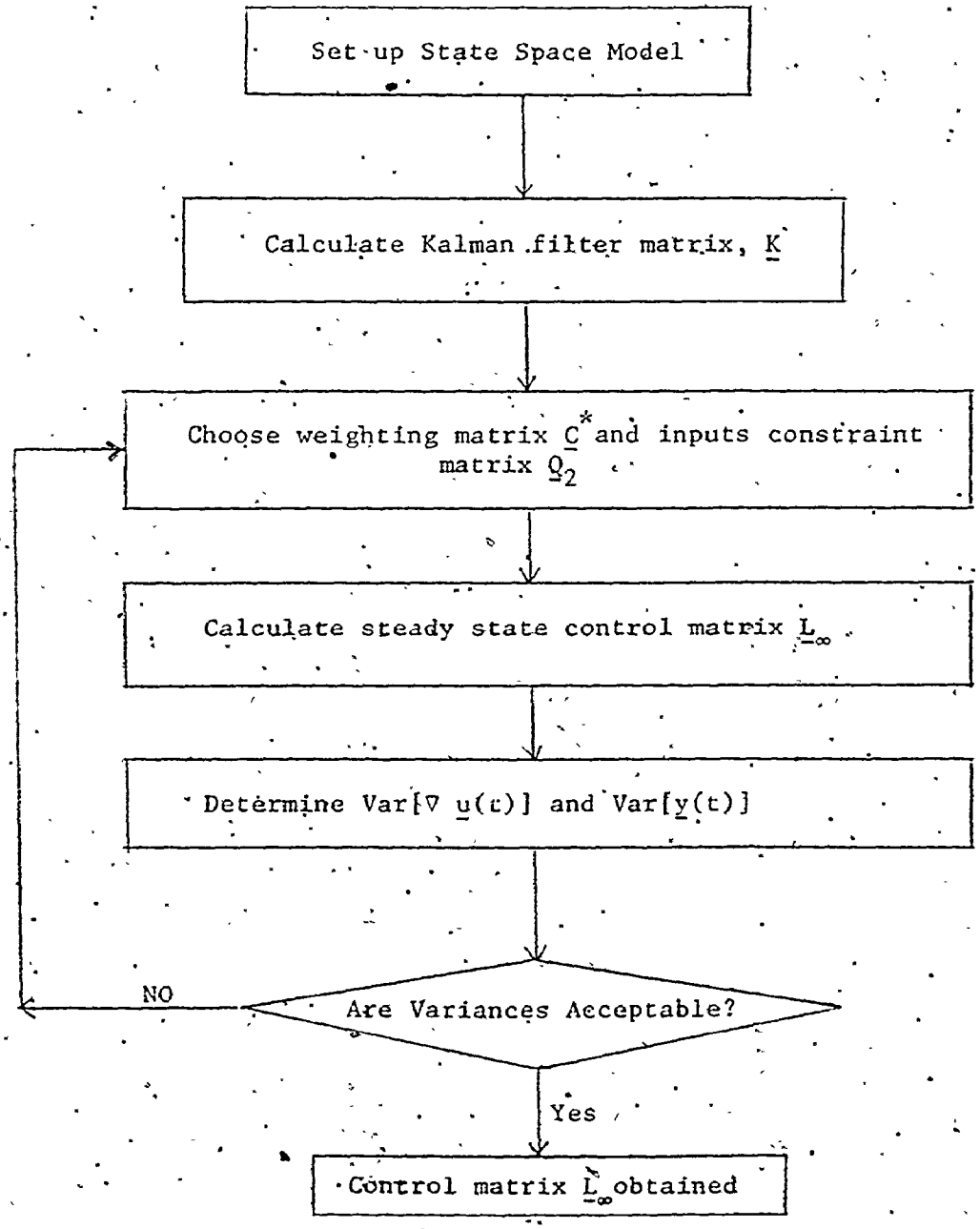

unweighted sum of the output variances of propane and butane extents. Various constraint matrices Q_2 for the input are tested and the theoretical results on the variances of input-output are given in Table 5.1. Optimal stochastic controllers have been designed for a number of different input variance constraint matrices Q_2. In general, as Q_2 becomes larger the variances of the output propane and butane extents increase. With equal weights on the input variances (2nd case), the variance of the hydrogen flow decreases rapidly while that of butane goes up. This is due to the fact that hydrogen flow variance is so much larger. The last three Q_2 matrices use unequal weighting in order to emphasise reduction on the variance of the butane manipulation. The control matrix L_∞ corresponding with the various Q_2 are given in Appendix 4. Generally, the output variance increases as larger restrictions are placed on the inputs manipulation, as indicated in Table 5.1. Some of the discrepancies may be due to computation round-off error. It is observed that a higher constraint is placed on the butane manipulation, thus ensuring a gradual butane flowrate change and preventing a sudden flux of this stream.

5.2.3 Simulation Studies on Controller Performance

Simulation studies of optimal stochastic control on the reactor are carried out in this section using the identified dynamic-stochastic model equation (4.44) of the reactor and the derived optimal stochastic controller equation (5.16) and (5.17). The simulations are used to confirm the optimal controller design

calculations prior to implementing the controller on the actual reactor. They also provide an insight of the performance of various optimal feedback controllers from the information of the predicted input manipulation and the output data. All the design cases discussed in the previous section are simulated. Two white noise sequences are used to simulate the output propane and butane extents. In this case, for simplicity, the residuals resulted from the model fitting in Chapter 4 are fed into Equation (5.25) with $\nabla \underline{u}(t)$ and $\underline{x}(t)$ set initially to be zero. The states $\underline{x}(t+1)$ and its estimators $\hat{\underline{x}}(t+1)$ are updated simultaneously with Equation (5.17) for the calculation of the $\nabla \underline{u}(t)$ and $\underline{y}(t)$. An algorithm of this simulation is outlined in Figure 5.2, given the state space model

$$\begin{aligned} \underline{x}(t+1) &= \underline{A}\,\underline{x}(t) + \underline{G}\,\nabla\underline{u}(t) + \underline{\Gamma}\,\underline{a}(t) \\ \underline{y}(t+1) &= \underline{H}\,\underline{x}(t+1) \end{aligned} \tag{5.25}$$

The simulation results corresponding to the cases of Table 5.1 are given in Table 5.2. It can be seen that the simulation results on the input-output variances agree quite well with the theoretical cases. The simulated outputs in extent deviates and the control actions in terms of input flowrates related to the 4th case in Table 5.2 are plotted in Figure 5.3 and 5.4. The large variation of the simulated hydrogen flowrate could be resulted from its slightly inadequate transfer functions with the output responses in Equation (4.41).

TABLE 5.1: THEORETICAL VARIANCES OF INPUTS AND OUTPUTS OF THE TWO INPUTS-TWO OUTPUTS DYNAMIC-STOCHASTIC MODEL EQUATION (4.44) UNDER VARIOUS INPUT CONSTRAINTS

	Constraint Matrix Q_2	$Var[\nabla u_{C_4H_{10}}]$	$Var[\nabla u_{H_2}]$	$Var[y_t]$
1	$\begin{bmatrix} 0 & 0 \\ 0 & 0 \end{bmatrix}$	0.103	8.22	$\begin{bmatrix} 48.5 & 76.4 \\ 76.4 & 124.6 \end{bmatrix}$
2	$\begin{bmatrix} 1 & 0 \\ 0 & 1 \end{bmatrix}$	0.140	3.14	$\begin{bmatrix} 49.0 & 75.9 \\ 75.9 & 125.4 \end{bmatrix}$
3	$\begin{bmatrix} 50 & 0 \\ 0 & 1 \end{bmatrix}$	0.046	4.02	$\begin{bmatrix} 49.2 & 76.8 \\ 76.8 & 125.9 \end{bmatrix}$
4	$\begin{bmatrix} 75 & 0 \\ 0 & 10 \end{bmatrix}$	0.057	1.13	$\begin{bmatrix} 51.3 & 74.2 \\ 74.2 & 132.6 \end{bmatrix}$
	$\begin{bmatrix} 100 & 0 \\ 0 & 25 \end{bmatrix}$	0.052	0.0625	$\begin{bmatrix} 53.8 & 70.9 \\ 70.9 & 139.5 \end{bmatrix}$

where $\underline{y}_t = \begin{bmatrix} C_{1,t} \\ C_{2,t} \end{bmatrix}$

and the control equation is given by Equation (5.16) $\nabla \underline{u}(t) = -L \underline{x}(t/t)$.

TABLE 5.2: SIMULATION RESULTS FOR THE VARIANCES OF INPUT FLOWRATE MANIPULATIONS AND OUTPUT PROPANE AND BUTANE EXTENTS

	Constraint Matrix Q_2	$\mathrm{Var}[\nabla u_{C_4H_{10}}]$	$\mathrm{Var}[\nabla u_{H_2}]$	$\mathrm{Var}[\underline{y}(t)]$
1	$\begin{bmatrix} 0 & 0 \\ 0 & 0 \end{bmatrix}$	0.101	8.57	$\begin{bmatrix} 48.9 & 76.9 \\ 76.9 & 125.2 \end{bmatrix}$
2	$\begin{bmatrix} 1 & 0 \\ 0 & 1 \end{bmatrix}$	0.142	3.08	$\begin{bmatrix} 49.6 & 76.4 \\ 76.4 & 125.7 \end{bmatrix}$
3	$\begin{bmatrix} 50 & 0 \\ 0 & 1 \end{bmatrix}$	0.046	3.97	$\begin{bmatrix} 50.5 & 78.3 \\ 78.3 & 125.9 \end{bmatrix}$
4	$\begin{bmatrix} 75 & 0 \\ 0 & 10 \end{bmatrix}$	0.061	0.927	$\begin{bmatrix} 53.3 & 76.3 \\ 76.3 & 131.0 \end{bmatrix}$
5	$\begin{bmatrix} 100 & 0 \\ 0 & 25 \end{bmatrix}$	0.058	0.430	$\begin{bmatrix} 55.9 & 74.6 \\ 74.6 & 132.2 \end{bmatrix}$

$$\underline{y}(t) = \begin{bmatrix} \text{propane extent deviates} \\ \text{butane extent deviates} \end{bmatrix}$$

FIGURE 5.2: ALGORITHM OF THE SIMULATION STUDY

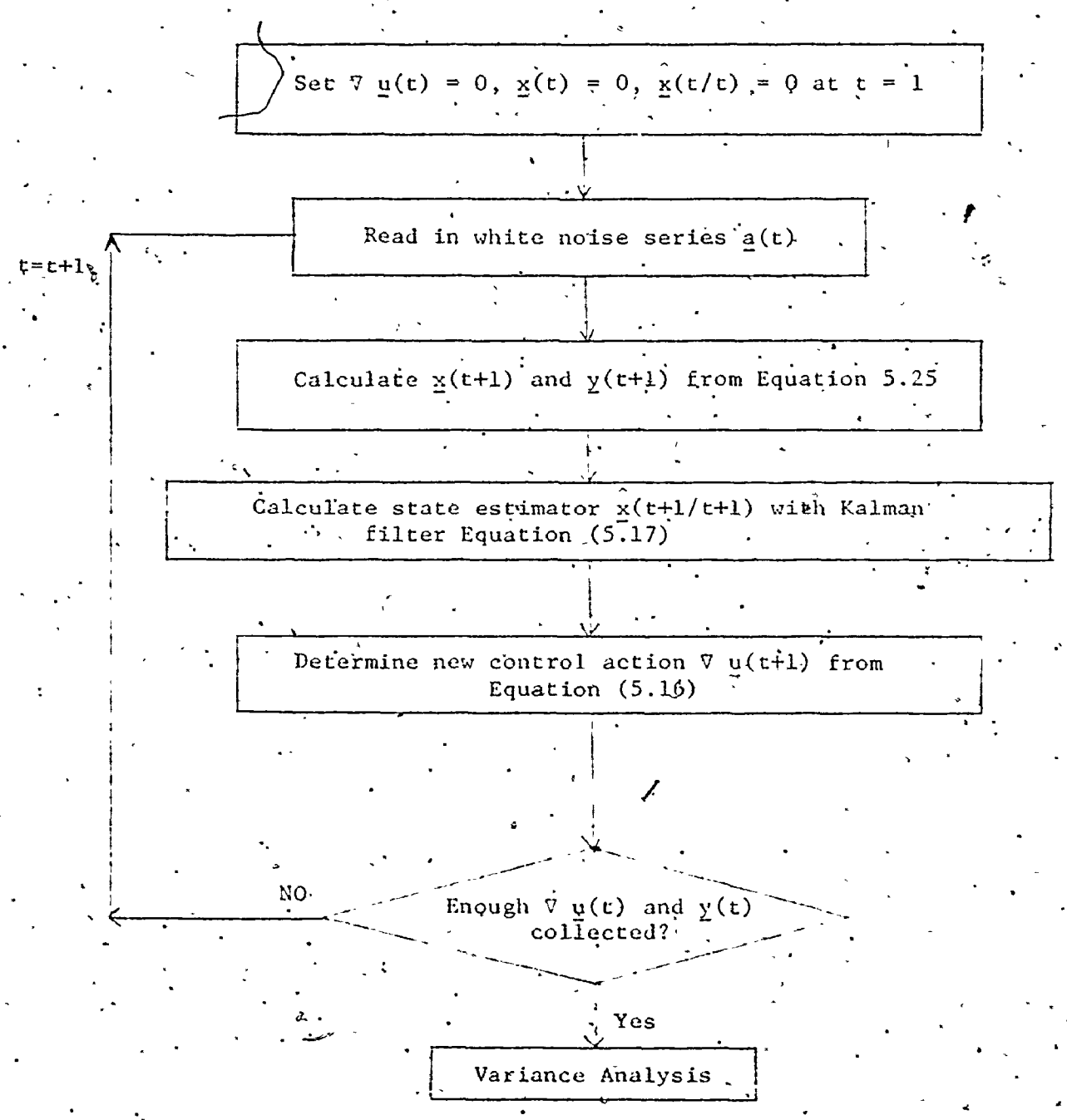

FIGURE 5.3: SIMULATED OUTPUT EXTENTS

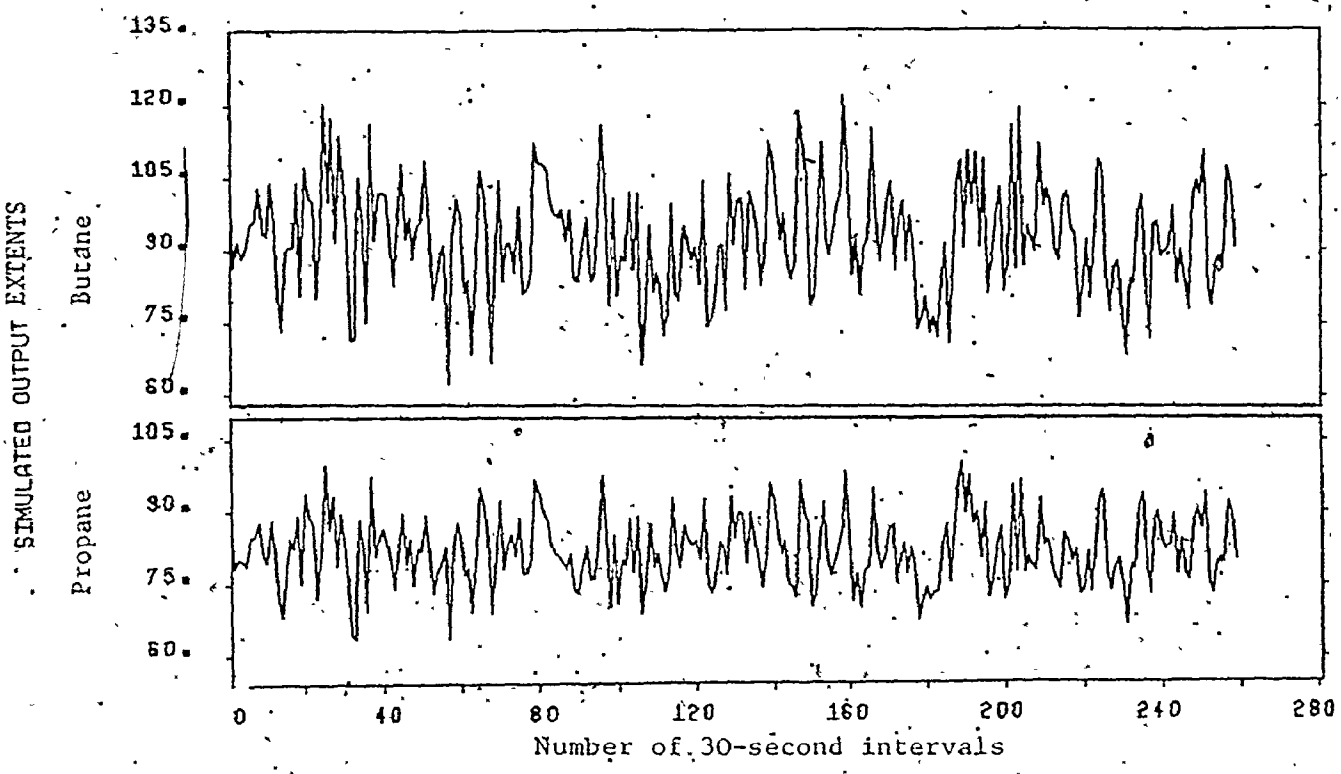

FIGURE 5.4: SIMULATED INPUT FLOWRATES

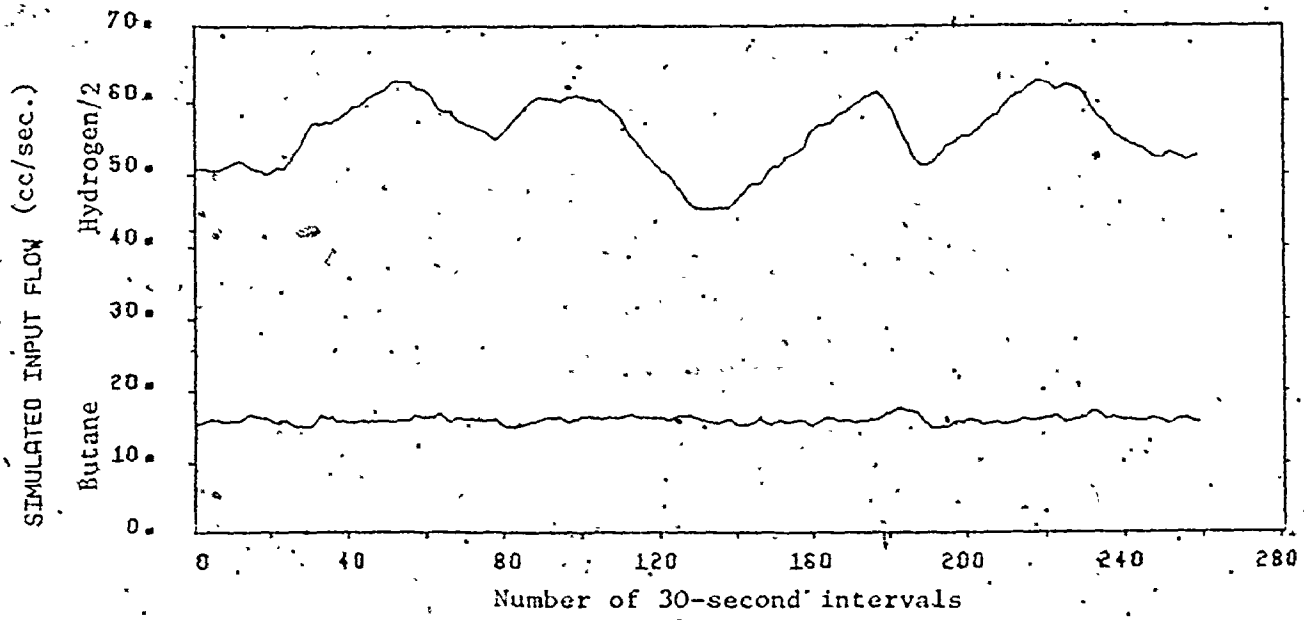

5.3 On-Line Control Studies

5.3.1 Controller Implementation

With the optimal stochastic feedback controller properly selected, a schematic control flow diagram is shown in Figure 5.5. Because the coolant oil temperature dynamic response is very slow the wall temperature cannot be used as the manipulated variable, although it is used to adjust the reactor conditions to give the desired level of steady state conversion and selectivities. Also it is used in this study as a load disturbance to test the control algorithm. The axial temperature profile and the flowrates during the preceding interval are used to predict the output responses every 30 seconds. The parameters of the prediction equation (4.14) are updated by RLS whenever new concentration data are available, presumably every 6 minutes. The multivariate feedback controller will then adjust the input flow accordingly.

The control software written in real time Fortran IV was developed and incorporated into the basic reactor software in Section 3.3.3. The sampling interval is arbitrarily chosen to be 30 seconds. Jután [1976] used an interval of 60 seconds while Tremblay [1977] chose 30 seconds for the model reference control scheme on this reactor. It had been shown that (MacGregor [1975]) more frequent control i.e. a short sampling interval does not necessarily improve the control efficiency. No attempt was made at selecting the optimal sampling interval. Since in previous work, a 30 second period was shown to be adequate, it was used in this study. In hindsight, this was probably

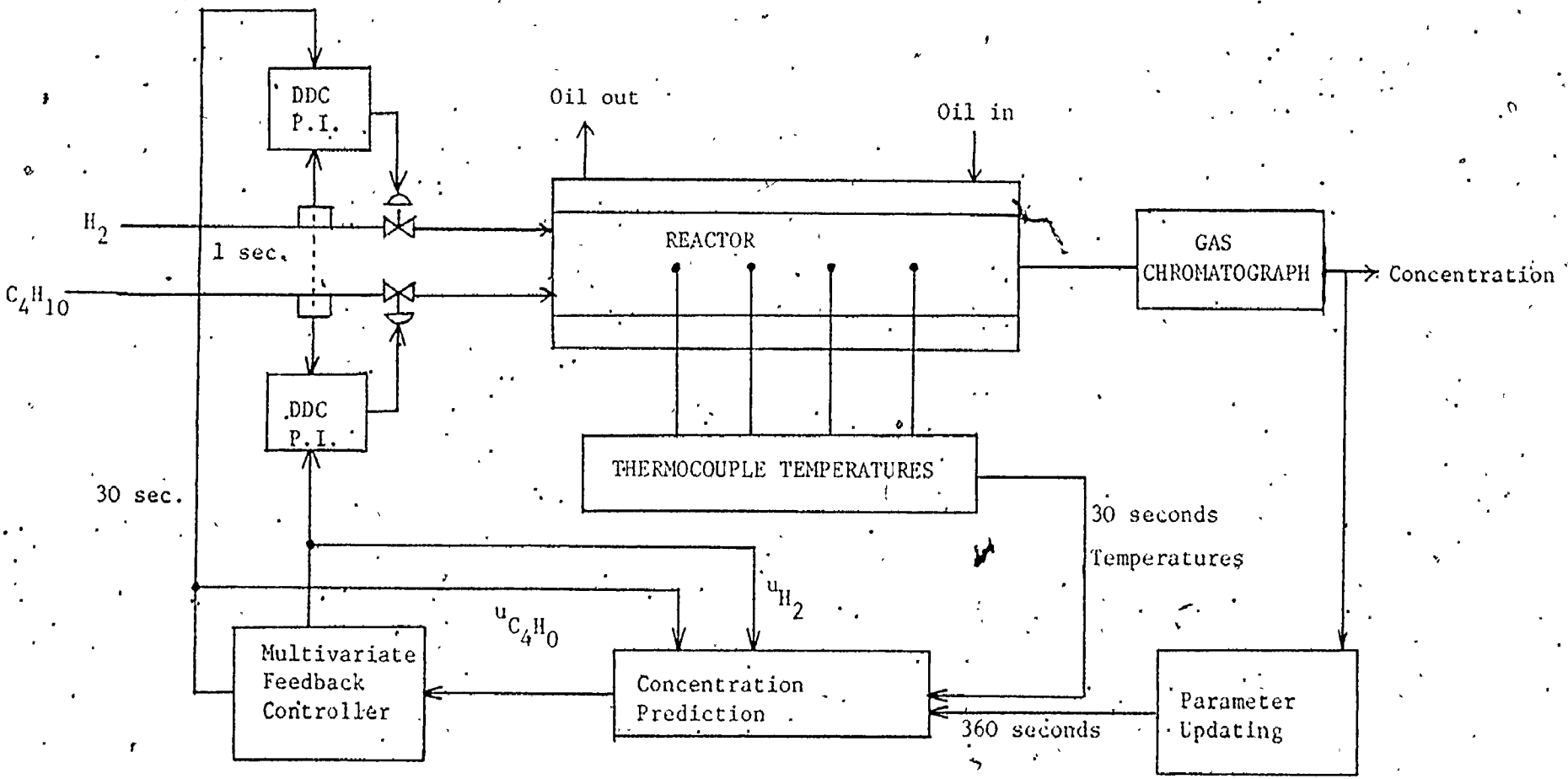

FIGURE 5.5: SCHEMATIC DIAGRAM OF ON-LINE CONTROL STUDY

a poor choice because it was not an integral multiple of the basic 12-second cycle time of the thermocouple multiplexer. However, all the 12-second temperature measurements were filtered by the digital filter $T(t) = 0.5T(t-1) + 0.5\ T_r$ and the error from this lack of synchronization of temperature can be somewhat reduced. The overall control algorithm is given in Figure 5.6.

The objective of the control algorithm is to hold the predicted propane and butane extents about their set points. Thus, the performance index used in this study is defined as the sum of squares of the output extent deviates from these set points.

In order to improve the parameter updating procedure, a modified version of Equation (4.16) is adopted here. An extra parameter β_o which is initially set to zero is added in each row with the corresponding variate Z_o being 1. These β_o's are used to provide extra flexibility in the prediction equation in case the reaction conditions during the implementation are different from those at the time the data was collected for fitting. The prediction parameters can then adapt to the new conditions more rapidly. On the other hand, if the shift in reaction condition is minimal, these β_o parameters will remain small. Thus, the inferential concentration prediction can be rewritten as:

$$\underline{C}_t = [\underline{\beta}_o \;\vdots\; \underline{\beta}] \left[\frac{1}{\underline{Z}_t}\right] \qquad (5.26)$$

The controller matrix corresponding to the uneven constraint matrix of case 4 in Table 5.1 was chosen for this study. The constraints placed on the input streams are high enough such that drastic change in

FIGURE 5.6: MULTIVARIATE FEEDBACK CONTROL ALGORITHM

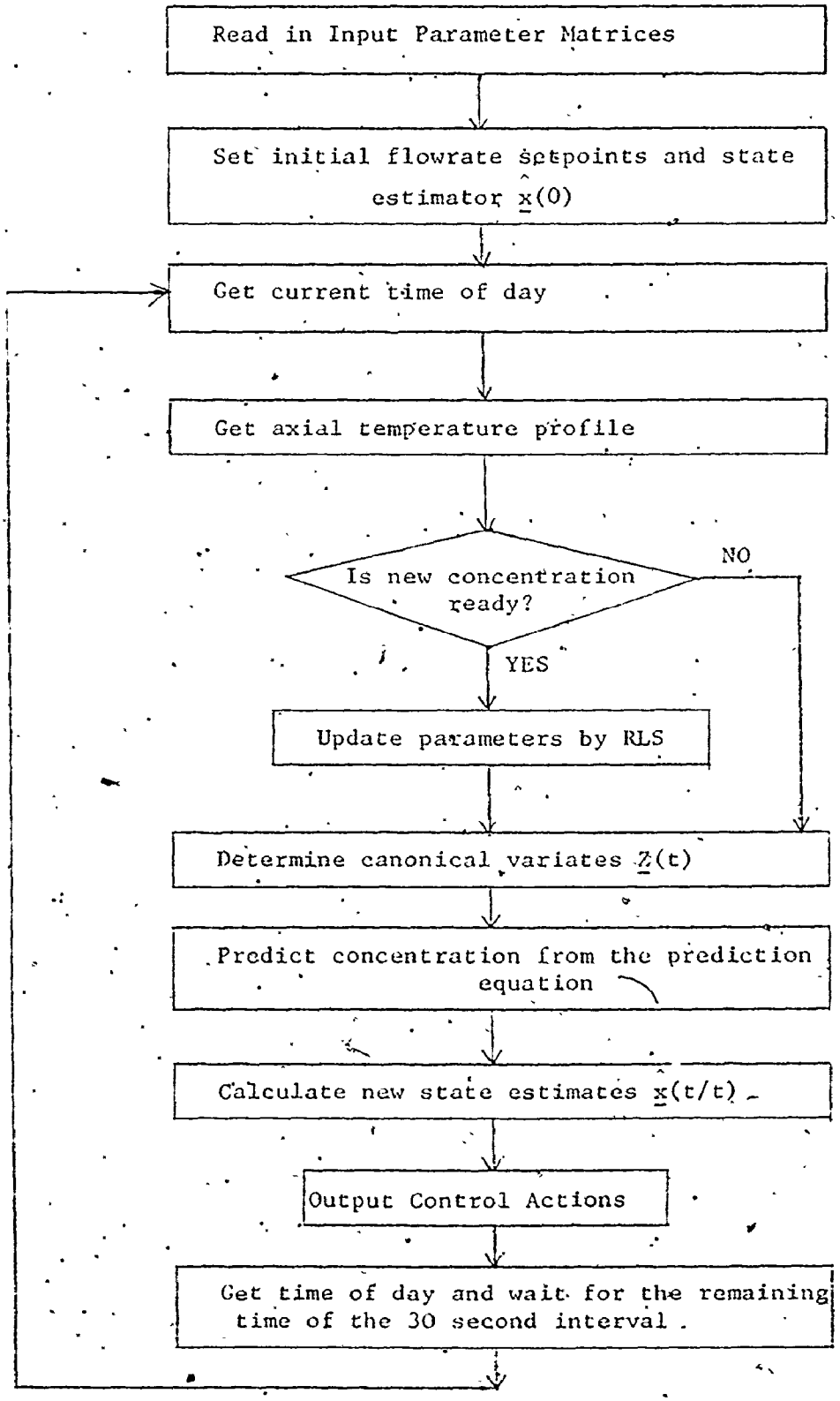

flowrate is avoided. At the same time, the variance of the controlled variables increases about only 5 to 10 percent from the unconstrained controller. Although theoretically the first two cases show smaller variances of the output responses, the variations of the manipulated inputs may be too large in practice and these lower values may not be attained easily.

5.3.2 Controller Performance

During the implementation some problems were encountered in the operation of the contact senses which supervise the transmission of analyzed output concentrations from the chromatograph to the computer. In most cases, only 9 to 10 analysis cycles of concentration were obtained before contact sense failure occurred. Thus, a compromise approach was adopted during the control run. Before the implementation of the multivariate controller, a univariate PI controller which manipulated the butane flowrate was used to bring up the reactor axial temperatures to the desired profile. The gas chromatograph was then initiated for analysis and the parameter updating procedure was also started. After a few cycles of parameter updating, the multivariate feedback controller was implemented. The results from one such control run are given in Figure 5.7 to 5.11, with the wall temperature set at 245°C.

From Figure 5.7 it can be seen that the switch from PI control to multivariable control induces large changes in the input flowrates. These transient effects also cause large fluctuations of the predicted

FIGURE 5. 7: PREDICTED EXTENTS x 10^6 AND HOT SPOT TEMPERATURE

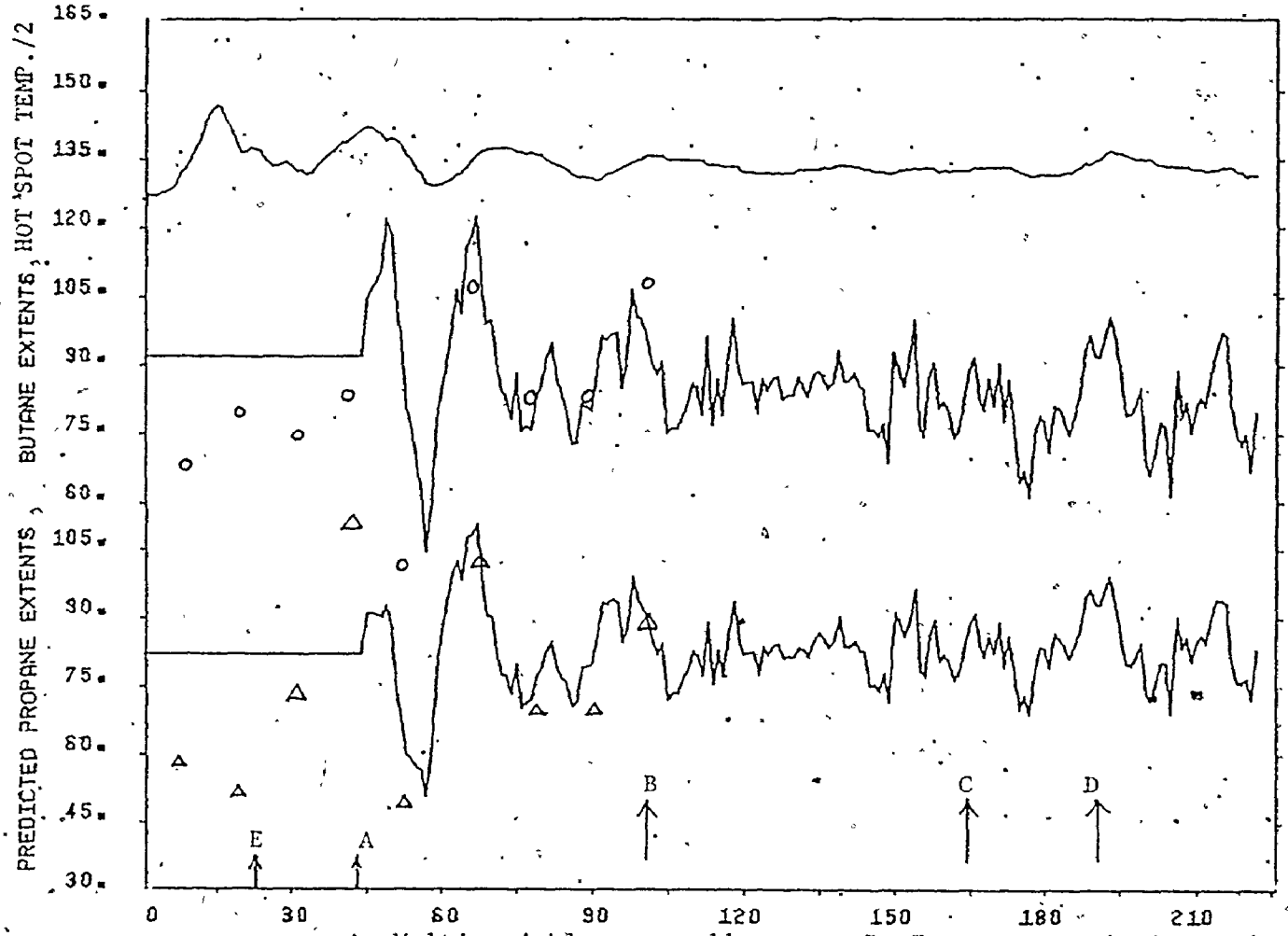

FIGURE 5.8: ACCUMULATED OBJECTIVE FUNCTION x 10^8

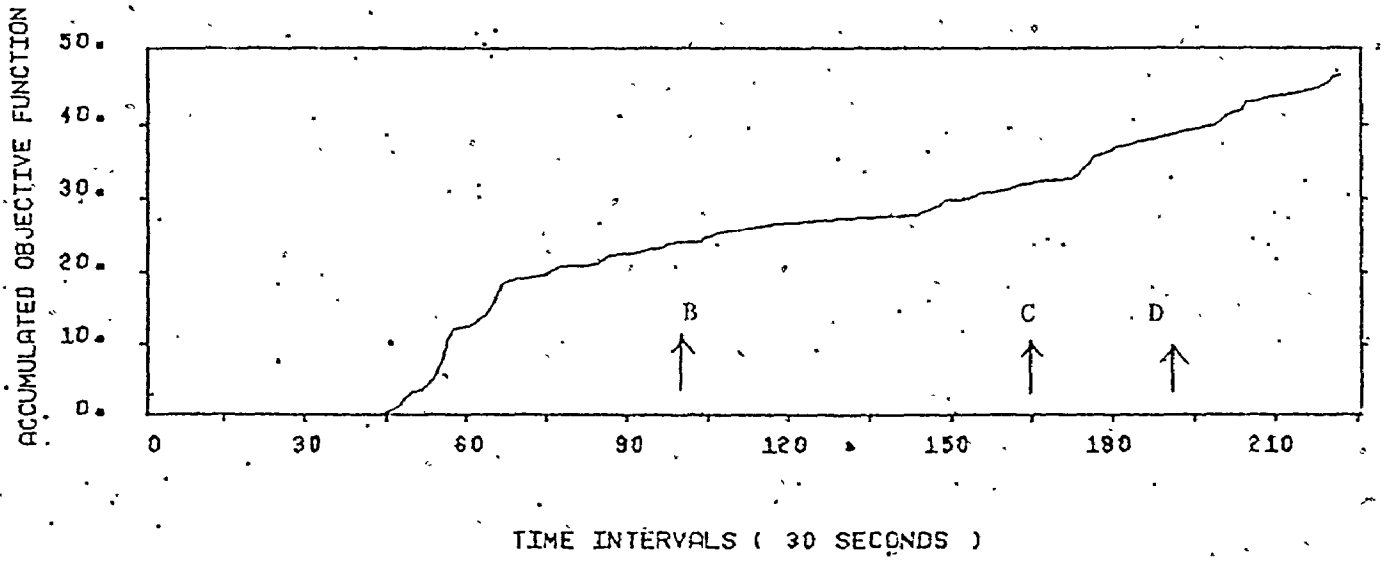

FIGURE 5.9: HYDROGEN AND BUTANE FLOWRATE

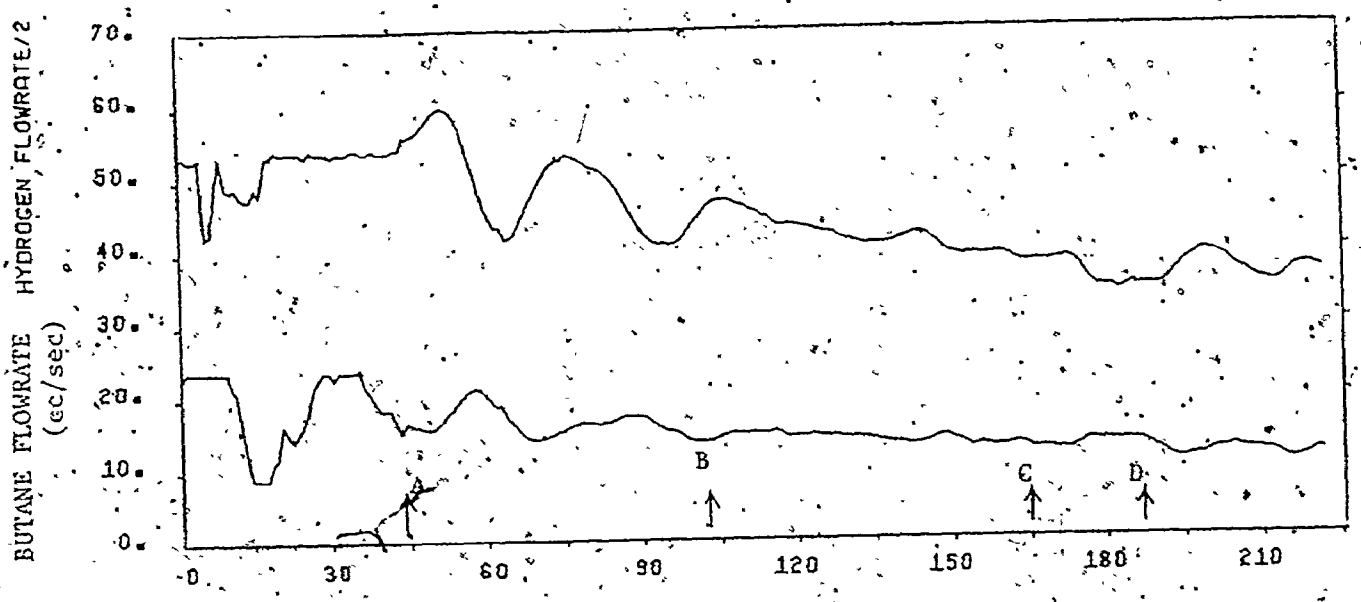

FIGURE 5.10: TOTAL INPUT FLOWRATES AND FLOW RATIO

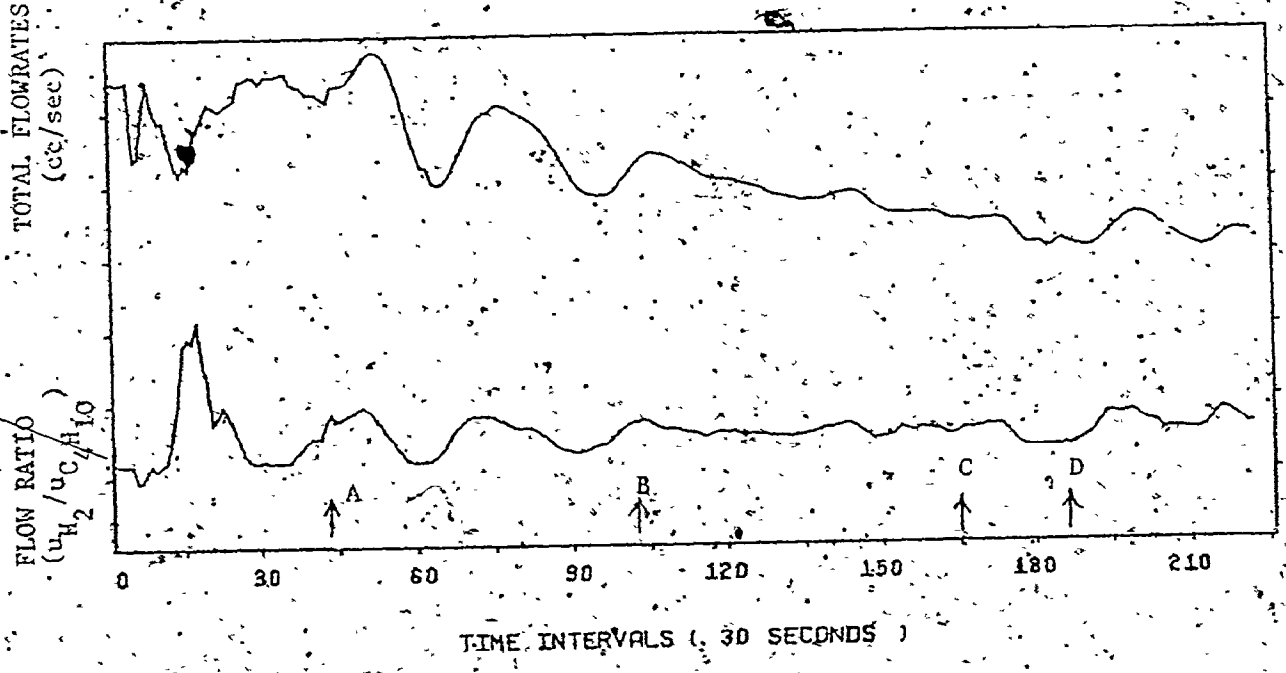

FIGURE 5.11: AVERAGE TEMPERATURE PROFILE

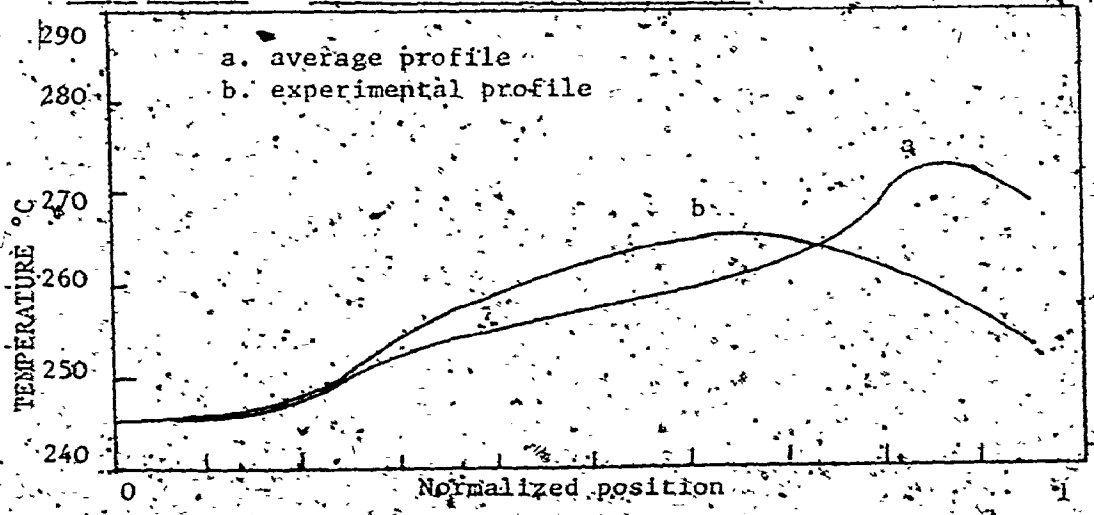

extent values. In addition, since the parameters in the prediction equation for the extents were updated only three times, the estimation equation may not be satisfactory at the time of switching to the multivariable controller. As the prediction model parameter estimates improve, so will the predicted extents. After approximately 100 30-second time intervals and nine chromatograph analyses the contact sense failed and no more analyses were available. By this time (point B in Figure 5.7) the β parameters are apparently reasonably satisfactory, and the predicted propane and butane extents are close to the measured values. Due to the limited availability of measured output extents, a more detailed comparison of the predicted and the measured extents is not feasible. However, it can be seen from the few comparisons that the predicted extents adapt quite well to fit the measured values.

The performance of the multivariable controller must also be evaluated on the basis of the predicted extents because of the absence of actual measured extents in the latter part of the run. After the initial transients due to switch over from the PI controller and updating of the prediction equation have died out, the multivariable controller performs very well as seen by the fact that the predicted extents are held very close to their target values between points B and C in Figure 5.7. The variances of propane and butane extents are found to be 27.8×10^{-12} and 43.3×10^{-12} respectively, during this period. They are considerably lower than the theoretical and simulated values in Table 5.1 and 5.2. The rate of rise of the performance index (Figure 5.8) is quite small during this period and the manipulated

input flows are much amoother and more stable than they were under PI control. The hot spot temperature was maintained relatively constant compared with that during PI control and the normalized position of the hot spot (0.61 from the top of the reactor) had shifted somewhat towards the centre of the reactor. Also, the hot spot temperature is lower than the one under PI control (a 19°C rise opposed to 27°C) and generally the temperature profile is flattened out. Yet, the production rate of propane and butane were maintained under this lower temperature profile.

In order to test the robustness of the controller, the wall temperature was dropped to 243°C at point C in Figure 5.7. The butane flowrate increased slightly while the hydrogen flow decreased. The controller performed quite well and was able to keep the reaction from dying out. After an initial drop in the predicted extents they soon recovered to near their target values. This can be seen as a slightly steeper rise in the objective function just after the drop in the wall temperature followed by a return to a more gentle rise. Because a low hydrogen flow limit had been imposed at 65 cm^3/sec at STP, the hydrogen flowrate remained at that level. After 10 minutes, the oil temperature was raised back to 245°C (point D) and consequently, the hydrogen and butane flowrates returned to near their level prior to the step change. Due to the controller encountering the hydrogen flow lower limit and due also to the relatively short duration of the test, the controller performance to such a change may be inconclusive.

It is noted that both hydrogen and butane flowrates decrease continuously although their flow ratio ($u_{H_2}/u_{C_4H_{10}}$) is maintained relatively constant, about 6:1 as shown in Figure 5.10.

A plausible explanation for the falling flowrate could be that the heat losses from the reactor are becoming less and gradually an equilibrium would be reached as the run proceeds.

The parameters in the inferential concentration prediction equation after 9 cycles of updating are shown in Equation (5.27):

$$\begin{bmatrix} C_1 \\ C_2 \\ C_3 \end{bmatrix} = \begin{bmatrix} -.6364E\text{-}06 & .2269E\text{-}04 & .1904E\text{-}05 & -.1316E\text{-}05 \\ -.1122E\text{-}05 & .2806E\text{-}04 & -.2807E\text{-}06 & -.6293E\text{-}06 \\ -.3817E\text{-}05 & .3732E\text{-}04 & -.2740E\text{-}05 & .1298E\text{-}05 \end{bmatrix} \begin{bmatrix} 1 \\ Z_1 \\ Z_2 \\ Z_3 \end{bmatrix} \quad (5.27)$$

Comparing with the fitted parameters in the prediction equation (4.14), large changes are observed except for those parameters corresponding to the most significant canonical variate Z_1. This is expected because the parameters associated with Z_3 and to a certain extent Z_2 had very large confidence intervals as shown in Table 4.1b. This confirms the belief that Z_1 and Z_2 contain most of the prediction information in the set of temperatures and flowrates. The β_o parameters are changed from o to some values in the first column, thus different operating conditions from those during data collection were encountered. Unfortunately, since only a limited amount of measured concentration data was available, the parameters were not updated continuously.

Throughout the run, the slight offset in butane extent prediction in Figure 5.7 could have resulted from these imperfect parameters which cannot adapt efficiently to any further changes in the reactor system. However, the inclusion of integral action in the controller should be able to eliminate this offset. The inability to cancel out the offset might be due to the integral action not being large enough. If the reactor is under controlled for an extended period of time the offset is expected to disappear eventually.

The catalyst used in this particular run was prepared about 5 days before the run and thus was quite fresh. Because this catalyst and the one used for the model fitting were not from the same batch, discrepancies in the catalyst characteristics are expected to exist, such as the catalyst activity. From previous experiments, it is believed that catalyst activity does not change significantly during a run. Rather, gradual deactivation probably occurs during reactor startup or shutdown sequences. The different catalyst properties may account for most of the changes in reactor conditions.

From this and several other similar control runs, it can be concluded that proper parameter updating is the key to successful implementation of this particular multivariable controller from an empirical model. A performance comparison with the controller designed by Jutan from theoretical physical equations may be premature due to the contact sense problem. Nevertheless, it can be seen that this controller is able to control the output production rates about their target values and the control action is considerably smoother than a univariate PI controller.

CHAPTER 6.

CONCLUSION AND FUTURE WORK

The modelling of complex chemical systems has always been a major problem in the studies of the application of modern control theories. Traditional process modelling based on theoretical material and energy balances are usually time consuming and tedious. In view of this, an alternative modelling route is presented here, which is relatively simple and easily applicable to chemical processes.

An empirical multivariate transfer function-noise model describing the dynamic and stochastic behaviour of a pilot plant catalytic reactor was built, based on plant input-output data. A statistical approach using the concept of multivariate time series and transfer functions was applied. Efficient modelling was achieved by the identification of process dynamics and stochastic noise structures, the estimation of the model parameters and the diagnostic checking of the fitted model by some statistical tests. A fairly adequate two input-two output model was obtained for the reactor. A low order (9th) state space model was then obtained by the minimal realization of the multivariate transfer function-noise model.

Reactor exit concentrations were inferred from measured temperature and input flowrate variables using a prediction equation

based on canonical predictor variables. This procedure was found to give better predictions and to be successful in reducing the correlations among the temperature variables. Also, the dimensionality of the effluent extent series was reduced to two by another canonical analysis, while still retaining most of the information on the process.

Multivariate optimal stochastic controllers were derived from the identified 9-th order state space model using Kalman filtering theory and dynamic programming. Despite the difficulties in the contact sense operations encountered during the implementation run, the performance of the controller was quite satisfactory and considerably better than a univariate PI controller. Parameter updating on the prediction of exit concentrations played a key role in this particular case due to the shifting of reactor conditions.

As a comparison with Jutan's [1976] theoretical multivariate model on this reactor, the empirical model is relatively easy to be developed. However, there is no intention to claim this approach to be superior. Rather, an alternate modelling procedure is presented here and the modelling choice will depend on the particular circumstances. The addition of integral actions to the controller should eliminate the offsets of the controlled exit extents despite the presence of load changes, thus maintaining a steady output product rate.

Future Work on the Reactor

Certain improvements on this work can be suggested here. Because of the success of dimensionality reduction, it might be interesting

to express the outputs as linear combinations of the various extents. This would eliminate the high correlations among the predicted extents as well as the occurrence of the highly correlated parameter estimates in the transfer function model. Also, perturbation with higher variations could be added to the hydrogen flowrate during the data acquisition, thus improving the identification of the corresponding dynamics.

After eliminating the problem with the contact sense it might be worthwhile performing further, more comprehensive runs with the present multivariate stochastic controller in order to evaluate its performance better.

NOMENCLATURE

$\underline{A}$	Dynamic state matrix.
$\underline{a}_t$	Vector of white noise sequence.
$\underline{B}$	Control matrix.
B	Backward shift operator.
$\underline{b}_t$	Intermediate series.
b	Dead time delay.
$\underline{C}^*$	Weighting matrix.
C_i	Concentrations of outputs in extents, g.mole/sec. $i = \begin{cases} 1, \text{ propane} \\ 2, \text{ butane} \\ 3, \text{ hydrogen} \end{cases}$
$\underline{D}$	Dispersion matrix of residuals.
d_t	'dither' noise series.
d	Order of differencing.
E( )	Expectation value.
e_t	Univariate output residual series.
$\underline{F}$	Vector of temperature functions.
$\underline{G}$	Control matrix.
$\underline{H}$	Measurement matrix.
$\underline{I}$	Identity matrix.
$\underline{J}$	Element matrix of the Hankel matrix.
$\underline{K}$	Kalman filter matrix.

$\underline{K}_w$ Weighting matrix, (4.16).

k Number of lags.

$\underline{L}$ Matrix for the non-singular canonical transformation.

$\underline{L}_\infty$ Steady state feedback gain.

$\underline{\ell}$ Vector of linear combination.

$\underline{M}$ Vector of measured variables.

m Number of output variables.

N Terminating time period of control.

$\underline{N}_t$ Stochastic noise series.

$\dot{\underline{N}}$ Vector of canonical variates.

$\hat{\dot{\underline{N}}}(1)$ One step ahead forecast of $\dot{\underline{N}}$.

n Number of input variables.

$\underline{P}$ Parameter matrix, (4.1), covariance matrix of $\hat{\underline{x}}$, (5.11).

p Order of autoregressive operator.

$\underline{Q}$ Parameter matrix, (4.1).

$\underline{Q}_i$ Positive definite matrices, (5.1) and (5.2).

q Order of moving average operator.

$\underline{R}_i$ Variance-covariance of white noise series, (2.31).

$\underline{R}^*$ Parameter matrix for prediction equation, (4.2)

R Rate of reaction.

r	Sample autocorrelation function.
r_{ij}	Order of δ parameters in transfer function.
$\underline{S}_{ij}$	Hankel matrix, (2.34).
$\underline{S}^*$	Parameter matrix for prediction equation, (4.2).
s_{ij}	Order of ω parameters in transfer function.
T	Temperature deviations, °K.
t	Discrete time interval, sec.
$\underline{U}(B)$	Canonical form of transfer function, (2.18).
$\underline{U}_j$	Controllability matrix, (2.34).
$\underline{u}_t$	Vector of input variables.
$\underline{V}(B)$	Transfer function matrix.
$\underline{V}_i$	Observability matrix, (2.34).
$v_{ij,k}$	Impulse response function.
$\underline{v}_t$	White noise sequence due to measurement error.
$\underline{w}_t$	White noise sequence due to disturbances and modelling error.
$\underline{X}$	Vector of independent variables.
$\underline{x}_t$	State vector at sample time t.
$\hat{\underline{x}}(t/t)$	State estimate (simultaneous) of $\underline{x}$.
$\underline{Y}$	Vector dependent variables.
$\underline{y}$	Vector of output variables.
$\underline{V}_x$	Variance matrix of state estimator.

$\underline{Z}$ Vector of canonical variates.

$\underline{\alpha}_t$ Input white noise series.

α_f Filtering constant, (4.1).

$\underline{\beta}$ Parameter vector of the prediction equation, (4.11).

σ Standard deviation of series.

λ Eigenvalues of the generalized eigen problem, (4.8).

λ_f Forgetting factor, (4.18).

$\underline{\lambda}$ Vector of constraint, (5.8).

$\underline{\xi}$ Independent variable vector, (4.18).

ε Output error.

δ Dynamic parameter (denominator) of transfer function.

ω Dynamic parameter (numerator) of transfer function.

ϕ Autoregressive operator.

θ Moving average operator.

ψ Ratio of θ to ϕ polynomial.

π Ratio of ϕ to θ polynomial.

δ_{ts} Unit variable (either 0 or 1).

τ Total time intervals or continuous time

μ Mean value of time series.

μ_i Roots of the determinantal equation, (4.36).

Σ	Variance-covariance matrix.
χ^2	Chi-square statistics.
$\underline{\Gamma}_u(k)$	Autocovariance matrix at lag k.
$\underline{\Gamma}_{u\alpha}(k)$	Cross-covariance matrix at lag k.
$\underline{Y}$	Eigenvectors.
Λ	Ratio of generalized variances, (4.40).
∇^d	dth difference operator.
ρ_k	Autocorrelation function.
ϕ_{kk}	Partial correlation function.

Subscripts and Superscripts:

T	Transpose of a matrix.
$\hat{}$	Denotes estimates e.g. $\underline{\hat{x}}(t)$.
∞	Subscript infinity refers to steady state.
$-$	Denotes vector or matrix.
$\cdot$	Denotes derivative with respect to time $\dot{x} = dx/dt$ or canonical variate $\dot{N}_t$
i	Denotes individual output.
j	Denotes individual input.
+	Dynamic part of state vector, $\underline{x}^+(t)$.
*	Stochastic part of state vector, $\underline{x}^*$ or canonical form of eigenvalues, λ^*

REFERENCES

1. Akaike, H., "A New Look at the Statistical Model Identification", IEEE, Automatic Control, 716, Vol. AC-19, No. 6, Dec. (1974).

2. Alavi, A.S., "Multivariable Extensions of Box-Jenkins Time Series", Ph.D. Thesis, University of Lancaster, England. Nov. (1973).

3. Anderson, T.W., "An Introduction to Multivariate Statistical Analysis", John Wiley & Sons Inc., New York, (1958).

4. Astrom, K.J., "Introduction to Stochastic Control Theory", Academic Press, New York, (1970).

5. Astrom, K.J., Borisson, V., Ljung, L., and Wittenmark, B., "Theory and Application of Adaptive Regulators Based on Recursive Parameters Estimation", Preprint, 6-th IFAC World Congress, Boston, (1975).

6. Box, G.E.P., Hunter, W.G., MacGregor, J.F. and Erjavec, J., "Some Problems Associated with the Analysis of Multiresponse Data", Technometrics, Vol. 15, No. 1, Feb. (1973).

7. Box, G.E.P. and Jenkins, G.M., "Time Series Analysis - Forecasting and Control", Holden Day, San Francisco, (1970).

8. Box, G.E.P. and MacGregor, J.F., "Parameter Estimation with Closed-Loop Operating Data", Technometrics, Vol. 18, No. 4, 371, Nov. (1976).

9. Box, G.E.P. and Tiao, G.C., "A Canonical Analysis of Multiple Time Series", Tech. Report No. 428, Department of Statistics, University of Wisconsin, Madison, Wisconsin, (1976).

10. Beckman Instrument Inc., Analyzer and Programmer Units, Model 6700 Process Gas Chromatograph Systems Operating Manual, Fullerton, California, (1973).

11. Data General Corporation, Real Time Disk Operating System Reference Manual, 7th Revision, 093-000075-07, Southboro, Massachusetts, (1975).

12. Data General Corporation, User's Manual Program: Relocatable Math Library Files, Tape 099-000001, Southboro, Massachusetts, (1973).

13. Ferguson, N.B. and Finlayson, B.A., "Transient Chemical Reaction Analysis by Orthogonal Collocation", Chem. Eng. J., 1, 372, (1970).

14. Finlayson, B.A., "Method of Weighted Residuals and Variational Principles", Acad. Press, New York, (1972).

15. Fisher, D.G. and Seborg, D.E., "Multivariable Computer Control, A Case Study", North Holland, (1976).

16. Froment, G.F., Chemical Eng. Techn., 46, (9), 381, (1974).

17. Hickin, J., Sinha, N.K., Law, S. and Tom, A., "Computer Programs for Control Applications", Report SOC-121, Faculty of Engineering, McMaster University, (1976).

18. Hu, Y.C. and Ramirez, W.F., "Application of Modern Control Theory to Distillation Column", AIChE J., 18, (3), 479, (1972).

19. Hong, H.M. and MacGregor, J.F., "Identification and Direct Digital Stochastic Control of a Continuous Stirred Tank Process", CJChE, Vol. 53, 211, April (1975).

20. Jackson, W.D., "Preliminary Design and DDC of an Extractive Distillation Column", M.Eng. Thesis, McMaster University, Hamilton, (1974).

21. Jazwinski, A.H., "Stochastic Process and Filtering Theory", Academic Press, New York, (1970).

22. Jutan, A., "State Space Modelling and Multivariate Stochastic Control of a Pilot Plant Packed-Bed Reactor", Ph.D. Thesis, McMaster University, Hamilton, Canada, (1976).

23. Jutan, A., Tremblay, J.P., MacGregor, J.F. and Wright, J.D., "Multivariable Computer Control of a Butane Hydrogenolysis Reactor, Part I - State Space Reactor Modelling", Submitted to AIChE J., (1976a).

24. Jutan, A., MacGregor, J.F. and Wright, J.D., "Multivariable Computer Control of a Butane Hydrogenolysis Reactor, Part II - Parameter Estimation and Noise Model Fitting", Submitted to AIChE J., (1976b).

25. Jutan, A., Wright, J.D. and MacGregor, J.F., "Multivariable Computer Control of a Butane Hydrogenolysis Reactor, Part III - On-Line Linear Quadratic Stochastic Control Studies", Submitted to AIChE J., (1976).

26. Kalman, R.E., "Mathematical Description of Linear Dynamical System", SIAM J. on Control, 1, 152, (1963).

26a. Kalman, R.E., J. Basic Eng., 82, 35 (1960).

27. Lee, W. and Weekman, V.W., "Advanced Control Practice in the Chemical Process Industry: A View from Industry", AIChE J., 22, (1), 27, (1976).

28. Ljung, L., Gustavesson, I. and Soderstrom, T., "Identification of Linear Multivariable Systems Operating Under Linear Feedback Control", IEEE Trans. on Aut. Control, 19, 836 (1974).

29. MacGregor, J.F.; "Topics in the Control of Linear Process Subject to Stochastic Disturbances", Ph.D. Thesis, University of Wisconsin at Madison, Wisconsin, U.S.A.; (1972).

30. MacGregor, J.F., "Optimal Discrete Stochastic Control Theory for Process Application", CJChE, Vol. 51, August (1973).

31. MacGregor, J.F., "Optimal Choice of the Sampling Interval for Discrete Process Control", Report SOC-82, Faculty of Engineering, McMaster University, Hamilton, Canada, (1975).

32. MacGregor, J.F. and Box, G.E.P., "The Analysis of Closed-Loop Dynamic-Stochastic Systems", Technometrics", Vol. 16, No. 3, August (1974).

33. Marroquin, G. and Luyben, W.L., "Practical Control Studies of Batch Reactors Using Realistic Mathematical Models", Chem. Eng. Sci., 28, (4), 993, (1973).

34. Meditch, J.S., "Stochastic Optimal Linear Estimation and Control", McGraw-Hill, New York, (1969).

35. Noble, B., "Applied Linear Algebra", Prentice-Hall, (1969).

36. Noton, A.R.M., "Introduction to Variational Methods in Control Forecasting", Pergamon Press, (1965).

37. Orlikas, A., "Kinetic Study of the Hydrogenolysis of n-Butane on Nickel Catalyst", M.Eng. Thesis, McMaster University, Hamilton, Canada, (1970).

38. Orlikas, A., Hoffman, T.W., Shaw, I.D. and Reilly, P.M., CJChE., 50, 628, (1972).

39. Parzen, E., "Some Recent Advances in Time Series Modelling", IEEE, Automatic Control, Vol. AC-19, No. 6, 723, Dec. (1974).

40. Quenouille, M.H., "The Analysis of Multiple Time Series", Griffin, London, (1957).

41. Rao, A.R. and Kashyap, R.L., "Dynamic Stochastic Models from Empirical Data", Academic Press, (1976).

42. Shaw, I.S.D., "Modelling and Discrimination Studies in a Catalytic Fluidized Bed Reactor", Ph.D. Thesis, McMaster University, Hamilton, Canada, (1974).

43. Smith, C.L., "Digital Computer Process Control", Intext Educational Publ., New York, (1972).

44. Sinai, J. and Foss, A.S., "Experimental and Computational Studies of the Dynamics of a Fixed Bed Chemical Reactor", AIChE J., 16, (4), 658, (1970).

45. Sinha, N.K., "Minimal Realization of Transfer Function Matrices: A Comparative Study of Different Methods", Vol.00, Int. J. Control, (1975).

46. Sinha, N.K. and Rozsa, P., "Efficient Algorithm for Irreducible Realization of a Rational Matrix", Int. J. Control, Vol. 20, No. 5, 739, (1974).

47. Soderstrom, T., Gustavesson, I. and Ljung, L., "Identifiability Conditions for Linear Systems Operating Under Closed-Loop", Int. J. Control, 21, 243, (1975).

48. Soderstrom, T., Ljung, L. and Gustavesson, I., "A Comparative Study of Recursive Identification Method", Report 7427, Lund Institute of Technology, Lund, Sweden, 20, (1974).

49. SSP, System/360 Scientific Subroutine Package (360A-CM-03x) Version 3, IBM publication, No. H20-0205-3.

50. Tremblay, J.P., Ph.D. Thesis, McMaster University, Hamilton, Canada, (to be published).

51. Tremblay, J.P. and Wright, J.D., "Computer Control of a Butane Hydrogenolysis Reactor", Joint CSChE-AIChE Conference, Vancouver, B.C., (1973).

52. Tremblay, J.P., "Generalized Operating System Executive", Report SOC-NOVA-3.01, Faculty of Engineering, McMaster University, Hamilton, Canada, (1975).

53. Vakil, H.B., Michelsen, M.L. and Foss, A.S., "Fixed-Bed Reactor Control with State Estimation", Ind. Eng. Chem. Fund., Vol. 12, No. 3, 328, (1973).

54. West, B., "Mini-Computer Control of a Chemical Plant", 26th Canadian Chemical Engineering Conference, CSChE, Toronto, Ontario, (1976).

55. Wilson, G.T., "Modelling Linear Systems for Multivariate Control", Ph.D. Thesis, University of Lancaster, England, August (1970).

56. Wilson, G.T., "The Estimation of Parameters in Multivariate Time Series Models", J.R. Statist. Soc., Vol. 35, 76, (1973).

57. Ho, B.L. and Kalman, R.E., Proc. Third Allerton Conf., 449, (1965).

58. Rosenbrock, H.H., "State-Space and Multivariable Theory", Nelson (1970).

APPENDIX 1

APPLICATION OF MULTIVARIATE TIME SERIES AND TRANSFER FUNCTION IDENTIFICATION

The modelling sequence of the model example in Section 2.3 are presented here. The procedure in Section 2.1 and 2.2 are followed for the construction of Equation (2.26). A total of 347 sets of two-inputs, two-outputs data are available and are given in Figure A1.1 and A1.2.

FIGURE A1.1: INPUT SERIES, $u_{1,t}$

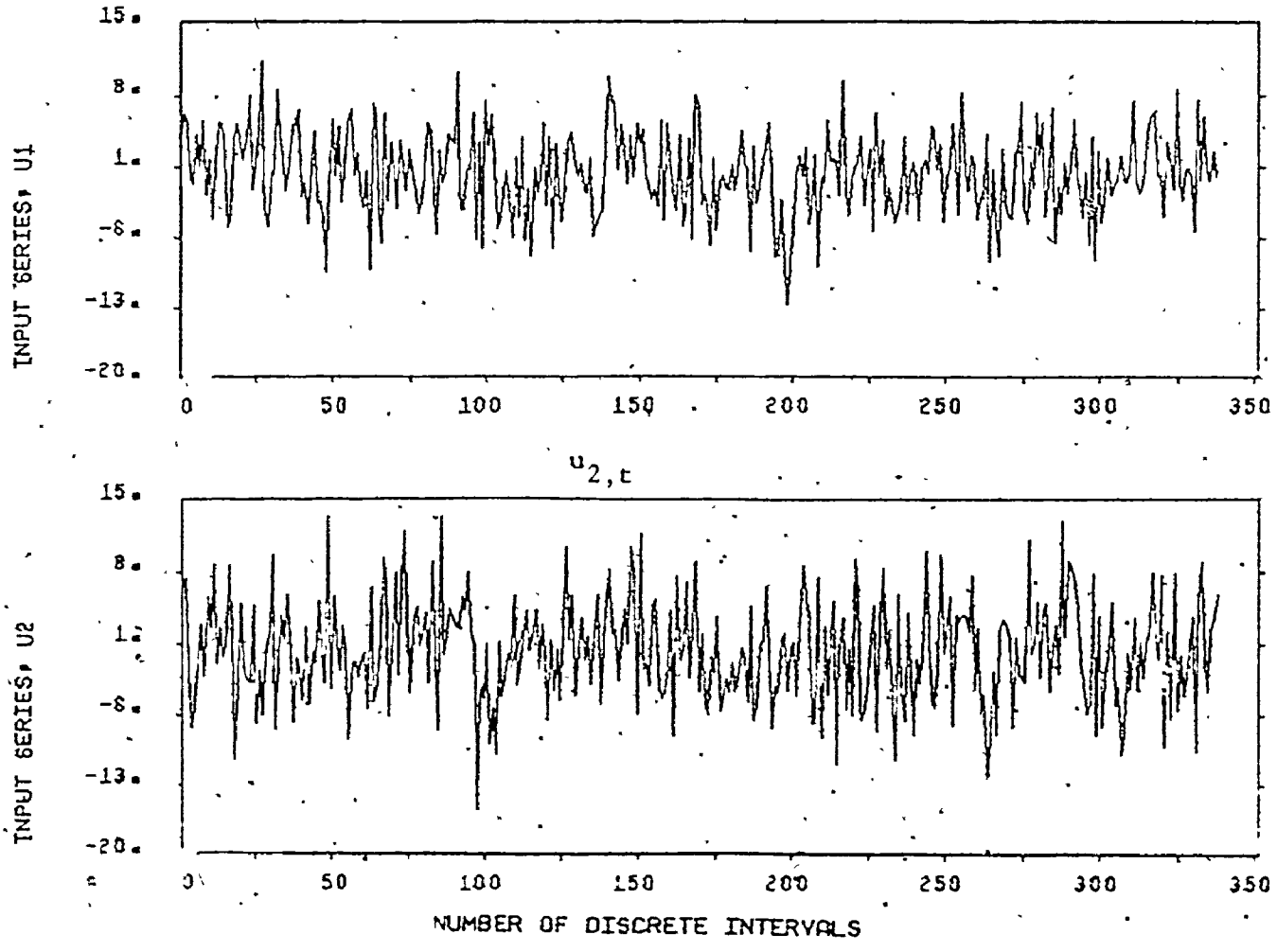

(a) Identification of Input, Output Series

The autocorrelation and partial correlation functions of each input and output series with no differencing are shown in Table A1.1, with the approximate 95% confidence limits. It is obvious that the inputs are uncorrelated white noise series and $y_{1,t}$, $y_{2,t}$ are stationary AR(1) processes. The fact that the inputs are white noise sequences simplifies the modelling procedure.

(b) Transfer Function Identification

Crosscorrelation functions between each input and output are given in Figure A1.3 to A1.6. Individual transfer functions can be identified as the following, with the preliminary parameters determined.

(i) $y_{1,t}$ and $x_{1,t}$: order r = 1, s = 0, b = 1

$$y_{1,t} = \frac{10.5}{1 - 0.47\ B}\ u_{1,t-1} \qquad \text{(A1.1a)}$$

(ii) $y_{1,t}$ and $x_{2,t}$: order r = 1, s = 0, b = 1

$$y_{1,t} = \frac{2.31}{1 - 0.41\ B}\ u_{2,t-1} \qquad \text{(A1.1b)}$$

(iii) $y_{2,t}$ and $x_{1,t}$: order r = 1, s = 1, b = 1

$$y_{1,t} = \frac{3.74 + 0.75\ B}{1 - 0.91\ B}\ u_{1,t-1} \qquad \text{(A1.1c)}$$

(iv) $y_{2,t}$ and $x_{2,t}$: order r = 1, s = 0, b = 1

$$y_{2,t} = \frac{2.12}{1 - 0.47\,B}\, u_{2,t-1} \qquad \text{(A1.1d)}$$

(c) Univariate Output Noise Series Regeneration

The regenerated univariate noise series are shown in Figure A1.7 to A1.8. Each $n_{i,t}$ is identified and the results are shown in Figure A1.9 to A1.10. A stationary ARMA(1,1) model can be tentatively assigned to each series.

$$n_{1,t} = \frac{1 + 0.25\,B}{1 - 0.6\,B}\, a_{1,t} \qquad \text{(A1.2a)}$$

$$n_{2,t} = \frac{1 + 0.7\,B}{1 - 0.7\,B}\, a_{2,t} \qquad \text{(A1.2b)}$$

(d) Preliminary Estimation and Diagnostic Checking of Two Inputs-Univariate Output Model

The two transfer function-noise models corresponding to the two outputs are fitted and checked. The fitted models are:

$$y_{1,t} = \left(\frac{10.13 - 2.49\,B}{1 - 0.52\,B}\right) u_{1,t-1} + 1.93\, u_{2,t-1} + n_{1,t} \qquad \text{(A1.3)}$$

$$n_{1,t} = \left(\frac{1 + 0.27\,B}{1 - 0.36\,B}\right) a_{1,t}$$

and

$$y_{1,t} = \left(\frac{2.93 - 1.00\,B}{1 + 0.53\,B}\right) u_{1,t-1} + \left(\frac{2.05}{1 + 0.41\,B}\right) u_{2,t-1} + n_{2,t} \qquad \text{(A1.4)}$$

$$n_{2,t} = \left(\frac{1 - 0.09\,B}{1 - 0.86\,B}\right) a_{2,t}$$

(e) Multivariate Output Noise Model Identification

The crosscorrelation between the univariate output noise series is shown in Figure A1.11. Significant crosscorrelations are observed and a multivariate stochastic model is thus necessary. The bivariate intermediate series $\underline{b}_t$ is generated and again the crosscorrelation between $b_{1,t}$ and $b_{2,t}$ is determined in Figure A1.12. The crosscorrelation has a cut off lag of 1, indicating the maximum order of the multivariate moving average matrix is at most one. Therefore, the multivariate noise model was assumed to be a multivariate ARMA(1,1) form.

(f) Estimation and Diagnostic Checking of Multivariate Transfer Function-Noise Model

With the off diagonal elements in the $\underline{\theta}(B)$ matrix initially set to zero and assumed to be of order 1, Equation (A1.3) and (A1.4) were combined for the final estimation and checking. The final model Equation (2.27) was obtained, and the autocorrelations among the residuals and the crosscorrelations between the inputs and the residuals are insignificant and thus the model equation (2.27) is adequate.

TABLE A1.1: IDENTIFICATION OF INPUT AND OUTPUT SERIES

a. Autocorrelation Functions, ρ_k

lag k	$u_{1,t}$	$u_{2,t}$	$y_{1,t}$	$y_{2,t}$
1	.071	-.007	.492	.845
2	.112	.054	.326	.706
3	-.026	.089	.149	.586
4	-.033	-.031	.089	.494
5	.070	.108	.112	.435
6	.045	.018	.100	.369
7	.063	-.074	.091	.300
8	-.045	.062	.038	.252
9	.082	-.033	.074	.200
10	-.050	-.034	.011	.151

b. Partial Correlation Functions, ϕ_{kk}

lag k	$u_{1,t}$	$u_{2,t}$	$y_{1,t}$	$y_{2,t}$
1	.071	-.007	.492	.845
2	.107	.054	.110	-.026
3	-.042	.090	-.064	-.013
4	-.041	-.033	.011	.027
5	.085	.099	.093	.065
6	.043	.015	.019	-.050
7	.038	-.080	.009	-.044
8	-.059	.042	-.036	.038
9	.089	-.021	.075	-.042
10	-.049	-.038	-.060	-.036

Approximate 95% confidence limit on correlation = .107

FIGURE A1.2: OUTPUT SERIES, $y_{1,t}$ AND $y_{2,t}$

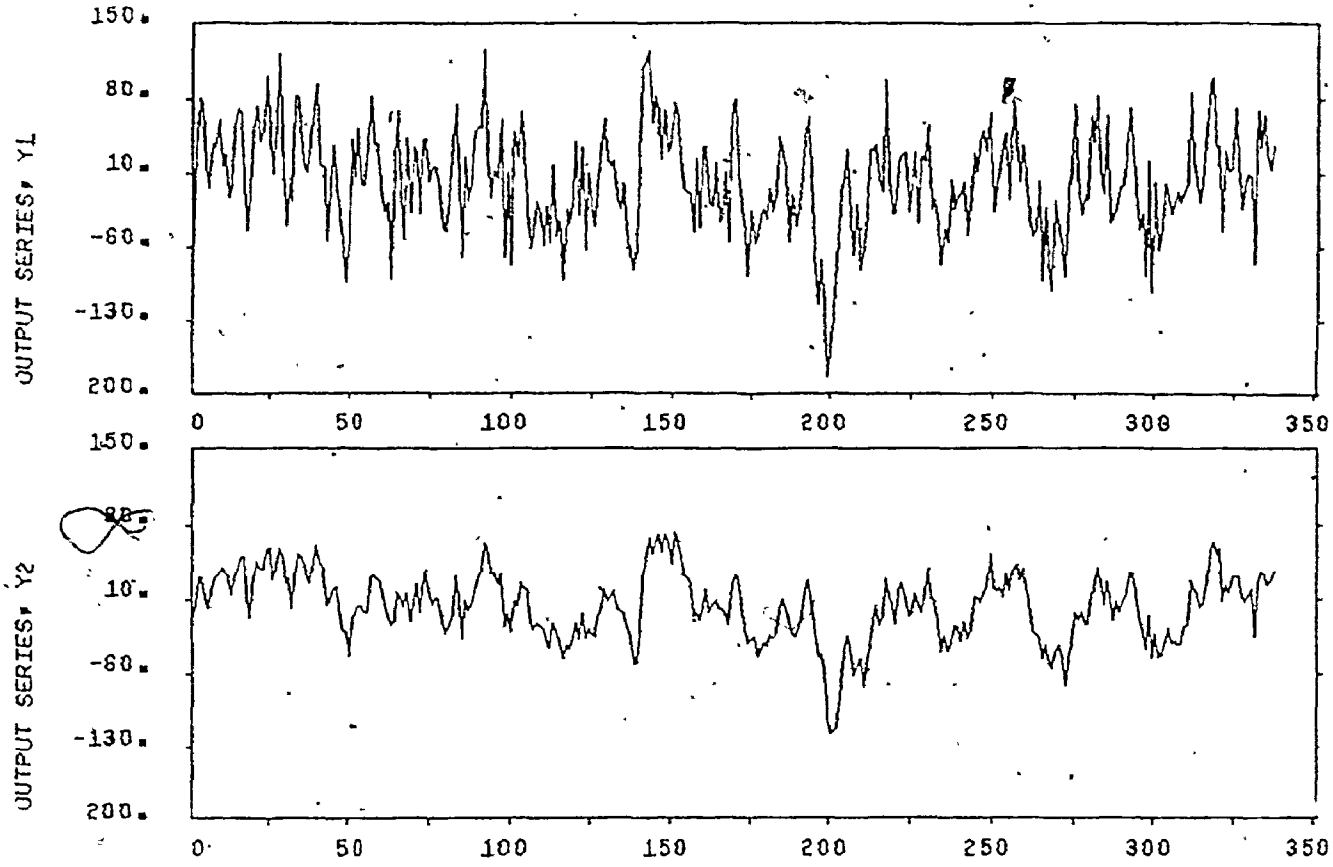

FIGURE A1.7 & A1.8: REGENERATED NOISE SERIES, $n_{1,t}$ and $n_{2,t}$

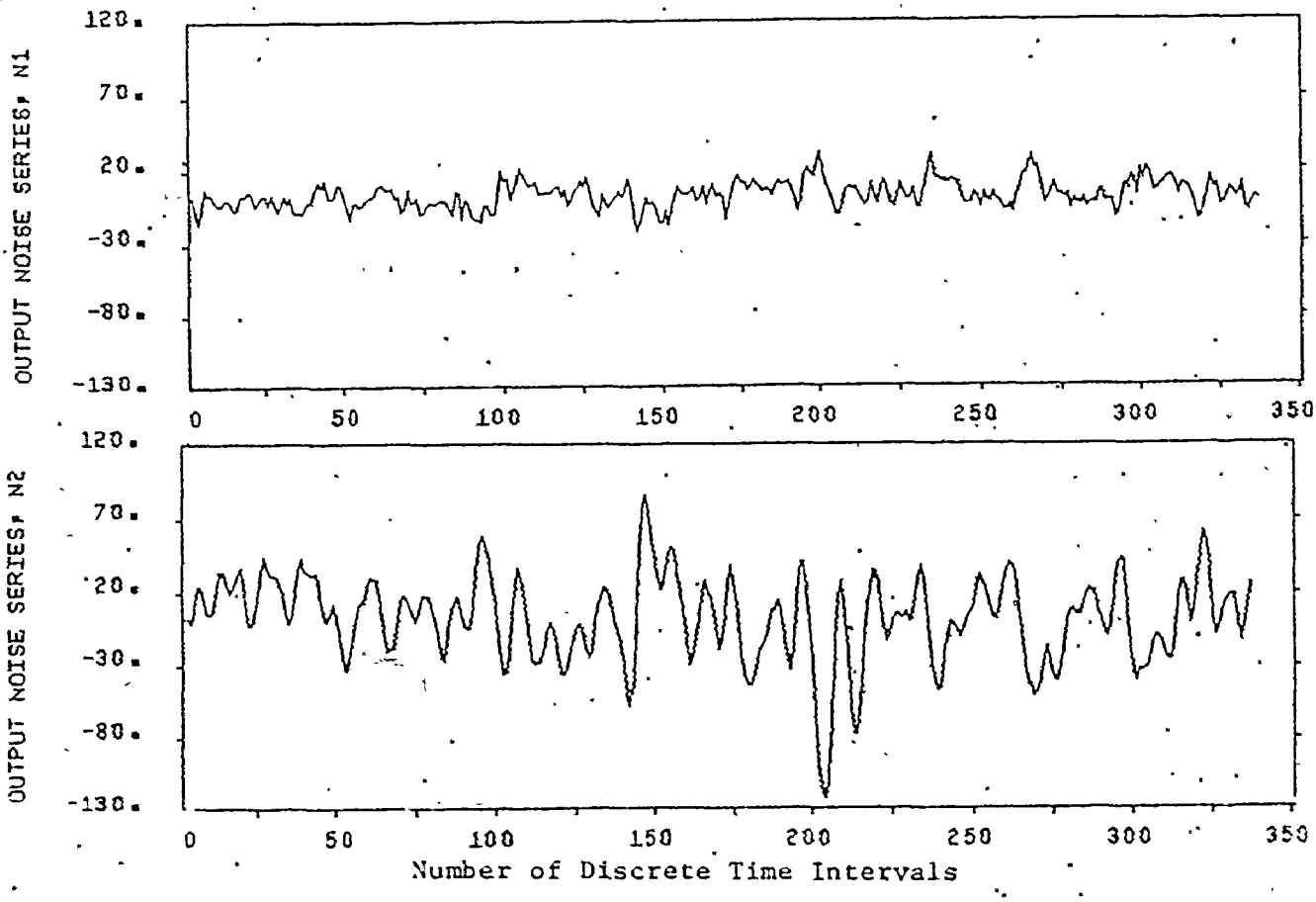

Impulse Response Function Between Input and Output

FIGURE A1.3: $y_{1,t}$ and $u_{1,t}$

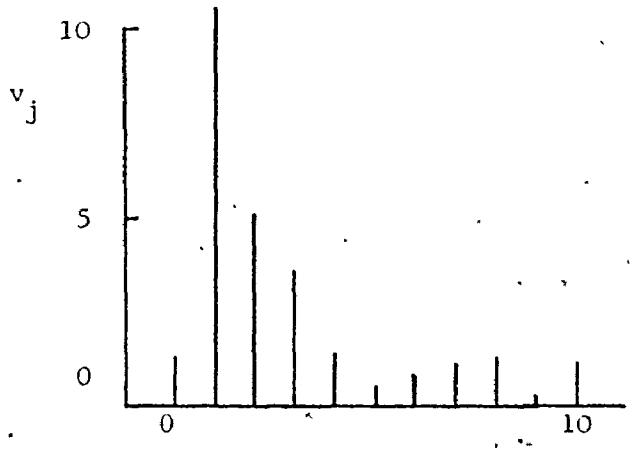

FIGURE A1.4: $y_{1,t}$ and $u_{2,t}$

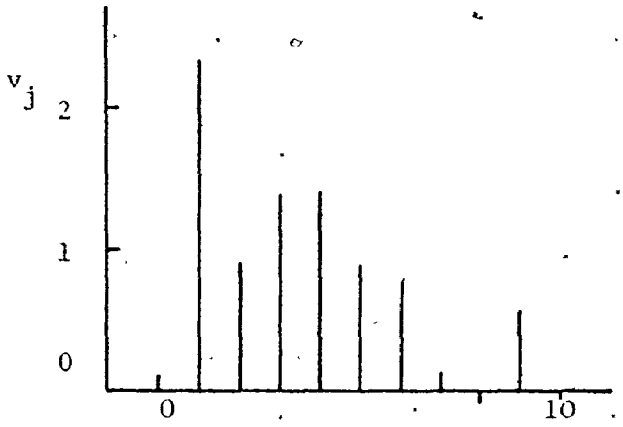

FIGURE A1.5: $y_{2,t}$ and $u_{1,t}$

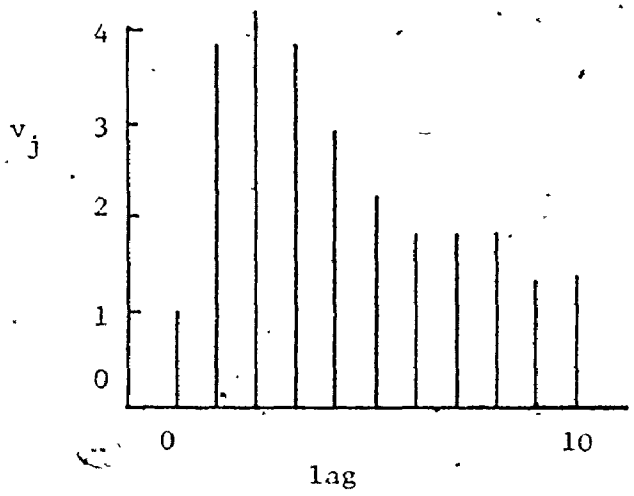

FIGURE A1.6: $y_{2,t}$ and $u_{2,t}$

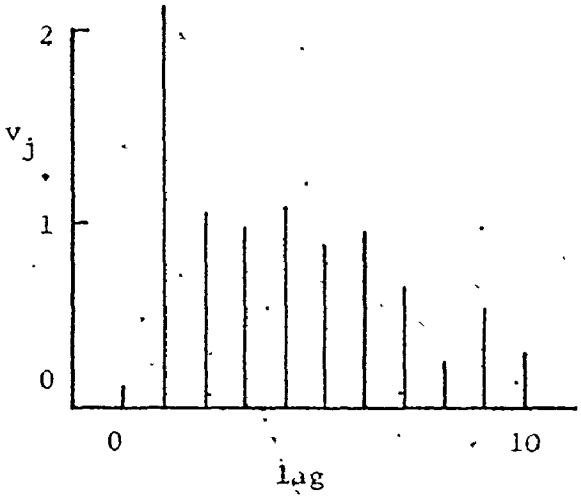

FIGURE A1. 9: $n_{1,t}$ Identification

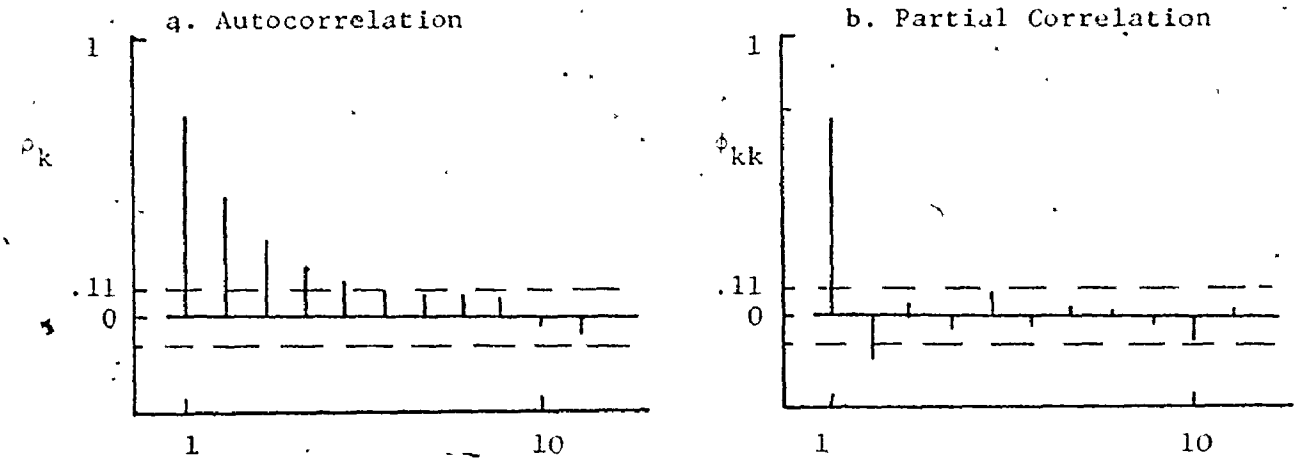

FIGURE A1.10: $n_{2,t}$ Identification

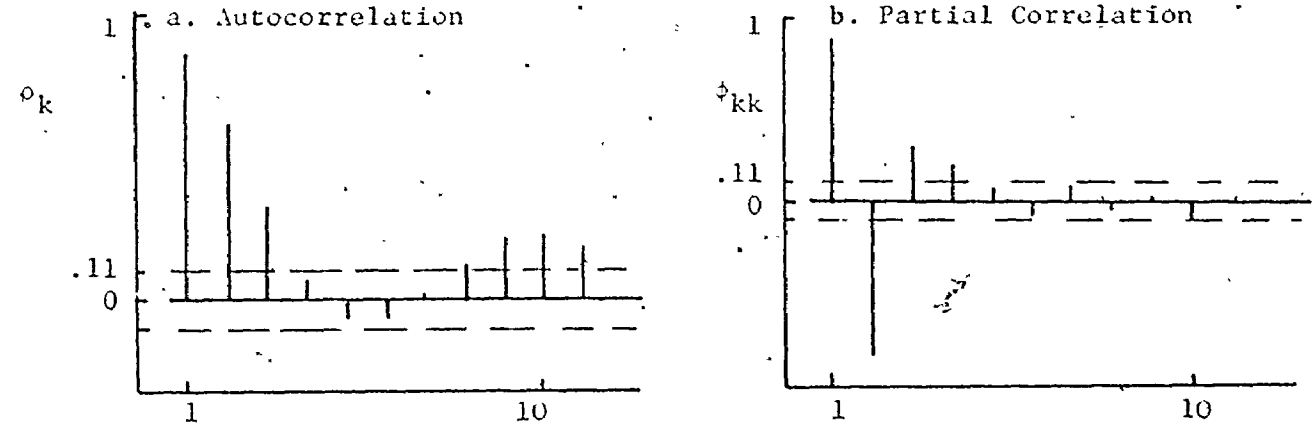

FIGURE A1.11. CROSS-CORRELATION BETWEEN $n_{1,t}$ and $n_{2,t}$

FIGURE A1.12: BIVARIATE SERIES CROSS-CORRELATION

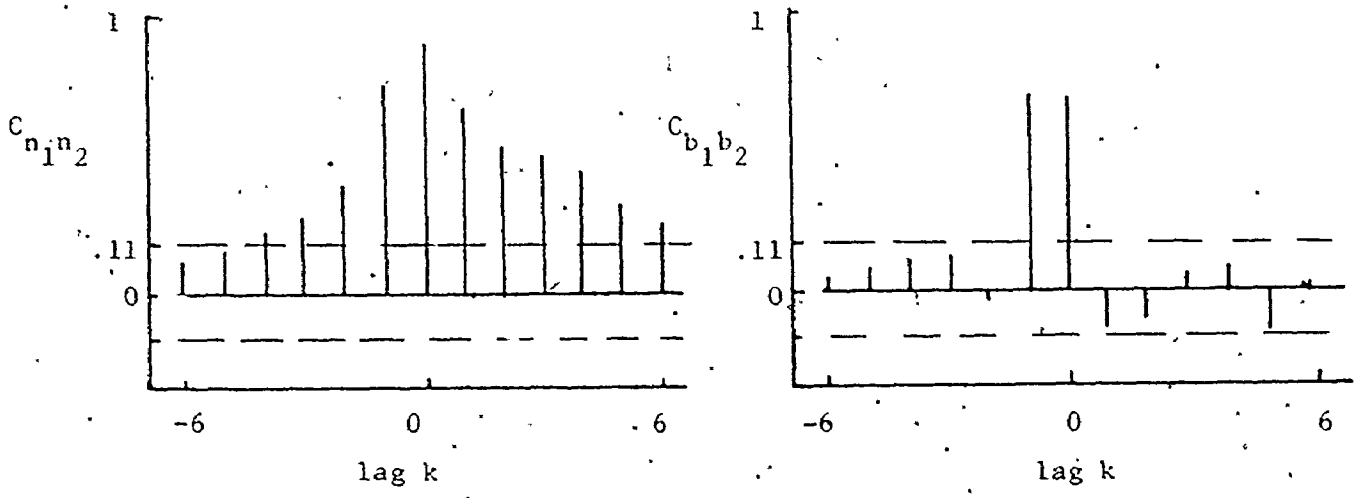

APPENDIX 2

DATA ACQUISITION

A2.1 Added 'dither' Noise Structure

In order to facilitate closed-loop identification, a 'dither' noise series was added to the manipulated butane flow under feedback control. Another perturbation was imposed on the hydrogen flow to excite its variations for efficient model identification. It was arbitrarily decided that an AR(1) noise process would be added to the hydrogen flow while the 'dither' noise was a series of random variables. These two disturbance series were generated by computer software. Evenly distributed random numbers were first generated, which were then converted into normally distributed random series. The desired noise series structure was obtained by filtering the random variables through the appropriate process $\phi(B)$ operators.

(a) Generation of Evenly Distributed Random Numbers

The algorithm is based on the Data General's Relocatable Math Library File [1973]. Evenly distributed random number R_e is calculated by

$$R_e(t+1) = [R_e(t) + A + C] \bmod (2^{16}) \qquad (A2.1)$$

where

$A = (2^{11} + 2^2 + 1)$

$C = 33031$ (octal)

and arg 1 mod (arg 2) is defined as arg 1 -(arg 1/arg 2) arg 2, with (arg 1/arg 2) being the truncated value of the quotient. Theoretically, the routine produces numbers in the range $0 \leq R_e \leq 2^{16} - 1$ and has a maximum cycling period of 2^{16}. The fractional value R_N between the range 0 and 1 can be obtained by dividing R_e by 2^{16}, i.e. $R_N = R_e/2^{16}$. A modified version of the supplied routine was used for the random number generation. Starting $R_e(t)_{t=1}$ values which must be odd numbers are chosen to be 1001 and 789, both of which produce random numbers with a cycle period of more than 1300 numbers without repeating itself. It is critical that the starting $R_e(t)$'s should be selected carefully so that the resulting random numbers have long cycling periods, otherwise repeated cycling effects will be resulted.

(b) Conversion Into Normally Distributed Random Variables

The formation of random number series with normal distribution is developed by the following formulae:

Let

$$\text{ARG1} = [-2.0 * \log_{10} (R_{N1})]^{1/2}$$

$$\text{ARG2} = 2.0 * \pi * R_{N2} \qquad \text{(A2.2)}$$

and

$$a_{1,t} = [\text{ARG1} * \cos (\text{ARG2}) * \sigma_1^+ * (1 - \phi_1^2)^{1/2}]/2.0$$

$$a_{2,t} = [\text{ARG2} * \sin (\text{ARG2}) * \sigma_2^+ * (1 - \phi_2^2)^{1/2}]/2.0 \qquad \text{(A2.3)}$$

where

$a_{i,t}$ - normally distributed random numbers

σ_i^+ = 2 * standard deviation of series

subscript $i = \begin{cases} 1, & \text{noise added to butane flow} \\ 2, & \text{noise added to hydrogen flow} \end{cases}$

The AR parameters are specified and σ_i^+ values can be adjusted on-line. The two noise series were generated by

$$d_{C_4,t} = \text{IFIX}[\phi_{C_4} * d_{C_4,t-1} + a_{1,t}]$$

$$d_{H_2,t} = \text{IFIX}[\phi_{H_2} * d_{H_2,t-1} + a_{2,t}] \qquad \text{(A2.4)}$$

A2.2 Operating Conditions of the Data Collection Run

For the data acquisition run, the following parameters in Table A2.1 were adopted. It is noted that all these parameters can be changed on-line until the optimal conditions are attained. The σ^+ values (2 times the standard deviations) of the AR(1) process and the random dither noise series were adjusted constantly on-line and their variations are increased up to a value of 25.

A2.3 Transformation of Product Mole Fractions Into Extents

Total input flowrate, $u_T = u_{C_4H_{10}} + u_{H_2}$ cc/sec. Converting the flowrates into gm mole/sec,

$$\text{Molar flowrate } G_c = \frac{u_T * P_{atm}}{R * T_{room}} \qquad \text{(A2.5)}$$

where

P_{atm} - atmospheric pressure, 1 atm.

R - universal gas constant, 82.06 (cc.atm)/(g.mole)(°K)

T_{room} - room temperature, 298°K

TABLE A2.1: PARAMETER SETTING DURING THE DATA ACQUISITION RUN

Parameters	Values
Filtering Constant, α_f	0.5
Coolant Oil Setpoint	246°C
Hot Spot Temperature Setpoint	273°C
Hydrogen Flow Setpoint at STP	100 cc/sec
Butane Flow Setpoint at STP	15 cc/sec
Hydrogen Flow Upper Limit	160 cc/sec
Hydrogen Flow Lower Limit	85 cc/sec
Butane Flow Upper Limit	22 cc/sec
Butane Flow Lower Limit	8 cc/sec
$\phi_{C_4H_{10}}$	0
ϕ_{H_2}	0.6

$$G_c = \frac{u_T * 1}{82.06 \times 298} \qquad \text{g mole/sec}$$

The extents of propane, butane and hydrogen are defined as:

$$C_{C_3H_8} = G_c * MF_{C_3H_8}$$

$$C_{C_4H_{10}} = G_c * (u_{C_4H_{10}}/u_T - MF_{C_4H_{10}})$$

$$C_{H_2} = G_c * (u_{H_2}/u_T - MF_{H_2})$$

where

MF - mole fraction of components in product stream

C_i - extents of component.

APPENDIX 3

DYNAMIC-STOCHASTIC MODEL CONSTRUCTION

A3.1 Comparison of Canonical Correlation and The Fitting of Temperature Functions on the Formulation of Predicted Equation

The concentration predicting equation (4.11) can be formulated by two approaches - the canonical correlation analysis in this thesis and the discrete selection of functions of temperatures and flowrates for the independent variables as adopted by Tremblay [1977]. A comparison of the standard deviations (shown in brackets) of individual parameters β_{ij} is given in the following equations. The parameters were fitted with the same set of 61 concentration data, and the normalized correlation matrix of the parameter estimates in each approach is also given.

(a) Canonical Correlation Analysis

(i) Prediction Equation Parameters with Standard Deviation:

$$\begin{bmatrix} C_1 \\ C_2 \\ C_3 \end{bmatrix} = \begin{bmatrix} (\pm.81) & (\pm.81) & (\pm.81) \\ 21.02 & -1.39 & -0.231 \\ (\pm1.86) & (\pm1.86) & (\pm1.86) \\ 36.55 & 15.54 & 1.109 \\ (\pm3.64) & (\pm3.64) & (\pm3.64) \\ 60.78 & 45.14 & 0.325 \end{bmatrix} \begin{bmatrix} Z_1 \\ Z_2 \\ Z_3 \end{bmatrix} \times 10^{-6} \quad \text{(A3.1)}$$

(ii) Normalized Correlation Matrix of Parameters:

$$\begin{bmatrix} 1 & -0.0006 & -0.0001 \\ -0.0006 & 1 & -0.0002 \\ -0.0001 & -0.0002 & 1 \end{bmatrix}$$

(b) Fitting With Input Flowrates and Selected Functions of Temperature

$$\begin{bmatrix} C_1 \\ C_2 \\ C_3 \end{bmatrix} = \begin{bmatrix} (\pm 4.86) & (\pm 2.53) & (\pm 1.65) & (\pm 6.70) & (\pm 2.34) \\ 5.99 & -0.222 & -0.353 & 10.30 & -1.88 \\ (\pm 2.57) & (\pm 1.33) & (\pm 8.68) & (\pm 3.53) & (\pm 1.24) \\ 1.37 & -0.537 & -8.11 & 4.71 & -0.864 \\ (\pm 9.3) & (\pm 4.82) & (\pm 3.14) & (\pm 12.7) & (\pm 4.47) \\ 13.7 & 0.686 & -0.728 & 20.2 & -3.55 \end{bmatrix} \begin{bmatrix} F_1 \\ F_2 \\ F_3 \\ u_{1,t-1} \\ u_{2,t-1} \end{bmatrix} \times 10^{-6} \quad \text{(A3.2)}$$

(ii) Normalized Correlation Matrix of Parameters:

$$\begin{bmatrix} 1 & -0.612 & 0.738 & -0.297 & -0.246 \\ -0.612 & 1 & -0.400 & 0.850 & 0.173 \\ 0.738 & -0.400 & 1 & -0.132 & -0.272 \\ -0.297 & 0.850 & -0.132 & 1 & 0.075 \\ -0.246 & 0.173 & -0.272 & 0.075 & 1 \end{bmatrix}$$

The eigenvalues and eigenvector of the generalized symmetric matrix in Equation (4.6) were computed by subroutine RSG of the Fortran SSP library routines package [1973]. The resulting eigenvectors from this routine are normalized such that

$$\underline{Y}^T \underline{\Sigma}_{22} \underline{Y} = \underline{I} \tag{A3.3}$$

where $\underline{Y}$ and $\underline{\Sigma}_{22}$ are defined in Section 4.2.2.

Examining individual eigenvector $\underline{Y}_i$ separately:

$$\underline{Y}_i^T \underline{\Sigma}_{22} \underline{Y}_j = \begin{cases} 1 & \text{when } i = j \\ 0 & \text{when } i \neq j \end{cases}$$

From the formulation of canonical variates Z_i in Equation (4.8):

$$Z_i = \underline{Y}_i^T \underline{A}_2 \tag{4.10}$$

In matrix form,

$$\underline{Z} = \underline{Y}^T \underline{A}_2 \tag{A3.4}$$

Since $\underline{\Sigma}_{22} = E(\underline{A}_2 \underline{A}_2^T)$, the variance-covariance matrix of the canonical variates is given by:

$$E(\underline{Z}\underline{Z}^T) = E(\underline{Y}^T \underline{A}_2 \underline{A}_2^T \underline{Y})$$

$$= \underline{Y}^T \underline{\Sigma}_{22} \underline{Y} = \underline{I} \tag{A3.5}$$

From Equation (A3.5), the canonical variates are orthogonal to each other, as shown by the normalized correlation matrix. In this case, the variance-covariance matrix is equivalent to the normalized correlation matrix.

A3.2 Results From Model Building

(a) Univariate Transfer Function Between Butane Conversion and Hydrogen Flow Under Closed Loop

Due to the closed-loop nature of the data collected in this work, it was not possible to identify the form of the transfer function involving the hydrogen input flowrate. However, earlier work on univariate transfer function identification between butane conversion and hydrogen flowrate under open loop gave an indication of the system dynamics although the operating conditions were quite different in that case. Using 143 data sets, the impulse response and the step response functions are given in Figure A3.1 and A3.2. They have the same characteristics as those between the butane flow and the various outputs (Figure 4.9 to 4.14) in Section 4.3.1, except that a negative dynamic behaviour is involved. Thus, the selection of model Equation (4.25) is valid, at least for the purpose of preliminary identification.

(b) Modelling

The closed loop identification in Section 4.3.1 together with the information from the open-loop results in (a) above give a transfer function matrix with element of the form Equation (4.21). The transfer function matrix is fitted with 145 data and the residuals represent the stochastic noise of the system. The deterministic model is given below, with a total of 18 dynamic parameters and their standard deviations in brackets.

$$\begin{bmatrix} Y_{1,t} \\ Y_{2,t} \\ Y_{3,t} \end{bmatrix} = \begin{bmatrix} \underset{(\pm.03)}{\left(\frac{5.42 - 3.21\,B}{1 - 0.76\,B}\right)} B & \underset{(\pm.35)}{\left(\frac{-0.85 - 0.16\,B}{1 - 0.12\,B}\right)} B \\ \underset{(\pm.03)}{\left(\frac{6.44 - 3.66\,B}{1 - 0.80\,B}\right)} B & \underset{(\pm.28)}{\left(\frac{-0.55 - 0.27\,B}{1 - 0.26\,B}\right)} B \\ \underset{(\pm.03)}{\left(\frac{8.24 - 4.09\,B}{1 - 0.81\,B}\right)} B & \underset{(\pm.20)}{\left(\frac{0.37 - 0.83\,B}{1 - 0.30\,B}\right)} B \end{bmatrix} \begin{bmatrix} u_{C_4H_{10},t} \\ u_{H_2,t} \end{bmatrix}$$

(A3.6)

where $Y_{i,t}$ is the deterministic output such that $\underline{C}_t = \underline{Y}_t + \underline{N}_t$.

The univariate residual series were identified (Figure 4.15 to 4.20) as either AR(1) or IMA(1,1) processes. High correlation among these stochastic disturbances were observed and hence a multivariate stochastic model was required. The IMA(1,1) model was chosen and the off-diagonal polynomials in terms of B's of the operator matrix $\underline{\theta}(B)$ were all assumed to be of order one. Combining the multivariate transfer function model equation (A3.6) and the multivariate IMA(1,1) stochastic model, the integrated model with 27 continuous parameters was refitted. In subsequent estimations, poor convergence for this model was observed and those parameters from the same output response were highly correlated. The difficulty in convergence might be due to the relatively small added noise perturbation in the hydrogen stream which was at least five times larger than that of butane.

Thus, a much higher perturbation should be added to the hydrogen flowrate so that the flow variation patterns are more apparent. In view of this problem, the δ parameters in the transfer functions involving u_{H_2} were omitted and the data was refitted. This meant that the responses were directly proportional to the hydrogen flowrates, and essentially, equally good fits can still be obtained under this situation. Two fitted models from two sets of 145 data are shown below, with the standard deviations of the parameters in the brackets.

(i) First 145 Data Set Set:

Average standard deviation of hydrogen flow = 8 cm^3/sec

Average standard deviation of butane flow = 10 cm^3/sec

$$10^6 \times \begin{bmatrix} C_{1,t} \\ C_{2,t} \\ C_{3,t} \end{bmatrix} = \begin{bmatrix} \underset{(\pm.04)}{\left(\frac{5.77 - 3.99\,B}{1 - 0.84\,B}\right)} B & \underset{(\pm.18)}{(-0.810 - 0.201\,B)}\,B \\ \underset{(\pm.03)}{\left(\frac{6.99 - 4.67\,B}{1 - 0.86\,B}\right)} B & \underset{(\pm.30)}{(-0.465 - 0.359\,B)}\,B \\ \underset{(\pm.04)}{\left(\frac{9.19 - 5.58\,B}{1 - 0.87\,B}\right)} B & \underset{(\pm.55)}{(0.501 - 0.664\,B)}\,B \end{bmatrix} \begin{bmatrix} u_{C_4H_{10},t} \\ u_{H_2,t} \end{bmatrix} + \underline{N}_t \qquad \text{(A3.7a)}$$

$$\nabla \underline{N}_t = \begin{bmatrix} 1 - 0.553\,B & 0.179\,B & -0.202\,B \\ 0.362\,B & 1 - 0.514\,B & -0.305\,B \\ 0.313\,B & 0.774\,B & 1 - 1.37\,B \end{bmatrix} \underline{a}_t \qquad \text{(A3.7b)}$$

Covariance matrix of residual vector

$$\underline{D} = \begin{bmatrix} 47.9 & 76.4 & 136.1 \\ 76.4 & 125.5 & 225.9 \\ 136.1 & 225.9 & 411.6 \end{bmatrix} \times 10^{-12} \qquad \text{(A3.7c}$$

(ii) Second Set of 145 Data:

Average standard deviation of hydrogen flow = 10 cm^3/sec

Average standard deviation of butane flow = 12 cm^3/sec

$$10^6 \times \begin{bmatrix} C_{1,t} \\ C_{2,t} \\ C_{3,t} \end{bmatrix} = \begin{bmatrix} (\pm.20)\ (\pm.30) & (\pm.17)\ (\pm.17) \\ \left(\frac{6.17 - 4.58\,B}{1 - 0.896\,B}\right) B\ (\pm.03) & (-0.45 - 0.050\,B)\,B \\ (\pm.31)\ (\pm.40) & (\pm.27)\ (\pm.27) \\ \left(\frac{7.51 - 5.18\,B}{1 - 0.904\,B}\right) B\ (\pm.02) & (0.049 - 0.141\,B)\,B \\ (\pm.54)\ (\pm.64) & (\pm.48)\ (\pm.27) \\ \left(\frac{10.04 - 6.28\,B}{1 - 0.908\,B}\right) B\ (\pm.02) & (1.298 - 0.304\,B)\,B \end{bmatrix} \begin{bmatrix} u_{C_4H_{10},t} \\ u_{H_2,t} \end{bmatrix} + \underline{N}_t$$

(A3.8a)

$$\nabla \underline{N}_t = \begin{bmatrix} (\pm.194) & (\pm.167) & (\pm.079 \\ 1 - 0.45\ B & -0.137\ B & 0.032\ B \\ \\ (\pm.288) & (\pm.214) & (\pm.110) \\ 0.375\ B & 1 - 0.573\ B & -0.148\ B \\ \\ (\pm.503) & (\pm.385) & (\pm.199) \\ 0.187\ B & 1.336\ B & 1 - 1.435\ B \end{bmatrix} \underline{a}_t \quad \text{(A3.8b)}$$

Covariance matrix of residual vector:

$$\underline{D} = \begin{bmatrix} 47.5 & 73.6 & 128.9 \\ 73.6 & 118.6 & 210.4 \\ 128.9 & 210.4 & 377.5 \end{bmatrix} \quad \text{(A3.8c)}$$

Correlation Between Univariate H_2 Series and Butane Conversion

FIGURE A3.1: Impulse Response Function

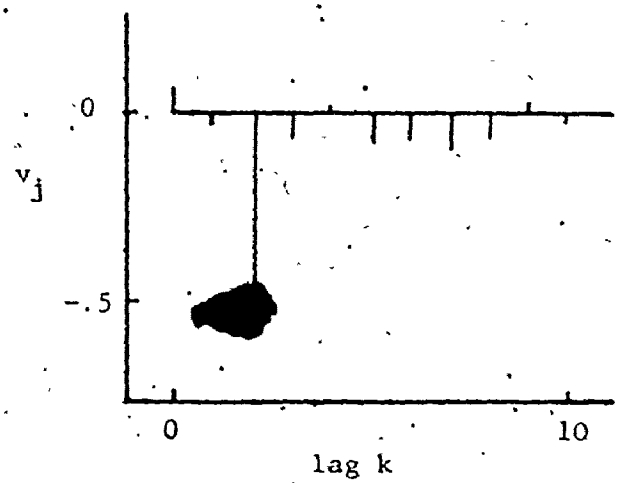

FIGURE A3.2: Step Response Function

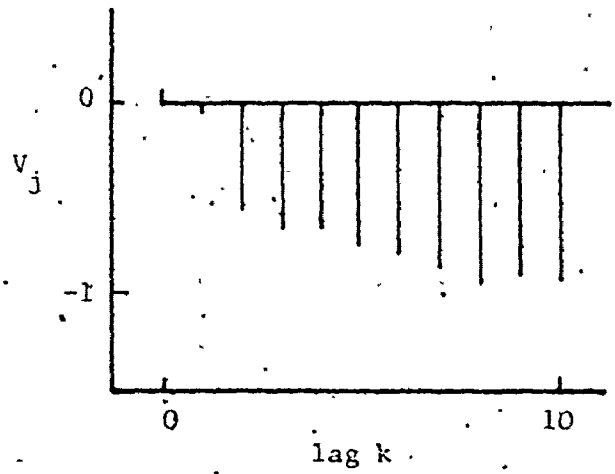

A3.3. Transformation of Transfer Function Matrix Into State Space Model Form

The dynamic-stochastic behaviour of the catalytic reactor system has been developed and is represented by Equation (4.41) and (4.42). Anticipating that integral control action will be involved, a modified version of the model in which $\nabla \underline{u}_t$ is used is shown by Equation (4.43). The transformation is to realize the dynamic transfer function matrix $(\underline{I} - \underline{I}\, B)^{-1}\underline{V}(B)$ and the stochastic 'transfer function' matrix $(\underline{I} - \underline{I}\, B)^{-1}\, \underline{\vartheta}(B)$ into the corresponding state forms. Augumenting the dynamic and stochastic state space model forms into the final model Equation (4.44):

$$\underline{x}(t+1) = \underline{A}\, \underline{x}(t) + \underline{G}\, \nabla\, \underline{u}(t) + \underline{\Gamma}\, \underline{a}(t+1)$$

$$\underline{y}(t) = \underline{H}\, \underline{x}(t) \qquad (4.44)$$

where

$$\underline{A} = \left[\begin{array}{ccccc|cccc} 0 & 0 & 0 & -2.525 & 0 & & & & \\ 0 & 0 & 0 & 0 & 0 & & & & \\ 0 & 1 & 1 & 0 & 0 & & \underline{0} & & \\ 1 & 0 & 0 & 2.755 & 0 & & & & \\ 0 & 0 & 0 & -0.770 & 0 & & & & \\ \hline & & & & & 0 & 0 & 0 & 0 \\ & & & \underline{0} & & 0 & 0 & 0 & 0 \\ & & & & & 1 & 0 & 1 & 0 \\ & & & & & 0 & 1 & 0 & 1 \end{array}\right]$$

$$\underline{\Gamma}^T = \left[\begin{array}{c|cccc} & 1 & 0 & 0 & 0 \\ \underline{0} & & & & \\ & 0 & 1 & 0 & 0 \end{array}\right]$$

$$\underline{H} = \left[\begin{array}{ccccc|cccc} 8.664 & -0.183 & -0.420 & 9.989 & 7.170 & 1 & 0 & 0.674 & -0.221 \\ 7.563 & -0.735 & -0.735 & 8.234 & 6.790 & 0 & 1 & 0.698 & -0.121 \end{array}\right]$$

$$\underline{G}^T = \left[\begin{array}{ccccc|c} 0 & 0 & 0 & 0 & 1 & \\ & & & & & \underline{0} \\ 0 & 1 & 0 & 0 & 0 & \end{array}\right] .$$

APPENDIX 4

RESULTS ON OPTIMAL STOCHASTIC CONTROLLER DESIGN

The Kalman filter matrix $\underline{K}$ defined in Equation (5.11) is given here:

$$\underline{K}^T = \begin{bmatrix} 0 & 0 & 0 & 0 & 0 & 1 & 0 & 0 & 0 \\ 0 & 0 & 0 & 0 & 0 & 0 & 1 & 0 & 0 \end{bmatrix}$$

With the $\underline{A}$, $\underline{G}$ and $\underline{H}$ matrices determined in Appendix 3, the simultaneous state estimator $\underline{x}(t/t)$ can then be set up from Equation (5.12). The controller matrix L_∞ of Equation (5.14) corresponding to various constraint matrices in Table 5.1 and 5.2 are given below:

$$\begin{bmatrix} \nabla u_{C_4,t} \\ \nabla u_{H_2;t} \end{bmatrix} = -\underline{L}_\infty \underline{x}(t/t)$$

(1) $\underline{Q}_2 = \begin{bmatrix} 0 & 0 \\ 0 & 0 \end{bmatrix}$

$$\underline{L}_\infty = \begin{bmatrix} 1.449 & -.043 & -.043 & 1.636 & 1.238 & .091 & -.035 & .091 & -.035 \\ 2.182 & .600 & .600 & 3.121 & 1.143 & -.106 & -.157 & -.106 & -.157 \end{bmatrix}$$

(4) $\underline{Q}_2 = \begin{bmatrix} 75 & 0 \\ 0 & 10 \end{bmatrix}$

$$\underline{L}_\infty = \begin{bmatrix} .867 & -.043 & -.043 & .946 & .778 & .058 & -.016 & .058 & -.016 \\ -.266 & .118 & .115 & -.263 & -.268 & -.071 & -.002 & -.071 & -.002 \end{bmatrix}$$

(5) $\underline{Q}_2 = \begin{bmatrix} 100 & 0 \\ 0 & 25 \end{bmatrix}$

$$\underline{L}_\infty = \begin{bmatrix} .813 & -.041 & -.041 & .885 & .732 & .054 & -.015 & .054 & -.015 \\ -.143 & .067 & .067 & -.143 & -.143 & -.041 & -.001 & -.041 & -.001 \end{bmatrix}$$

(2) $\underline{Q}_2 = \begin{bmatrix} 1 & 0 \\ 0 & 1 \end{bmatrix}$

$$\underline{L}_\infty = \begin{bmatrix} 1.323 & -.063 & -.063 & 1.463 & 1.166 & .090 & -.027 & .090 & -.027 \\ .401 & .257 & .257 & .596 & .189 & -.100 & -.037 & -.100 & -.037 \end{bmatrix}$$